ICLIAD 63 (1), 1-110, 2022

p-ISSN 0535-5133
e-ISSN 2477-9393

Volumen 63
No. 1
Marzo 2022

Investigación Clínica

Universidad del Zulia
Facultad de Medicina
Instituto de Investigaciones Clínicas
"Dr. Américo Negrette"
Maracaibo, Venezuela

Investigación Clínica

https://sites.google.com/site/revistainvestigacionesclinicas

Revista arbitrada dedicada a estudios humanos, animales y de laboratorio relacionados con la investigación clínica y asuntos conexos.

La Revista es de Acceso Abierto, publicada trimestralmente por el Instituto de Investigaciones Clínicas "Dr. Américo Negrette", de la Facultad de Medicina, de la Universidad del Zulia, Maracaibo, Venezuela.

Investigación Clínica está indizada en Science Citation Index Expanded (USA), Excerpta Medica/EMBASE y Scopus (Holanda), Tropical Diseases Bulletin y Global Health (UK), Biblioteca Regional de Medicina/BIREME (Brasil), Ulrich's Periodicals, Journal Citation Reports (USA), Index Copernicus (Polonia), SIIEC Data Bases, Sección Iberoamérica (Argentina) e Infobase Index (India), Redalyc y las bases de datos: SciELO (www.Scielo.org.ve), Revencyt, LILACS, LIVECS, PERIODICA y web de LUZ: http://www.produccioncientificaluz.org/revistas

Para cualquier otra información dirigir su correspondencia a:

Dra. Elena Ryder, Editora
Instituto de Investigaciones Clínicas
"Dr. Américo Negrette"
Facultad de Medicina, Universidad del Zulia
Maracaibo, Venezuela.

Teléfono:
+58-0414-6305451

Correos electrónicos:
elenaryder@gmail.com
riclinicas@gmail.com

Páginas web:
https://sites.google.com/site/revistainvestigacionesclinicas

http://www.produccioncientificaluz.org/revistas

For any information please address correspondence to:

Dr. Elena Ryder, Editor
Instituto de Investigaciones Clínicas
"Dr. Américo Negrette"
Facultad de Medicina, Universidad del Zulia
Maracaibo, Venezuela.

Phone:
+58-0414-6305451

E-mails:
elenaryder@gmail.com
riclinicas@gmail.com

Web pages:
https://sites.google.com/site/revistainvestigacionesclinicas

http://www.produccioncientificaluz.org/revistas

Universidad del Zulia
Publicación auspiciada por el
Vicerrectorado Académico
Serbiluz-CONDES

CODEN: ICLIAD
Versión impresa ISSN: 0535-5133
Depósito legal pp 196002ZU37
Versión electrónica ISSN: 2477-9393
Depósito legal ppi 201502ZU4667

Artes finales:
Lisbeny Valencia
lisbenyvalencia@gmail.com

Invest Clin 63(1): 1 - 5, 2022 https://doi.org/10.54817/IC.v63n1a00

EDITORIAL
¿Diabetes post COVID-19?

La diabetes mellitus (DM) es una de las enfermedades crónicas que supone una enorme carga para los sistemas sanitarios del mundo. Esta es una enfermedad de etiología multifactorial caracterizada por hiperglucemia crónica asociada con resistencia a la insulina (RI) y una respuesta compensatoria inadecuada en la secreción de esta hormona [1]. La DM es un síndrome que comprende una serie de etiologías moleculares progresivamente emergentes que pueden presentarse con diferentes subfenotipos [2].

Es reconocido que la DM, independientemente del tipo, aumenta el riesgo de presentar otras comorbilidades incluyendo las complicaciones propias de la enfermedad, así como un riesgo elevado de sufrir cualquier clase de infección, con particular énfasis en infecciones respiratorias bajas. Numerosos estudios indican que la fisiopatogenia de esta enfermedad está íntimamente relacionada con un proceso inflamatorio sistémico, el mismo que podría estar activo antes de que se desarrollen las alteraciones metabólicas detectables clínicamente, alteran la inmunidad y disminuyen la resistencia a la infección, lo que favorece la sobreinfección por bacterias y hongos; facilitan la aparición de polineuropatías y disfunción multiorgánica y en definitiva, incrementan la mortalidad de los pacientes [3].

Actualmente, el mundo está combatiendo una pandemia de enfermedad por coronavirus 2019 (COVID-19), que, al unirse a otra como la de DM, han planteado una relación bidireccional entre estas dos condiciones de salud. Está indudablemente demostrado que la DM está asociada a un mal pronóstico de COVID-19. Más interesante aún, investigaciones recientes evidencian que los pacientes diabéticos con COVID-19 experimentan con frecuencia hiperglucemia descontrolada y sostenida que requieren dosis excepcionalmente altas de insulina, o episodios de crisis hiperglucémica aguda, incluyendo en este último caso, pacientes sin antecedente de DM, muy probablemente dentro de la población de riesgo con prediabetes que ante un proceso infeccioso podrían presentar estas alteraciones [4, 5].

Aunque las principales causas de la DM son ampliamente conocidas (RI y obesidad asociada a hábitos de vida poco saludables como el sedentarismo y consumo excesivo de calorías, que predispone al desarrollo de la diabetes mellitus tipo 2 (DM tipo 2) o con la destrucción de las células beta pancreáticas por el propio sistema inmunitario (DM tipo 1), recientemente se ha puesto de manifiesto una posible asociación entre la infección por el síndrome respiratorio agudo severo coronavirus 2 (SARS-CoV-2), el virus que causa la COVID-19 y el desarrollo de diabetes. El mecanismo de infección de SARS-CoV-2 comienza con la unión del virión a receptores (enzima convertidora de angiotensina-2 o ACE2) de las células beta del páncreas, lo que podría causar un deterioro agudo en la secreción de insulina. La ACE2 no solo es una enzima, sino también un receptor funcional en las superficies celulares a través del cual el SARS-CoV-2 ingresa a las células huésped y se expresa en gran medida en el corazón, los riñones y los pulmones. ACE2 es un regulador clave del sistema renina-angiotensina-aldosterona (RAAS). La interacción de la

proteína viral S con su receptor ACE2 induce el bloqueo del paso de la Angiotensina II (altamente proinflamatoria) a Angiotensina 1-7 (anti-inflamatoria) con las consecuencias de dejar a la Angiotensina II ejerciendo un mayor efecto pro-inflamatorio a través de la activación del factor NF-kB y producción de varias citocinas y factores que inducen daño tisular por inflamación y estrés oxidativo. El SARS-CoV-2 provoca la interrupción del equilibrio ACE/ACE2 y la activación de RAAS, lo que finalmente conduce al incremento de los procesos inflamatorios y a la progresión de COVID-19, especialmente en pacientes con comorbilidades, como hipertensión, DM y enfermedad cardiovascular, que tienen una activación inflamatoria de base. Por lo tanto, la expresión de ACE2 puede tener efectos paradójicos, ayudando a la patogenicidad del SARS-CoV-2 y, al mismo tiempo, limitando la infección viral [6].

En este contexto, es importante mencionar que estos hallazgos han creado la preocupación sobre si los bloqueadores del receptor de angiotensina II (BRA) y los inhibidores de la enzima convertidora de angiotensina (IECA) pueden tener efectos nocivos sobre la morbimortalidad de los pacientes con COVID-19, basados en la especulación de que estos medicamentos aumentarían la regulación ACE2, que aumentaría la carga viral y la lesión pulmonar. Los estudios recientes concuerdan con las recomendaciones de las sociedades científicas que plantean evitar la suspensión o cambio de medicación antihipertensiva, pues no hay evidencia que muestre que estos puedan ser tomados como factores de riesgo para gravedad o mortalidad por COVID-19 [7].

Asimismo, al igual que se ha postulado ocurre con otras patologías virales, la infección de las células productoras de insulina por SARS-CoV-2 puede inducir una respuesta autoinmune contra ellas. Esto podría provocar que el sistema inmunitario las ataque por error, las destruya y cause la aparición de DM tipo 1 (DM1). Sin embargo, en un estudio reciente, no fue posible demostrar una asociación clara entre la infección por SARS-CoV-2 y la DM1 de nueva aparición. Estos autores plantean estudiar, en grandes cohortes, si el SARS-CoV-2 aumenta la susceptibilidad a la diabetes al desencadenar la autoinmunidad de las células de los islotes y afecta el momento de la diabetes manifiesta en pacientes con autoinmunidad existente [anticuerpos contra las células de los islotes (ICA), contra la descarboxilasa del ácido glutámico (GAD-65), contra la insulina (IAA) y contra la tirosina fosfatasa (IA-2A)]; o con síndromes poliglandulares autoimmunes [8]. Mientras, otros investigadores, reportan tres casos de DM recién diagnosticada asociada con COVID-19 [9], lo que plantea la pregunta una vez más, si COVID-19 puede causar anomalías endocrinas y conllevar a la aparición de DM sin cetoacidosis, en el contexto donde se ha informado disfunción tiroidea con triyodotironina baja, hormona estimulante de la tiroides baja o tiroiditis subaguda [10]. Las complicaciones de otras glándulas endocrinas aún no están claras, junto a otra interrogante con relación a la acción del virus en células que no producen insulina y donde el receptor para insulina puede estar afectado, induciendo DM tipo 2.

Desde hace algún tiempo investigaciones previas han puesto de manifiesto la asociación entre citoquinas proinflamatorias (IL-6 e IL-1beta, entre otras) y la aparición y desarrollo de la DM2 [11], además la exposición de los islotes humanos a las citoquinas, especialmente IL-1β e IFN-γ, ha resultado en una mayor acumulación extracelular de proinsulina, lo que sugiere su conversión desproporcionada de proinsulina en insulina en la DM1. Esta evidencia apunta hacia el papel de las citocinas en la disfunción de las células beta [12]. Otras evidencias de estudios clínicos describen que la gravedad de COVID-19 se correlaciona positivamente con los niveles de citocinas inflamatorias, incluidas IL-1β, TNF-α, proteína quimioatrayente de monocitos 1 (MCP-1)/CCL2, IL-2, sIL-2RA, IL- 6, IL-7, IL-17, IL-18, factor estimulante de colonias de granulocitos (G-CSF), IP10, factor

estimulante de colonias de macrófagos (M-CSF) y MIP-1α/CCL3, MCP-3 en el plasma/suero de pacientes [13]; sin embargo, cuanto podría contribuir la tormenta de citoquinas proinflamatorias con la aparición de la DM, es un punto interesante a investigar, a sabiendas que la fisiopatología de esta enfermedad está íntimamente relacionada con un proceso inflamatorio sistémico de base.

Por otro lado, mucho se ha comentado sobre los niveles de ansiedad, depresión y miedo asociado a un diagnóstico de COVID-19 y a las medidas de confinamiento aplicadas [14], lo que conlleva a un aumento del estrés, acompañado de una producción incrementada de hormonas relacionadas, como los glucocorticoides, que tienen entre sus múltiples efectos la hiperglucemia. También, para evitar la tormenta de citoquinas que se produce en la COVID-19, y que es una de las principales causas del empeoramiento y mal pronóstico de la enfermedad, se incluye el uso de fármacos antiinflamatorios de tipo glucocorticoides. Este exceso de glucocorticoides exógenos o endógenos se caracteriza por una mayor susceptibilidad a las infecciones, debido al deterioro del sistema inmunitario innato y adaptativo [15]. Por lo tanto, en los pacientes con exceso de glucocorticoides, podría evidenciarse hiperglucemia y un alto riesgo de desarrollar una infección por COVID-19 con un curso clínico grave, por ende, la bidireccionalidad asociada a DM, vuelve a ser un factor clave a dilucidar.

Por ahora, es razonable considerar que las personas con DM tienen un mayor riesgo de complicación al desarrollar COVID-19, con implicaciones clínicas significativas e impacto en la morbimortalidad; razones de base para implementar una vigilancia oportuna. Es crucial que en la atención de este grupo de pacientes se tomen en cuenta los factores de riesgo metabólicos asociados con la gravedad de la enfermedad, las interacciones metabólicas entre los agentes antidiabéticos, los inhibidores y los fármacos potenciales. Todo ello contribuirá a disminuir otras complicaciones adicionales a las previamente conocidas en la DM, en especial cuando se desconoce el fin de la pandemia de COVID-19. Es evidente la necesidad de investigar sobre nuevas manifestaciones de aparición temprana y tardía de la DM, dado que hasta el momento los datos son limitados.

Nereida Valero Cedeño
nereida.valero@unesum.edu.ec
ORCID: 0000-0003-3496-8848

¿Diabetes post COVID-19?

The appearance of Diabetes Mellitus (DM) in patients who have suffered from COVID-19 could be added, if confirmed by subsequent studies, to the long list of consequences caused by this pandemic. Likewise, the impact of COVID-19 on the endocrine system is poorly studied. Previous coronavirus outbreaks, as well as other previously reported viral infections, have been associated with new-onset DM. However, there is little research in this regard and the question arises again as to how viruses can contribute to the onset of the disease or if they modify factors that ultimately trigger the lack of control of blood glucose, together with insulin resistance (IR). The recent COVID-19 pandemic has made it abundantly clear that DM increases the risk of more frequent and severe viral infections. At the same time, proinflammatory cytokines promote IR and constitute a risk factor for the development of DM. This raises the existence of a reciprocal and harmful interaction between the immune and endocrine systems in the context of DM. It is not clear why these two systems would interact by inducing transient changes in systemic metabolism as a strategy against viral infection. In people with DM, this system fails, negatively affecting the antiviral immune response. In addition, immune-mediated changes in systemic metabolism after infection may worsen glycemic control, laying the groundwork for future research.

REFERENCIAS

1. Stidsen JV, Henriksen JE, Olsen MH, Thomsen RW. Nielsen JS, Rungby J, Sinna P Ulrichsen SP, Berencsi K, Kahlert JA, Friborg SG, Brandslund I, Nielsen AA, Christiansen JS, Sørensen HT, Olesen TB, Beck-Nielsen H. Pathophysiology-based phenotyping in type 2 diabetes: A clinical classification tool. Diabetes Metab Res Rev 2018; 34:e3005. *https://doi.org/10.1002/dmrr.3005.*
2. Wagner R, Heni M, Tabák AG, Machann J, Schick F, Randrianarisoa E, Fritsche A. Pathophysiology-based subphenotyping of individuals at elevated risk for type 2 diabetes. Nature Medicine 2021; 27(1): 49-57. *https://doi.org/10.1038/s41591-020-1116-19.*
3. Nyunt TPK, Mullol J, Snidvongs K. Immune response to fungi in diabetic patients with invasive fungal rhinosinusitis. Asian Pac J Allergy Immunol 2020; 38(4):233-238. *Doi: 10.12932/AP-080620-0874.*
4. Rubino F, Amiel SA, Zimmet P, Alberti G, Bornstein S, Eckel RH, Mingrone G, Boehm B, Cooper ME, Chai Z, Del Prato S, Ji L, Hopkins D, Herman WH, Khunti K, Mbanya JC, Renard E. New-Onset Diabetes in Covid-19. N Engl J Med 2020; 383(8):789-790. *Doi: 10.1056/NEJMc2018688.*
5. Sathish T, Kapoor N, Cao Y, Tapp RJ, Zimmet P. Proportion of newly diagnosed diabetes in COVID-19 patients: A systematic review and meta-analysis. Diabetes Obes Metab 2021; 23(3):870-874. *Doi: 10.1111/dom.14269.*
6. Beyerstedt S, Casaro EB, Rangel ÉB. COVID-19: angiotensin-converting enzyme 2 (ACE2) expression and tissue susceptibility to SARS-CoV-2 infection. Eur J Clin Microbiol Infect Dis 2021; 40(5):905-919. *Doi: 10.1007/s10096-020-04138-6.*
7. Molina DI, Muñoz TM, Guevara K. Inhibidores de la enzima convertidora de angiotensina y bloqueadores de los receptores de angiotensina II: ¿aumentan el riesgo de padecer COVID-19? Rev Colom Cardiol 2020: 27(3): 132-136. *https://doi.org/10.1016/j.rccar.2020.05.003.*

8. Ata A, Jalilova A, Kırkgöz T, Işıklar H, Demir G, Altınok YA, Özkan B, Zeytinlioğlu A, Darcan Ş, Özen S, Gökşen D. Does COVID-19 predispose patients to type 1 diabetes mellitus? Clin Pediatr Endocrinol 2022; 31(1):33-37. *Doi: 10.1297/cpe.2021-0050.*
9. Suwanwongse K, Shabarek N. Newly diagnosed diabetes mellitus, DKA, and COVID-19: Causality or coincidence? A report of three cases. J Med Virol 2021; 93(2):1150-1153. *Doi: 10.1002/jmv.26339.*
10. Duntas LH, Jonklaas J. COVID-19 and thyroid diseases: A bidirectional impact. J Endocr Soc 2021;5(8):bvab076. *doi: 10.1210/jendso/bvab076.*
11. Spranger J, Kroke A, Möhlig M, Hoffmann K, Bergmann MM, Ristow M, Boeing H, Pfeiffer AF. Inflammatory cytokines and the risk to develop type 2 diabetes: results of the prospective population-based European Prospective Investigation into Cancer and Nutrition (EPIC)-Potsdam Study. Diabetes 2003; 52(3):812-7. *Doi: 10.2337/diabetes.52.3.812.*
12. Bender C, Rajendran S, von Herrath MG. New insights into the role of autoreactive CD8 T cells and cytokines in human Type 1 diabetes. Front Endocrinol (Lausanne) 2021;11:606434. *Doi: 10.3389/fendo.2020.606434.*
13. Katsogiannos P, Kamble PG, Pereira MJ, Sundbom M, Carlsson PO, Eriksson JW, Espes D. Changes in circulating cytokines and adipokines after RYGB in patients with and without Type 2 diabetes. Obesity 2021; 29(3):535-542. *Doi: 10.1002/oby.23093.*
14. Valero Cedeño NJ, Vélez Cuenca MF, Duran Mojica AA, Torres Portillo M. Afrontamiento del COVID-19: estrés, miedo, ansiedad y depresión? Enferm Inv 2020;5(3):63-70. *http://dx.doi.org/10.31243/ei.uta.v5i3.913.2020.*
15. Guarnotta V, Ferrigno R, Martino M, Barbot M, Isidori AM, Scaroni C, Ferrante A, Arnaldi G, Pivonello R, Giordano C. Glucocorticoid excess and COVID-19 disease. Rev Endocr Metab Disord 2021; 22(4):703-714. *Doi: 10.1007/s11154-020-09598-x.*

Invest Clin 63(1): 7 - 18, 2022 https://doi.org/10.54817/IC.v63n1a01

Arracacia xanthorrhiza Bancr compounds decrease β-actin, hypoxia-inducible factor-1 and nitric oxide production in HeLa cells.

Yenddy Carrero[1,2], Jenny Moya[2], Michael Acosta[2] and Jesús Mosquera-Sulbarán[3]

[1]Universidad Técnica de Ambato. Facultad Ciencias de la Salud. Ambato, Ecuador.
[2]Universidad Técnica de Ambato. Facultad de Ciencias de la Salud. Laboratorio de Biología Molecular y Celular. Ambato, Ecuador.
[3]Instituto de Investigaciones Clínicas "Dr. Américo Negrette". Facultad de Medicina, Universidad del Zulia, Maracaibo, Venezuela.

Key words: actin; nitric oxide; HIF-1; *Arracacia xanthorrhiza Bancr*; Hela cells.

Abstract. The treatment of cancer patients with anti-cancer drugs is often accompanied by the presence of undesirable side effects. The use of natural plant derivatives alone, or in conjunction with existing anti-neoplastic drugs, has been suggested to obtain better results and decrease these side effects. Nitric oxide (NO•), the hypoxia-inducible factor-1 (HIF-1), and decreased concentration of actin play important roles in cancer progression. The beneficial effects of polyphenols in various organ disorders including cancer has been reported. The aim of this study was to determine the effect of *Arracacia xanthorrhiza Bancr* extracts, white (WAXB) and red (RAXB) variants (compounds rich in polyphenols) on the concentrations of β-actin, NO• and HIF-1 in Hela cells cultures, to uncover possible anti-neoplastic effects. Extracts from the plant leaves were added to Hela cell cultures at a concentration of 10^{-3} mg/mL, and after 24 hours of culture, the concentrations of β-actin, NO• and HIF-1 were determined by immunohistochemical, biochemical and western blot assays. Both extracts reduced the concentrations of β-actin, NO• and HIF-1 ($p<0.001$), similar to the methotrexate effect. These results suggest an antineoplastic effect of the studied plant extracts and highlight the possibility of their use in the treatment of neoplasms.

Corresponding author. Yenddy Carrero. Universidad Técnica de Ambato. Facultad Ciencias de la Salud. C/ Salvador entre México y Colombia, Ingahurco. Ambato 180150, Ecuador. Tel: + 59 3 33730268 ext. 5239.
E-mail: yenddycarrero@yahoo.es

Los componentes de la *Arracacia xanthorrhiza Bancr* disminuyen las producciones de la actina β, del factor-1 inducible por la hipoxia y del óxido nítrico en células Hela.

Invest Clin 2022; 63 (1): 7 – 18

Palabras clave: actina; óxido nítrico; HIF-1; *Arracacia xanthorrhiza Bancr;* células Hela.

Resumen. El tratamiento de pacientes con cáncer utilizando drogas-antineoplásicas presenta problemas relacionados con efectos colaterales indeseables. Se ha sugerido el uso de derivados de plantas naturales solas, o en combinación con drogas antineoplásicas existentes para obtener mejores resultados y disminuir los efectos colaterales. Así mismo, se ha reportado que el óxido nítrico (NO•), el factor-1 inducible por hipoxia (HIF-1) y la disminución de la expresión de la actina tienen un papel en la progresión del cáncer. También se ha reportado los efectos beneficiosos de lo polifenoles en varios desordenes orgánicos, incluyendo el cáncer. El objetivo de este estudio fue determinar los efectos de los extractos procedentes de la *Arracacia xanthorrhiza Bancr* blanca (AXBB) y la variedad roja (AXBR) (compuestos ricos en polifenoles) en las concentraciones de la actina-beta, el NO• y el HIF-1 en cultivo de células Hela, para destacar sus posibles efectos antineoplásicos. A los cultivos de células Hela se les agregaron los extractos de las hojas de AXBB o AXBR (10^{-3} mg/mL, concentración final) y después de 24 horas de cultivo se determinaron las concentraciones de la actina-beta, el NO• y el HIF-1 por métodos inmunohistoquímicos, bioquímicos y western blot. Ambos extractos disminuyeron las concentraciones de la actina-beta, el NO• y el HIF-1 ($p<0,001$) de una manera similar al efecto del metotrexato. Estos resultados sugieren un efecto antineoplásico de estos extractos y destacan la posibilidad de ser usados para el tratamiento de las neoplasias.

Received: 13-08-2021 Accepted: 03-09-2021

INTRODUCTION

Cellular motility is the basis for cancer cell invasion and metastasis. Migration involves an intricate actin branched network. Regulation of cell migration is necessary for development, wound healing, and immune responses, whereas aberrant and uncontrolled cell motility is a feature in cancer cells [1]. Therefore, compounds capable of inducing degradation of actin, could be important in the production of anti-cancer drugs by decreasing the actin-dependent cell motility. In addition to the alterations of actin, nitric oxide (NO•), a vasodilator, has been shown to have a role in the regulation of cancer progression and metastasis [2]; effects that probably are mediated by angiogenesis, apoptosis and cellular motility [3,4]. In addition, NO• increases the hypoxia-inducible factor-1 (HIF-1), a transcription factor that enhances several hypoxia-inducible genes and induces cancer metastasis [5]. Previous studies have shown

that methotrexate is capable of inducing apoptosis [6], an important cytotoxic mechanism of anti-cancer drugs. It is well known that apoptosis is associated with alterations of the reorganization and concentration of actin [7, 8]. Therefore, drugs that target actin, NO•, and HIF-1may be important in the treatment of cancer. Thus, the aim of this study was determining the effect of two ecovariants of *Arracacia xanthorrhiza Bancr* extracts, white (WAXB) and red (RAXB) variants on the concentrations of β-actin, NO• and HIF-1 in Hela cells cultures (uterine cervix cancer cell line) and compared their effects with the effect of methotrexate, a well-known anti-cancer drug.

MATERIALS AND METHODS

Source of plants

Plants were obtained from the following localities: Red *Arracacia xanthorrhiza Bancr* (RAXB) from the province of Tungurahua, Quinchicoto (Municipality Tisaleo), Ecuador (Latitude: 1° 23' 54" S; Longitude: 78° 24' 41" W; Altitude: 3,260 meters above sea level). White *Arracacia xanthorrhiza Bancr* (WAXB) from El Triunfo (Municipality Baños), Ecuador (Latitude: 1°10' 18" S; Longitude: 78°32' 33" W; Altitude: 1,683 meters above sea level). Plant samples used for this research have been authorized by the Ecuadorian government under the framework of the United Nations Convention on Biodiversity.

Extract procedure

Fresh plant leaves were collected and dried in an oven at 40°C for 24 hours until a constant weight was obtained. The specimens were stored at room temperature in the dark prior to their extraction and subsequent testing. Stock solutions of RAXB and WAXB were prepared by dissolving 60 g of leaves in ethanol (20%) at 80°C for one hour. Ethanol was extracted by a rotary evaporator and active compounds remained in water. Extracts were grinded into a powder (VirTis Bench Top, SP Scientific, NY, USA), and then dissolved in PBS and filtered (0.22 μm). Filtered stock solutions (0.411 mg/mL) were stored at -80°C until use. Total phenolic content (TPC) and antioxidant activity (AA) assays in microplates were determined. An intra-laboratory validation was performed [9] of the Folin-Ciocalteu microplate method to measure TPC and the 2,2-diphenyl-1-picrylhydrazyl (DPPH) microplate method to measure AA.

Cell culture

The human cervical cell line (HeLa) was obtained from the American Type Culture Collection (CCL-2). Cells were maintained in DMEM media, supplemented with 10% fetal bovine serum, 100 U/mL penicillin, and 100U/mL streptomycin. The cells were then incubated at 37°C with 5% CO2 saturation. Cells were used in the linear phase of growth with a passage number of 5 to 7.

Viability assay

The cytotoxic effect of WAXB and RAXB on HeLa cells was evaluated by MTT assay according to the manufacturer's instructions (Thermo Fisher, MA, USA). The cells were seeded at $1x10^4$ cells per well in a 96-well plate and incubated at 37°C for 24 h. Cells were treated with increasing doses of WAXB or RAXB by 2-fold dilution, starting with 10^{-1}mg/mL until 10^{-11}mg/mL. Cells were treated for 24h. The MTT assay results were obtained using a spectrophotometer plate reader (Victor X3; Perkin Elmer, USA) at 570 nm. Half maximal inhibitory concentration (IC50: 10^{-3} mg/mL) was obtained by no lineal regression analysis (Graphpad Prism 7.0 Software Inc., San Diego, CA, USA). All experiments were performed in triplicate to evaluate half-maximal inhibitory concentration for both plant extracts against the HeLa cell line.

Western Blot

Untreated and WAXB or RAXB- treated Hela cell cultures (10^{-3} mg/mL) and metho-

trexate-treated cultures (10 μM), were lysed with RIPA buffer for 30 min on ice. Then, cells were centrifuged at 1200 rpm for 15 min at 4°C, and the supernatant was collected. The protein concentration was measured by the Bradford protein assay. Similar amount of protein from each sample was separated by SDS-PAGE and transferred onto PVDF membranes. The membranes were blocked with 7% skimmed milk for 2 h at room temperature and incubated overnight at 4°C with a primary anti- β actin antibody (Santa Cruz Biotechnology Inc, Texas, USA). After washing three times with TBST(10 mM Tris-HCL, pH 7.4, 150 mM NaCl, 0.05% Tween 20), the membranes were incubated with the appropriate horseradish peroxidase-conjugated secondary antibody (1:5000 dilution: Santa Cruz Biotechnology Inc, Texas, USA). Experiments were performed in triplicate and at least three independent experiments were done. Controls represent untreated HeLa cultures.

β-actin determination

HeLa cells were seeded on coverslips at $5x10^5$ cells per well. After 48 h of culture, cells were treated with WAXB, RAXB (10^{-3} mg/mL) or methotrexate (10 μM) for additional 24 h. Cells were fixed and permeabilized by a paraformaldehyde solution (4%, 15 min) and cold acetone (15 min), respectively. Then, cells were reacted with a monoclonal antibody against β-actin (β-Actin (C4): sc-47778 conjugated Alexa Fluor®647; Santa Cruz Biotechnology Inc, Texas, USA) for 30 min at 37°C. Thereafter, cells on coverslips were analyzed through a fluorescence microscopy (Leica-DMi8, Wetzlar, Germany). Experiments were performed in triplicate and at least three independent experiments were done. DAPI staining was used to identify nuclei. Results were expressed as fluorescence intensity units (502/530 nm) per x 630 field. Controls represent untreated HeLa cultures.

Nitric oxide determination

Nitric oxide was determined by detection of nitrite formed by the spontaneous oxidation of NO• using a Griess Reagent Kit (G-7921: Molecular Probe Inc. Eugene, USA) following the manufacture's indications. Results are expressed as μM per mg of protein.

Hypoxia-inducible factor-1 determination

HIF-1 was determined in WAXB, RAXB (10^{-3} mg/mL) treated Hela cell cultures using Image-iT™ Hypoxia Reagents (Invitrogen, Termo Fisher Scientific, Eugene, USA) following the manufacture's indications. Cells on coverslips were analyzed through a fluorescence microscopy (Leica-DMi8, Wetzlar, Germany). Experiments were performed in triplicate and at least three independent experiments were done. DAPI staining was used to identify nuclei. Results were expressed as fluorescence intensity units (502/530 nm) per x 630 field. Controls represent untreated HeLa cultures.

Statistical analysis

Experiments were in triplicate and performed at least three times. Results were expressed as the means ± standard deviation. Statistical analysis was performed using one way ANOVA and Bonferroni´s posttest using Graph Pad Prism software (version 7.0; Graph Pad Software Inc., San Diego, CA, USA). Statistical significance is expressed as $p<0.05$.

RESULTS

The antioxidant activity of WAXB and RAXB and their phenolic content are observed in Table 1. The cytotoxicity of both extract plants was determined by the MTT assay. The MTT assay indicated that both WAXB and RAXB have a half maximal inhibitory concentration (IC50) of 10^{-3} mg/mL (Fig. 1). Western blot analysis showed decreased thickness and intensity of the actin

Table 1
Phenolic content and antioxidant activity of *Arracacia xanthorrhiza Bancr* (white carrot and red carrot) extracts.

	WABX	RABX
Phenolic content (mg Eq AG/g powder)	78.6 ± 0.002	59.7 ± 0.001
Antioxidant activity		
(μg Eq Trolox/g powder)	0.595 ± 0.03	0.395 ± 0.02
(μmol Eq Trolox/100g powder)	237.7 ± 0.03	157.8 ± 0.02

WABX: White *Arracacia xanthorrhiza Bancr*; RAXB: Red *Arracacia xanthorrhiza Bancr.*

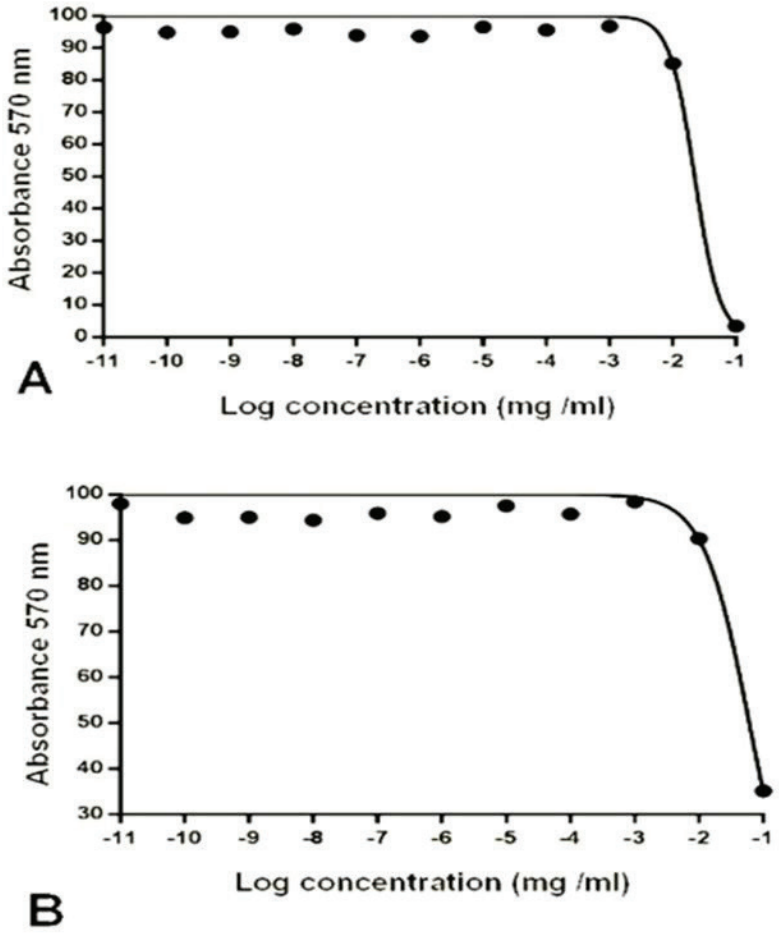

Fig. 1. Viability assay in Hela cell cultures. White (WABX) and red (RABX) *Arracacia xanthorrhiza Bancr* leaves cytotoxic effect on HeLa cells was evaluated by MTT assay. Cells were seeded at $1x10^4$ per well and treated with increased doses of WAXB (A) and RAXB (B) from 10^{-11}mg/mL to 10^{-1}mg/mL. Experiments were performed in triplicate to evaluate half-maximal inhibitory concentration (IC50: 10^{-3} mg/mL) for plant extracts.

bands in cultures treated with WAXB, RAXB or methotrexate compared with untreated cultures (Fig, 2). A similar anti-actin effect of plant extracts and methotrexate were observed. This finding was associated to decreased anti-β-actin antibody reactivity on Hela cells, as shown by immunofluorescence analysis (Fig. 3). WAXB, RAXB and methotrexate were capable of decreasing the nitrite (NO•) content in Hela cell cultures. Methotrexate had a higher NO• reducing effect when compared to plant extracts (Fig. 4). Hela cell cultures treated with WAXB, RAXB under culture conditions of 5% of CO_2, showed decreased expression of HIF-1in treated cultures compared to controls (Fig. 5).

DISCUSSION

Malignant cancer cells can invade surrounding tissues, progress to intravasation and, ultimately, to metastasize. Cellular membrane protrusion is related to local polymerization of actin filaments, and the molecules that link migratory signals to the actin cytoskeleton are upregulated in invasive and metastatic cancer cells [1]. Therefore, cellular actin cytoskeleton is very important for cancer cell migration during the formation of metastases [10]. Since modifications of the actin cytoskeleton are characteristic features of invasive tumor cells, it is likely that drugs inducing interactions of cytoskeletal proteins, can be useful to induce apoptosis

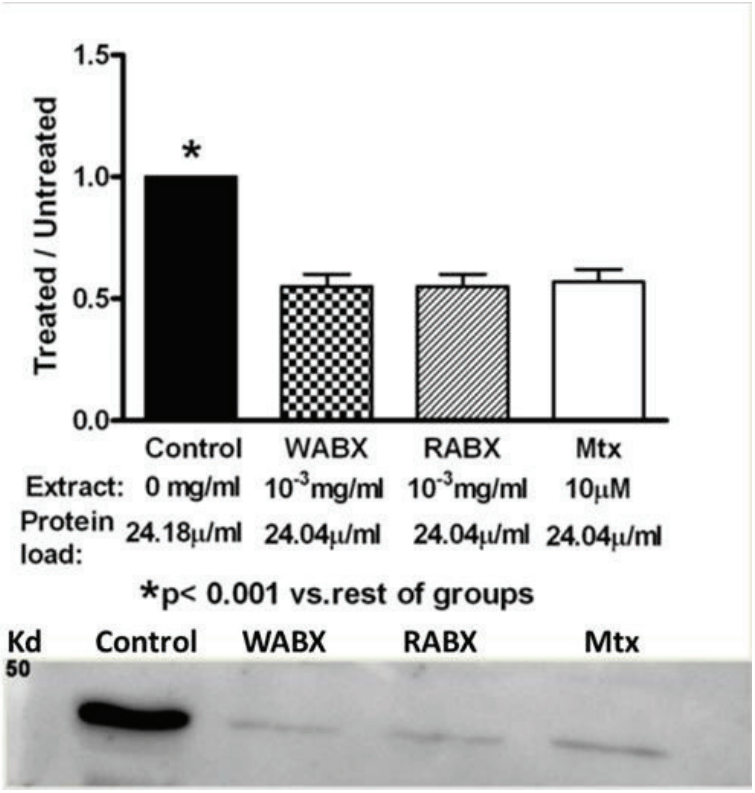

Fig. 2. β-actin expression in HeLa cell cultures treated with *Arracacia xanthorrhiza Bancr* extracts (10^{-3} mg/mL). In up panel: Decreased expression of β-actin was observed in plant extract treated cultures compared with untreated cultures. Similar effects of White *Arracacia xanthorrhiza Bancr* (WABX), Red *Arracacia xanthorrhiza Bancr* (RAXB) and methotrexate (Mtx: 10 μM) were observed. Low panel: Western blot analysis of β-actin in the same conditions observed in the upper panel. One way ANOVA with Bonferroni´s post-test.

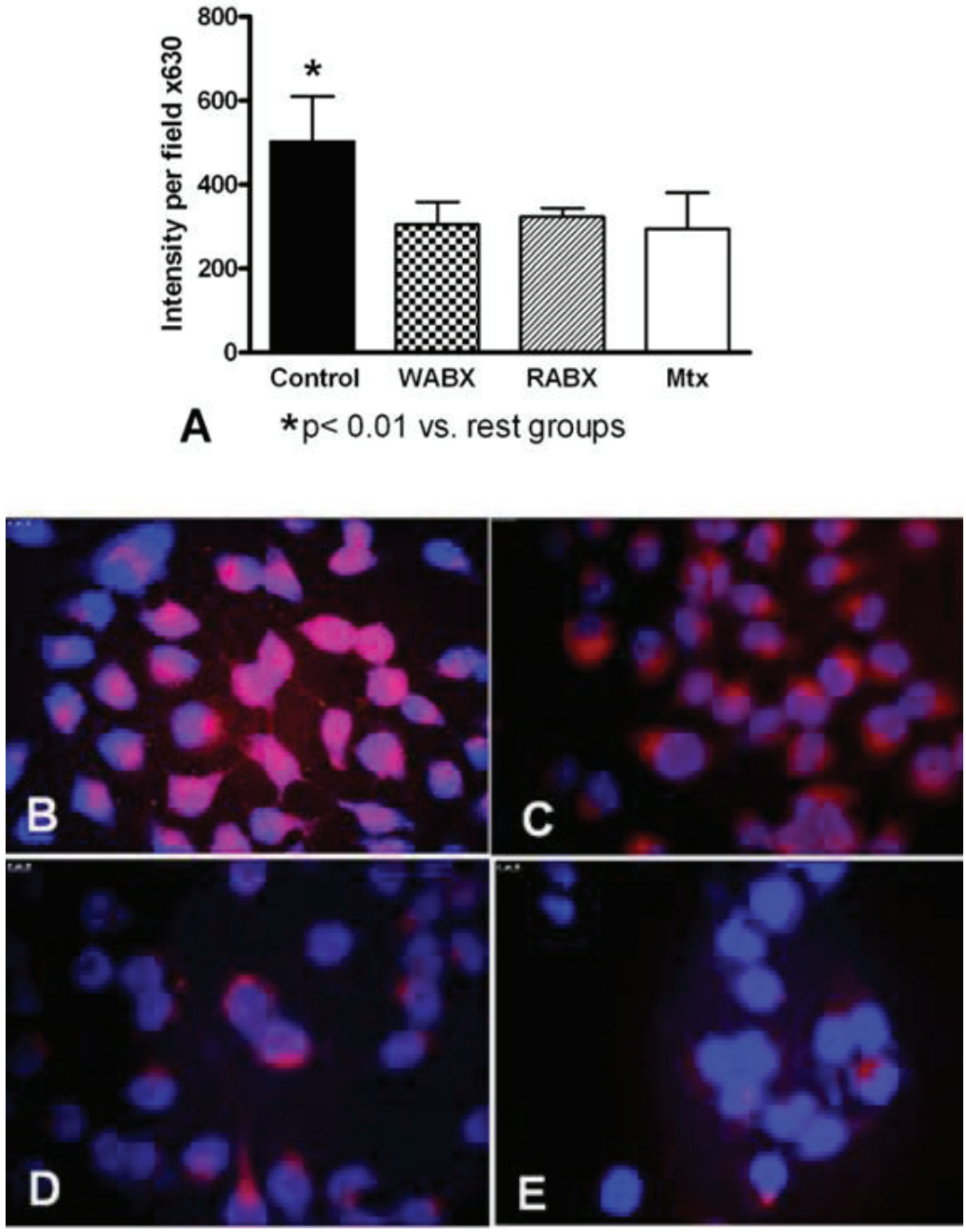

Fig. 3. β-actin expression in HeLa cell cultures treated with *Arracacia xanthorrhiza Bancr* extract. A) Decreased fluorescence intensity units were observed in White *Arracacia xanthorrhiza Bancr* (WABX), Red *Arracacia xanthorrhiza Bancr* (RAXB) (10^{-3} mg/mL) and methotrexate (Mtx: 10 μM) treated cultures compared with control without treatment. Low panel: β-actin positive cells in HeLa cell cultures. B) Control (untreated). C) WABX. D) RAXB. E) Methotrexate (10 μM). Monoclonal antibody against β-actin (β-Actin (C4): sc-47778 conjugated Alexa Fluor®647. One way ANOVA with Bonferroni´s post-test. Magnification X1000.

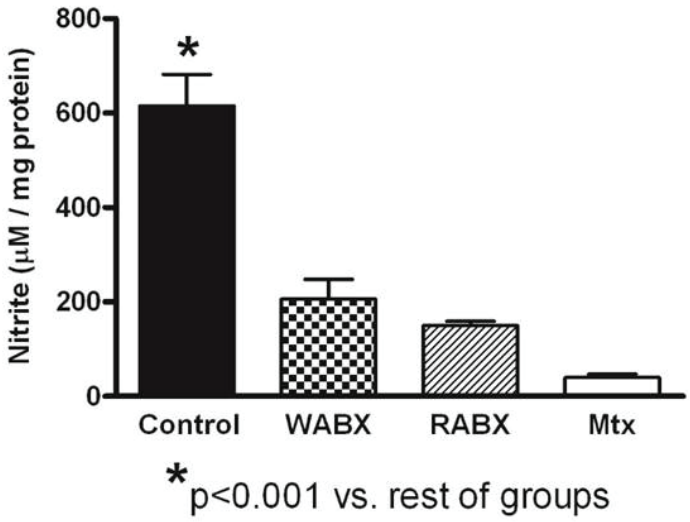

Fig. 4. Nitrite (NO•) production by HeLa cell cultures treated with *Arracacia xanthorrhiza Bancr* extracts. Decreased nitrite production was observed in White *Arracacia xanthorrhiza Bancr* (WABX), Red *Arracacia xanthorrhiza Bancr* (RAXB) (10^{-3} mg/mL) and methotrexate (Mtx: 10 μM) treated cultures compared with control (untreated). Methotrexate had higher reducer NO• effect compared to plant extracts. Griess Reagent Kit (G-7921: Molecular Probe Inc. Eugene, USA). One way ANOVA with Bonferroni´s post-test.

or inhibit cancer cell metastasis. In this regard, increased attention has been observed for drugs capable of modifying the state of actin (polymerization, microfilament organization) [11].

In this study, extracts from WAXB and RAXB could induce decreased expression of B-actin on Hela cells. The effects of WAXB and RAXB were like that observed using methotrexate. Methotrexate is an anti-folate used in the treatment of cancers and autoimmune diseases [12]. In previous a communication it has been reported that methotrexate is an actin affecting drug, acting mainly on its polymerized form [13]. In this study, all studied extracts and drug decreased the reactivity to an anti- β-actin antibody in Hela cells, suggesting an actin molecular alteration. We could not observe alterations in the actin cytoskeleton organization; however, some similar effects related to actin reorganization between methotrexate and extracts were observed. Methotrexate can induce alterations of the actin cytoskeleton in uterine cervix cancer cell line (CaSki) [6] as observed in Hela cells (uterine cervix cancer cell line) using extracts and methotrexate. Apoptosis is the major cytotoxic mechanism of anticancer therapies [8], and it is known that morphology alterations during apoptosis [7] correlate with the reorganization of the actin microfilaments and concentration of actin; in this study both, AXB extracts and methotrexate are capable of decreasing the actin concentration. These data suggest that the anticancer effects of WAXB and RAXB are like those observed in methotrexate. WAXB and RAXB actin degradation mechanisms remain unknown. Previous reports have shown that actin initiates apoptosis and that the final degradation of actin filaments enhances the apoptosis signaling [14]. A decreased actin band was observed in western blot analysis, suggesting degradation of actin molecule. Since plant extracts and methotrexate are capable of inducing apoptosis, activation of proteases during the apoptotic process may act on actin leading to its degradation. In

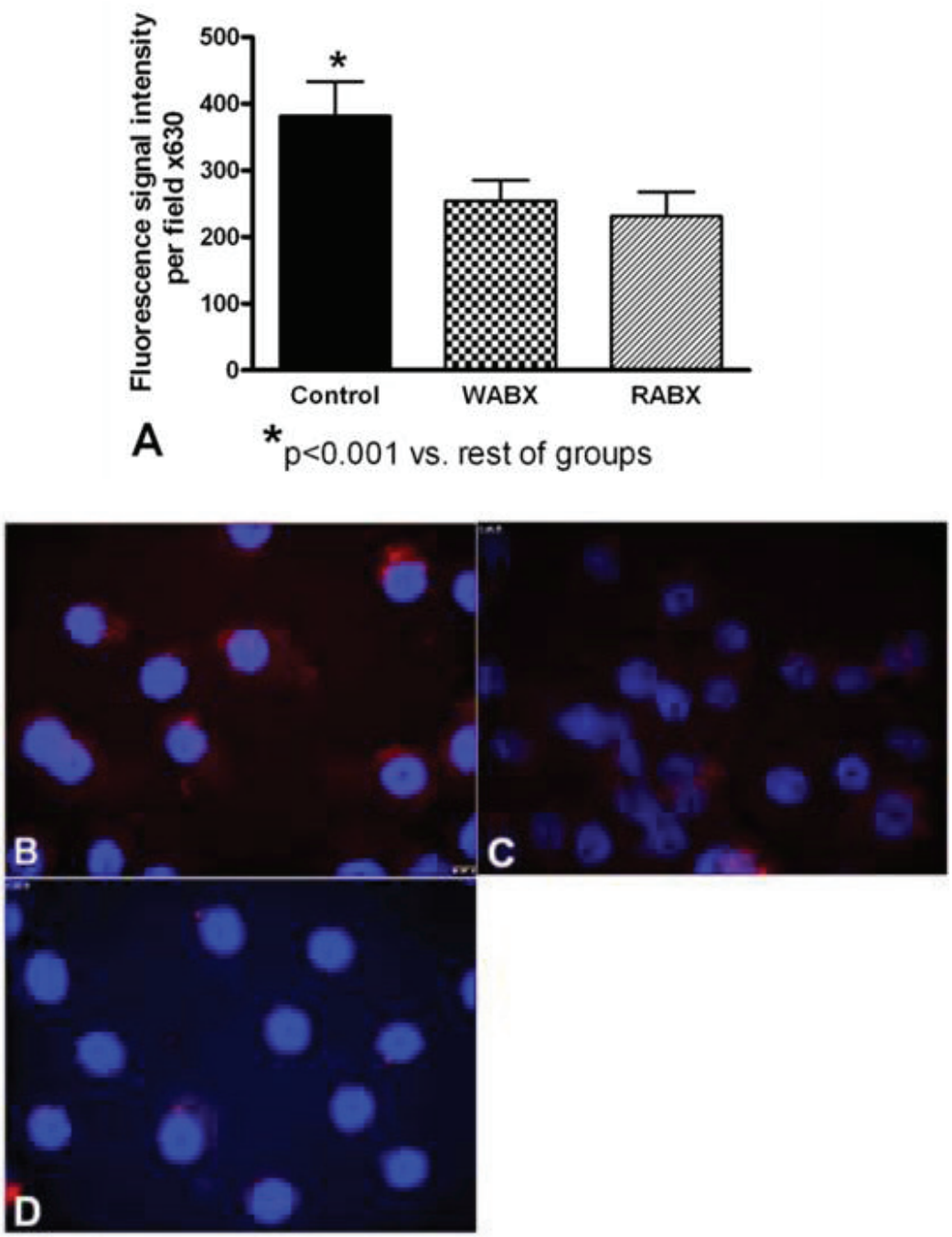

Fig. 5. Hypoxia-inducible factor-1expression (HIF-1)in HeLa cell cultures treated with *Arracacia xanthorrhiza Bancr* extracts. A) Decreased fluorescence intensity units were observed in White *Arracacia xanthorrhiza Bancr* (WABX) and Red *Arracacia xanthorrhiza Bancr* (RAXB) (10^{-3} mg/mL) treated cultures compared with control (untreated). Low panel: HIF-1positive cells in HeLa cell cultures. B) Control. C) WABX. D) RAXB. Image-iT™ Hypoxia Reagents (Invitrogen, Termo Fisher Scientific, Eugene, USA). One way ANOVA with Bonferroni´s post-test. Magnification X1000.

this regard, interleukin-1b-converting enzyme (ICE)-like family of proteases such as Nedd2 / Ich-1, CPP32 / Apopain / Yama, TX / ICE_{rel}II, TY / ICE_{rel}III, Mch 2, Mch 3 / ICE-LAP3, Mch 4, and FLICE are implicated in actin degradation during apoptosis [15].

Nitric oxide has been involved in the cancer biology probably by induction of angiogenesis, apoptosis, increased HIF-1 and alterations of cellular motility [3-5]. Some of these effects can induces cancer metastasis, spread and growth of tumor cells through angiogenesis and high production of HIF-1; however, other effects such as apoptosis and alterations of actin may impede or eliminate metastatic progression [2]. Angiogenesis is the growth of new blood vessels and is essential for tumor progression and metastasis [16]. It has been reported that increased activity of isoform enzyme iNOS (inducible nitric oxide synthase) facilitates tumor cell angiogenesis and metastasis [3], probably mediated by interleukin-33 [17].

HIF-1 is a transcription factor that regulates hundreds of genes, and it is activated by hypoxia (reduced oxygen availability) [18]. HIF-1 is stabilized by hypoxia-dependent or independent pathways and associated with pro-carcinogenic effects [19]. Stabilization of HIF-1 leads to changes in glycolysis, nutrient uptake, angiogenesis, cell migration and apoptosis promoting survival of tumor and metastasis [20, 21]. However, HIF can be activated by non-hypoxic pathways. In this regard, NO• can induce this transcription factor that enhances many hypoxia-inducible genes, via the PI3k/Akt pathway [5].

Previous studies have shown that plant extracts and polyphenolic compounds may have a beneficial role in several diseases including cancer [22-26]. Mechanisms related to the regulation of immune system, inactivation of arachidonic acids pathways, inactivation of NF-κB (nuclear factor kappa-light-chain-enhancer of activated B cells), suppression of toll-like receptor and antioxidant activity [27] may be involved. Biochemical analysis of WAXB and RAXB shows that both are phenolic compounds and the effects previously reported for phenolic compounds probably are implicated in ours results. In this regard, WAXB and RAXB have antioxidant activity as shown by the Trolox assay. In addition, these plant extracts induced a decreased content of NO•, suggesting that these extract plants can act on nitrogen reactive species and may represent one of their anti-cancer mechanisms.

In conclusion, in this study Hela cells were capable of producing NO• and HIF-1, compounds that are related to cancer progression. WABX and RABX extracts induced decreased expressions of NO• and HIF-1 and actin-β in treated cultures. These effects associated with anti-cancer progression were similar to the effect of methotrexate, a well-known anti-cancer drug. As an important point, not included in this study, it is necessary to determine the effect of WAXB and RWABX on other types of cancer to determine if these plant extracts have a general effect on cancer. Further investigation should explore the clinical benefits of WAXB and RWABX (dietary or alcoholic extract) in human cancer.

ACKNOWLEDGMENTS AND FUNDING

The authors express their gratitude to the Dirección de Investigación de la Universidad Técnica de Ambato (DIDE) for funding the Project ESTUDIO ETNOBOTÁNICO Y BIOENSAYOS DE PLANTAS MEDICINALES RELACIONADAS CON EL TRATAMIENTO DE CÁNCER DE CÉRVIX EN LA CIUDAD DE AMBATO, PROVINCIA DE TUNGURAHUA, ECUADOR, with resolution 0904-CU-P-2018.

Declaration of conflict of interest

The manuscript has no conflict of interest.

Authors' ORCID numbers

- Yenddy Carrero (YC) 0000-0003-4050-4468
- Jenny Moya (JM) 0000-0002-9846-0122
- Michael Acosta (MA) 0000-0001-9437-828X
- Jesús Mosquera-Sulbaran (JM-S) 0000-0002-1496-5511

Authors' Contribution

- Conception and design of the work YC/JM/JM-S
- Experimental work YC/JM/MA
- Data Collection/obtaining results YC/JM/MA
- Data analysis and interpretation YC/JM/MA/JM-S
- Drafting the article. YC/JM-S
- Critical revision of the article YC/JM-S
- Final approval of the version to be published. YC/JM/MA/JM-S.

REFERENCES

1. **Olson MF, Sahai E.** The actin cytoskeleton in cancer cell motility. Clin Exp Metast 2009; 26: 273–287.
2. **Cheng H, Wang L, Mollica M, Re AT, Wu S, Zuo L.** Nitric oxide in cancer metastasis. Cancer Lett 2014; 353: 1–7.
3. **Sun MH, Han XC, Jia MK, Jiang WD, Wang M, Zhang H, Han G, Jiang Y.** Expressions of inducible nitric oxide synthase and matrix metalloproteinase-9 and their effects on angiogenesis and progression of hepatocellular carcinoma. World J Gastroenterol 2005; 11: 5931–5937.
4. **Xie K, Huang S.** Contribution of nitric oxide-mediated apoptosis to cancer metastasis inefficiency. Free Rad Biol Med 2003; 34: 969–986.
5. **Sandau KB, Zhou J, Kietzmann T, Brune B.** Regulation of the hypoxia-inducible factor 1alpha by the inflammatory mediators nitric oxide and tumor necrosis factor-alpha in contrast to desferroxamine and phenylarsine oxide. J Biol Chem 2001; 276: 39805–39811.
6. **Mazur AJ, Nowak D, Mannherz HG, Malicka-Błaszkiewicz M.** Methotrexate induces apoptosis in CaSki and NRK cells and influences the organization of their actin cytoskeleton. Eur J Pharmacol 2009; 613: 24–33.
7. **Mills JC, Sone NL, Pittman RN.** Extranuclear apoptosis: the role of the cytoplasm in the execution phase. J Cell Biol 1999; 146: 703–707.
8. **Holdenrieder S, Stiebe P**. Apoptotic markers in cancer. Clin Biochem 2004; 37: 605–617.
9. **Bobo-García G, Davidov-Pardo G, Arroqui C, Vírseda P, Marín-Arroyo MR, Navarro M.** Intra-laboratory validation of microplate methods for total phenolic content and antioxidant activity on polyphenolic extracts, and comparison with conventional spectrophotometric methods. J Sci Food Agric 2015; 95: 204-209.
10. **Bhattacharya A, Kumar J, Hermanson K, Sun Y, Qureshi H, Perley D, Scheidegger A, Singh BB, Dhasarathy A.** The calcium channel proteins ORAI3 and STIM1 mediate TGF-β induced Snai1 expression. Oncotarget 2018; 9: 29468-29483.
11. **Rao J, Li N.** Microfilament actin remodelling as a potential target for cancer drug development. Curr Cancer Drug Targets 2004; 4: 267–283.
12. **Walling J.** From methotrexate to pemetrexed and beyond. A review of pharmacodynamic and clinical properties of antifolates. Invest New Drugs 2006; 24: 37–77.
13. **Otrocka M, Verschueren H, Malicka-Błaszkiewicz M.** The effect of methotrexate on actin and invasiveness of hepatoma Morris 5123 cells in culture. Acta Biochim Polonica 2001; 48: 1051–1060.
14. **Desouza M, Gunning PW, Stehn JR.** The actin cytoskeleton as a sensor and mediator of apoptosis. Bioarchitecture 2012; 2: 75–87.
15. **Song Q, Wei T, Lees-Miller S, Alnemri E, Watters D, Lavin M F.** Resistance of ac-

tin to cleavage during apoptosis. Proc Natl Acad Sci, USA 1997; 94: 157–162.

16. **Folkman J.** Role of angiogenesis in tumor growth and metastasis. Sem Oncol 2002; 29:15–18.
17. **Choi YS, Cho HJ, Min JK, Pyun BJ, Maeng YS, Park H, Kim J, KimYM, Kwon YG.** Interleukin-33 induces angiogenesis and vascular permeability through ST2/TRAF6-mediated endothelial nitric oxide production. Blood 2009; 114: 3117–3126.
18. **Jun JC, Rathore A, Younas H, Gilkes D, Polotskyn VY.** Hypoxia-inducible factors and cancer. Curr Sleep Med Rep 2017; 3: 1–10.
19. **Zheng SS, Chen XH, Yin X, Zhang BH.** Prognostic significance of HIF-1alpha expression in hepatocellular carcinoma: a meta-analysis. PloS One 2013; 8: e65753.
20. **Parks SK, Cormerais Y, Marchiq I, Pouyssegur J.** Hypoxia optimizes tumor growth by controlling nutrient import and acidic metabolite export. Mol Aspects Med 2016; 47–48: 3–14.
21. **Luo D, Wang Z, Wu J, Jiang C, Wu J.** The role of hypoxia inducible factor-1 in hepatocellular carcinoma. BioMed Res Int 2014; 2014: 409272.
22. **Andriantsitohaina R, Auger C, Chataigneau T, Étienne-Selloum N, Li H, Martínez M C, Schini-Kerth VB, Laher I.** Molecular mechanisms of the cardiovascular protective effects of polyphenols. British J Nutr 2012; 108: 1532-1549.
23. **Eberhardt MV, Lee CY, Liu RH.** Antioxidant activity of fresh apples. Nature 2000; 405: 903–904.
24. **Recio M, Andujar I, Rios J.** Anti-inflammatory agents from plants: progress and potential. Curr Med Chem 2012; 19: 2088–2103.
25. **Spagnuolo C, Russo M, Bilotto S, Tedesco I, Laratta B, Russo GL.** Dietary polyphenols in cancer prevention: the example of the flavonoid quercetin in leukemia. Ann New York Acad Sci USA 2012; 1259: 95–103.
26. **Vauzour D, Rodriguez-Mateos A, Corona G, Oruna-Concha MJ, Spencer JE.** Polyphenols and human health: Prevention of disease and mechanisms of action. Nutrients 2010; 2: 1106–1131.
27. **Yahfoufi N, Alsadi N, Jambi M, Chantal-Matar C.** The immunomodulatory and anti-Inflammatory. Role of polyphenols. Nutrients 2018; 10: 1618-1641.

Invest Clin 63(1): 19 - 31, 2022 https://doi.org/10.54817/IC.v63n1a02

Clinical related factors to neuroendocrine tumors in Ecuadorian patients: a logistic biplot approach.

Karime Montes Escobar [1,2], José Luis Vicente Villardón[2], Daniel Fabricio Alarcón Cano[3] and Aline Siteneski[4,5]

[1]Departmento de Matemática y Estadística. Instituto de Ciencias Básicas. Universidad Técnica de Manabí, Portoviejo, Ecuador.
[2] Departmento de Estadística. Universidad de Salamanca, Salamanca, España.
[3] Departamento de Docencia e Investigación. SOLCA, Manabí, Ecuador
[4] Instituto de Investigación, Universidad Técnica de Manabí, Portoviejo, Ecuador.
[5] Facultad de Ciencias de la Salud, Carrera de Medicina. Universidad Técnica de Manabí, Portoviejo, Ecuador.

Key words: neuroendocrine tumors; cancer symptoms; statistical method; logistic biplot.

Abstract. Neuroendocrine tumors (NETs) are relative rare, affecting neuroendocrine cells throughout the body. Most tumors are diagnosed at advanced stages. NETs prevalence has increased in the last years but there is little data available in developing countries. The aim of this study was to describe symptoms associated with NETs in patients of the Society for the Fight Against Cancer (SOLCA) in Ecuador from 2005 to 2020; using logistic biplots, in a hospital database, generating binary responses (presence/absence) relevant to this study. The results showed that the mean age was 59 and the study showed no difference in prevalence between genders. NETs were mainly found in lungs (19%), followed by stomach (18%) and skin (9%). Most patients had pathological diagnosis G2 and G3 (30% and 70%, respectively). Symptoms as cough, dyspnea, weight loss, diarrhea, constipation, abdominal pain, dyspepsia, hypertensive crisis, distended abdomen and intestinal obstruction had p values <0.05. Additionally, the statistical analysis showed that cough and intestinal obstruction were also common, bearing in mind that patients had most frequent NETs in the lungs and skin. In summary, our results indicate that symptoms of NETs patients were positively associated with lung and skin. Further investigation is needed focusing on the type of NETs and their symptoms in order to establish an early marker for diagnosis.

Corresponding author. Aline Siteneski. Instituto de Investigación y Facultad de Ciencias de la Salud, Carrera de Medicina. Universidad Técnica de Manabí, Portoviejo, Ecuador. Phone: (593) 99129 2040 .
E-mail address: aline.siteneski@gmail.com

Factores clínicos asociados a tumores neuroendocrinos en pacientes ecuatorianos: un análisis biplot logístico.

Invest Clin 2022; 63 (1): 19 – 31

Palabras clave: tumores neuroendocrinos; síntomas de cáncer; método estadístico; biplot logístico.

Resumen. Los tumores neuroendocrinos (TNE) son relativamente raros y afectan a las células neuroendocrinas de todo el cuerpo. La mayoría de los tumores se diagnostican en etapas avanzadas. La prevalencia de los TNE ha aumentado en los últimos años, pero hay pocos datos en los países en desarrollo. El objetivo de este estudio fue determinar los síntomas asociados a los TNE en pacientes de la Sociedad de Lucha contra el Cáncer (SOLCA) en Ecuador entre 2005 y 2020, utilizando biplots logísticos en una base de datos hospitalaria, generando respuestas binarias (presencia / ausencia) relevantes para este estudio. Los resultados mostraron que la edad promedio era de 59 años y el estudio no encontró diferencias en la prevalencia entre géneros. Los TNE se encontraron con mayor frecuencia en los pulmones (19%), seguidos del estómago (18%) y piel (9%). La mayoría de los pacientes tenían diagnóstico patológico G2 y G3 (30% y 70% respectivamente). Los síntomas como tos, disnea, pérdida de peso, diarrea, estreñimiento, dolor abdominal, dispepsia, crisis hipertensiva, abdomen distendido y obstrucción intestinal tuvieron valores de $p < 0,05$. Además, el análisis estadístico mostró que la tos y la obstrucción intestinal también eran comunes, teniendo en cuenta que los pacientes tenían TNE más frecuentes en los pulmones y la piel. En resumen, nuestros resultados indican que los síntomas de los pacientes con TNE se asociaron positivamente con los pulmones y la piel. Se necesitan más investigaciones que se centren en el tipo de TNE y sus síntomas a fin de establecer un marcador más temprano para el diagnóstico.

Received: 13-08-2021 Accepted: 03-09-2021

INTRODUCTION

Neuroendocrine tumors (NETs) are a group of malignant tumors appearing from neuroendocrine cells throughout the body that are defined as epithelial neoplasms with predominantly neuroendocrine differentiation [1]. NETs are commonly located in the pancreas, digestive tract, and the lungs although they can appear in any organ [2]. NETs grading is probably the most useful instrument for providing prognostic information for clinicians [3]. Currently, the classification recognizes that neuroendocrine cancer at any anatomical site is either well-differentiated defined as NETs, and poorly differentiated defined as neuroendocrine carcinoma [3]. Severity may be evaluated by grading the tumor between 1 and 3 and per proliferation fraction as measured by mitotic count by the Ki67-positive percentage [4,5]. Approximately one-third of the high-grade group are the most aggressive NETs fraction, predicting either a worst event-free

survival or overall survival compared with grade 2 NETs [6]. Unfortunately, most patients are diagnosed in late stage of NETs [7].

NETs symptoms vary depending on biological aggressiveness and the anatomical location of the tumor [8]. Vague and nonspecific symptoms may cause considerable delay and difficulty in diagnosis [9]. The clinical presentation of NETs is generally related to the secretion of hormones that may indicate carcinoid syndrome or hormonal symptoms [10]. Carcinoid syndrome commonly cause diarrhea, flushing, fatigue [9], abdominal pain and intermitted bowel obstruction [11]. It is worth mentioning that the number of bowel movements and flushing episodes significantly affect the quality of life of NETs patients [10]. The intensity of these symptoms can vary widely, depending primarily on the site of disease and grade of tumor. More studies are necessary for clinicians to become familiar with the natural history and patterns of disease progression, which are characteristic of NETs [7]. Therefore, the precocious diagnosis of tumor may increase survival and improve NETs patient's quality of life.

In Ecuador, the Cancer Fighting Society (SOLCA) Quito Nucleus and National Tumor Registry exists since 1984 (Minist Salud Pública) and cares for approximately 31% of the oncological cases of the country [12]. In Ecuador, the clinical management of NETs is significantly lower, compared to that of the United States and Europe and there are few specialized centers managing a multidisciplinary environment [13]. Despite the high prevalence and severity of NETs, this tumor has not been previously studied in people from Ecuador to the best of our knowledge. Consequently, the aim of this research was to investigate the presence of NETs patients in the hospital database over fifteen years. Based on the above, a logistic biplot is proposed as an alternative to identify the most frequent symptoms in patients with NET using binary variables (presence / absence) with binomial distribution [14]. This analysis allows us to obtain a graphic representation of the NETs types and the main associated symptoms. In this sense, the approach that provides a better interpretation to relate the type of tumor with its symptoms, taking into account the comparison with the classic classification / ordering techniques, is provided by the biplot methods [15, 16], where a simultaneous graph represents the columns (variables) and the rows (individuals) of the given data matrix.

MATERIAL AND METHODS

Collected database

The study was done using the hospital database of SOLCA Portoviejo, in the Province of Manabí, Ecuador, analyzing patients with NETs diagnosis between 2005 and 2020.

Statistical analysis

The main problem with our data is the very limited number of patients and the high number of variables (symptoms, types of tumor, locations, etc…) that prevents from using standard methods as logistic regression. An exploratory multivariate technique would be more adequate to explore possible patterns before trying to apply a more formal model using a relevant subset of symptoms obtained from it. This kind of techniques have also the advantage of showing the interrelations among all the variables.

For the exploratory analysis of our data, we used a multivariate technique called "logistic biplot" [14] that was specifically designed to treat binary data, as well as more traditional analyses. Although logistic biplots have not been extensively used with medical data, some authors [17] propose these kind of multivariate techniques as a mean to perform an exploratory analysis previous to a more formal analysis. Other authors [18] also propose the technique as an analysis of the residuals of a model, to check for the goodness of fit or the violation of some previous hypothesis about the data.

Because logistic biplots are less known, we include here a brief description. A biplot is a graphical representation of a data

matrix, containing the measures subjects on numerical variables [15], that jointly represents subjects and variables on the same plot. We have patients with different NETs and related symptoms (presence or absence) organized in a binary data matrix (0 for presence, 1 for absence).

The adequate method for binary data is the logistic biplot, originally proposed by Vicente-Villardón *et al* [14] and later extended by Demey *et al* [19] to binary matrices where the number of variables is high compared to the number of individuals. This extension was applied to the investigation of the single nucleotide polymorphisms related to different racial groups of people with data from the HAPMAP project [20]. The method has been applied in different fields as sustainability [21], dermatology [22] and lately it has also been extended to deal with nominal data [23].

Logistic biplots represent individuals as points on a Euclidean map (scattergram) and variables as directions (arrows) on the same map. Patients with similar combinations of symptoms tend to group together while distinct individuals tend to pull apart. The vectors for the variables on the plot are the directions more correlated to the presence of the symptom, so we can infer which symptoms are responsible for the grouping of the patients. To interpret the symptoms associated to the grouping of patients we project the points onto the direction of the vectors - the further (in the direction of the arrow) the point is projected, the higher is the probability of the symptom. The origin of the vector is the point predicting probability 0.5 and the arrow indicates the direction of increasing probabilities.

Angles among vectors can help with the identification of the relationships among the symptoms: small acute angles mean strong positive relations; plane angles (Formed by two right angles 180°), negative relations; and straight angles (formed by two perpendicular lines 90°), are not related. The position of the vectors can also help identifying the main gradients (or latent traits) summarizing the variation of the symptoms and its relation to the different locations of the cancer. It is called logistic biplot because the relation of the symptoms and the traits (dimensions) is logistic, it is like a Principal Component Analysis (or biplot) for binary data in which the relation to the components is logistic rather than linear. When data are binary, like those obtained in the analysis of neuroendocrine tumors, Classical Linear Biplots and Principal Components Analysis (PCA) are not suitable because the response along the dimensions is linear. This is the same reason why linear regression is not appropriate for binary or categorical data [14, 21].

The MULTBIPLOT [24] and MultBiplotR[25] packages were used to perform the calculations and obtain the graphical representations. For this study, we first performed a Principal Coordinates Analysis (Classical Multidimensional Scaling), with the simple matching coefficient, and then fitting separated logistic regressions to represent the directions on the Euclidean map [19]. The interpretation of the relevance of the symptoms to classify the patients was evaluated by traditional indicators for logistic regressions as Wald tests, pseudo R-squared coefficients or percentages of accurate classification.

RESULTS

Population characteristics and NETs symptoms

A total of 94 adult patients (aged 19 to 95 years-old) were diagnosed with NETs between 2005 and 2020 and included in our research. The most frequent primary location was the lungs (19%), followed by stomach (18%), rectum (8%) and skin (8%). Unknown primary location represents 8% of the tumors studied. The set symptoms present in our patients with different types of NETs are shown in Table 1.

Table 2 represent sociodemographic characteristic, mortality, primary site and histologic grade of NETs patients. The mean age in this study was 59 years-old and the prevalence was higher in men (57% versus

Table 1
Represent total symptoms found in NETs patients among eleven years in SOLCA, Manabí.

Primary location	Patient	Porcentage
LUNG	18	19%
STOMACH	17	18%
RECTAL	8	9%
SKIN	8	9%
UNKNOWN PRIMARY	8	9%
PANCREAS	5	5%
GANGLIA	4	4%
LIVER	4	4%
DUODENUM	3	3%
APPENDIX	2	2%
CECAL APPENDIX	2	2%
CERVIX	2	2%
COLON	2	2%
RETROPERITONEUM	2	2%
RIGHT COLON	2	2%
COLEDOCO	1	1%
ENDOMETRIC	1	1%
ILEUM	1	1%
LEFT COLON	1	1%
SOFT TISSUES	1	1%
UTERINE NECK	1	1%
VESICAL TUMOR	1	1%
TOTAL	94	100%

43%). The most prevalent stage in NETs patients was G3 (70%) while G1 and G2 represent 30% of the patients.

Logistic Biplot in types of NETs and our symptoms in patients of SOLCA

Fig. 1 shows the result of applying the logistic biplot to the binary matrix of 94 patients and 37 symptoms. Each patient (points) has been labeled using the primary location of its tumor and each symptom (arrow) using the name of the symptom. Only the symptoms significantly related to the patient's configuration were retained on the plot (See Table 3). We observe that most patients having lungs as the primary location are on the top of the plot, while tumors related to the digestive system (rectum, stomach, right colon, ileum and pancreas) are on the bottom part and well separated from the "lung" group, so we can conclude that the analysis has some power to classify the tumors.

Table 2
Represent sociodemographic characteristic, mortality, primary site and histologic grade of NETs patients.

Variable	Parameters	No. Patients (n)	Porcentage
Age	<40	11	12%
	40-54	22	23%
	55-70	30	32%
	> 70	31	33%
Sex	Man	54	57%
	Woman	40	43%
Mortality	Alive	38	40%
	Dead	56	60%
Histologic grade	Type 1 y 2	28	30%
	Type 3	66	70%

When projecting the patients' points onto the directions for the symptoms, we obtain the expected probability that the patient has the symptom. In order to predict the expected presence when the expected probability is higher than 0.5. For each arrow, we only represent the point predicting 0.5 and the direction of increasing probabilities. Thus, we can correctly predict 95.75% of the presences and absences. All the individual symptoms have percentages of correct predictions over 94%. The associated R-squared values are all over 70% and the information of each variable can be accurately interpreted. We can conclude that the representation is a good picture of our data matrix and can be used for exploration.

To search for the symptoms that characterize each group, we can look at the di-

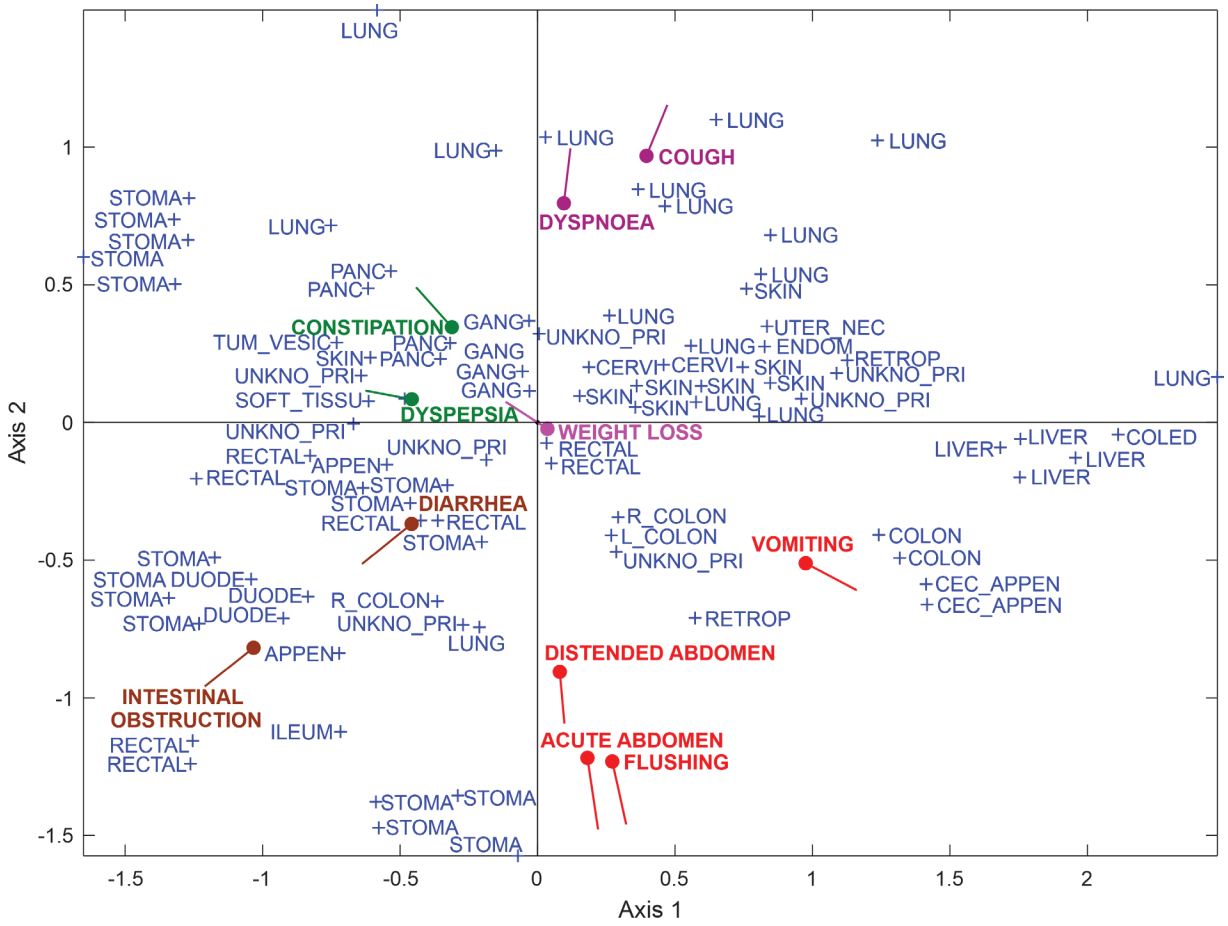

Fig. 1. Biplot representation of the relations among the type of disease and the symptom that determine the groups structure in the simulation. Small acute angles mean strong positive relations; plane angles (Formed by two right angles 180º), negative relations; and straight angles (Formed by two perpendicular lines 90º), are not related. Sign (+) represents each of the individuals. Segments (lines) represent each of the variables (symptoms). Point represents the value of 0.05. Direction of the vector predicts the increase in the probability. The colors: red, brown, green, purple represents group the variables with respect to the individuals.

rection they point. For example, *Dyspnea* and *Cough* are present in patients for which the primary location is *lungs*, while *Diarrhea, Stomach pains, Distended abdomen*, *Hypertensive Crisis* and *Intestinal obstruction* point to the direction of the tumors related to the digestive system. Both sets of symptoms point in opposite direction meaning that they are inversely related, that is, the symptoms present in one group are absent in the other. Together, they define the gradient that separate both types of tumors. *Dyspnea* and *Cough* point to the same direction, meaning that they are highly positively correlated and appear together in some patients. *Weight Loss* has a very good fit but is not clearly characterized in any of the groups. The same is true to *Dyspepsia* and *Constipation*. The three are closely related to the first dimension, but they are less important to separate between groups of tumors.

Table 3
Goodness of adjunct for the main symptoms in NETs patients.

Primary symptom	Deviance	p-value	R2	% Correct
Vomiting	5.326	2,22045E-14	0,9390	100
Dyspepsia	6.467	0	0,8622	91.489
Flushing	4.791	1,78129E-07	0,8474	100
Distended Abdomen	5.922	1,69207E-11	0,8167	97.872
Diarrhea	4.848	0	0,8136	94.681
Weight Loss	6.146	0	0,8129	94.681
Cough	5.591	8,95759E-10	0,7999	97.872
Intestinal Obstruction	4.953	1,40092E-09	0,7847	94.681
Dyspnoea	5.574	6,51029E-11	0,7410	94.681
Acute Abdomen	4.306	1,96949E-07	0,7350	98.936
Constipation	5.730	1,26565E-14	0,7266	92.553

DISCUSSION

Neuroendocrine cells have endocrine and neural properties and are widely distributed in the body [3]. Many organs contain this cell phenotype and may be affected by NETs. The tumor has a particular morphofunctional characteristic, such as the hormones production, and the immunohistochemical features staining pattern with chromogranin, synaptophysin, and neuron-specific enolase [26]. Moreover, the World Health Organization (WHO) advices characterizing NETs by proliferation fraction as measured by either mitotic count or (more easily) by the Ki67-positive percentage (Ki67 index) [6]. It is worth mentioning that, epidemiological studies indicate that the most frequent source of metastasis in NETs are the small intestine, lungs and colon [27]. In the present retrospective databased study, we found lungs and stomach as more frequent NETs followed by rectum, and skin. Here, the diagnosis was through synaptophysin, chromagranin or Ki67 by biopsy, and most patients had several pathological diagnostics. Despite the malignancies of the tumor, to the best of our knowledge, this is the first evidence about NETs in patients from the Ecuadorian coast.

An approach that facilitates the genetic interpretation, compared to the classic techniques of classification/ordination, is provided by the Biplot methods [28, 15, 16], that is, a simultaneous graphical representation of the rows (individuals) and the columns (variables) of a given data matrix. The main uses are exploratory, although it has also been used as a graphical representation for more formal models [29]. The biplot can be fitted by performing alternating regressions and interpolations [30-32]. However, when data are binary, like those obtained in the analysis of molecular information, Classical Linear Biplots and Principal Components Analysis (PCA) are not suitable because the response along the dimensions is linear. This is the same reason why linear regression is not appropriate for binary or categorical data.

There is a significant delay between the symptoms onset and diagnosis of NETs and, consequently, most patients are diagnosed at a late stage of the disease [7]. Our results demonstrated that most patients were diagnosed in histologic grade 3, metastatic or advanced NETs and do not survive. Previous works consider NETs as a low-grade, usually non-functioning, malignant cancer characterized by long survival of pa-

tients with prognosis depending on grade and stage [33]. In fact, WHO in 2017 classified NETs with a Ki67 >20% as either grade 3 NET (well-differentiated) or as grade 3 NEC (poorly differentiated) on the basis of morphological characteristics as necrosis and differentiation [34]. NETs account for about 0.5% of all currently diagnosed malignancies [35]. Given this scenario, our work presents most NETs cases registered in the advanced stage, which could explain, at least in part, the death rates from NETs found in the present data-based study. Furthermore, the retrospective characteristic of the study with a duration of fifteen years should be considered. Indeed, NETs origin and ranking grade can define patient survival if previously reported 103 months from disease originating in the small intestine and only 14 months for cancers originating in the colon [36]. A severity nation-wide multi-center study in Korea reported a high G1 percentage of 92.3% [37]. However, research in Kentucky found a population with 67% in G3 [38]. Reinforcing this notion, our study reports most patients in G3 - 70%. Nevertheless, of special importance is that lower grade NETs do not indicate a better outcome in terms of survival [38].

Given this background, retrospective studies in different populations are important as an alert for the early diagnosis of disease. In the present study, we decided to investigate NETs more frequently and its associated symptoms. Lungs were the most frequently NETs reported in our study and it was associated with the symptoms of cough and dyspnea. In line with our results, previous research as a nation-wide study from the Netherlands and SEER database reported pulmonary NETs as being the most prevalent [36]. The NETs are often misdiagnosed before the cause of the patient's symptoms is finally diagnosed and managed appropriately [9].

Our results demonstrated that after lung and stomach, the most incidence of NETs was in the rectum and skin. We found a significantly positive relationship between the most frequent symptoms and the NETs found during or study. Therefore, symptoms such as diarrhea, constipation, dyspepsia, and intestinal obstruction in addition to weight loss were more prevalent. We should note that our research found that NETs in the stomach and rectum were associated with syndromes such as carcinoid syndrome. It has been previously described that carcinoid syndrome occurs in 8% to 35% of NETs patients [39]. This event appears when vasoactive hormones secreted by metastases (i.e serotonin, histamine, or tachykinins), are no longer metabolized and inactivated by the liver and reach the general circulation [40]. The classic symptom of episodic diarrhea was previously described by more than 70% of patients as consequence of carcinoid syndrome [41]. This data point is similar with what we found in our study. Additionally, it is important to note that the clinical presence of diarrhea and/or abdominal pain can often lead to misdiagnosis, confusing carcinoid syndrome as small bowel obstructions or irritable bowel disease [42]. Unfortunately, there is a delay between the onset of symptoms and the diagnosis of carcinoid tumor; the median time reported range from 2 to 20 years [43]. It is well established that early diagnosis of any type of cancer can improve the quality of life and survival and patients with carcinoid syndrome have a significantly worse quality of life than patients with only NETs [44]. Supporting this fact, our findings underscore the need to further identify all symptoms associated with NETs in an effort to aid physicians to speed up the diagnosis.

Unsurprisingly, the lungs are the most frequently found NET during the fifteen years studied. Importantly, we demonstrated that skin was the fourth most frequently NETs discovered. Based on previous work, NETs in the skin or soft tissue delay late manifestations of disease when represent metastases from other organs [45]. However, notably, according to the World Health Organization

books on skin and soft tissue tumors stated that primary cutaneous and soft tissue NETs are extremely rare, except for Merkel cell carcinoma of the skin [46]. Therefore, only a few case studies of soft tissue NETs are available in the literature [47]. Our findings show that 8% of all cases in the fifteen years studied were skin NET, mostly in elderly men. Supporting this finding, previous studies showed that Merkel cell carcinoma are most commonly found in elderly and in sun-exposed skin [48, 49], patients typically have fair-skin and the median age of diagnosis of 65 years [49]. It is interesting to note that the most common symptom reported in our work is skin damage with unknown or asymptomatic causes. This evidence is corroborated by other studies. Despite the diversity of skin manifestations, the tumor is typically painless and develops as a small, less than 2 centimeters, violaceous papule, plaque, cyst, or infiltrative nodule [50]. The tumor has a multifactorial cause and the exact mechanism by which it acts in the organism it is not fully elucidated, but Merkel cell polyomavirus is thought to be a major contributor to the pathogenesis of this malignancy [51].

Altogether, the results provided suggest that the most frequent clinical symptoms (cough and intestinal obstruction) were positively related to the type of NETs. When looking at the prevalence of NETs, the lungs were the most frequent site, which reinforces the hypothesis of the vulnerability of this organ. Further research is needed and should focus on identifying symptoms of NETs with the objective of early diagnosis. Furthermore, the prevalence of NETs specific in each population must be underscored in future research.

The logistic biplot technique allows the generation of relevant information based on clinical antecedents, as it was for this study on the presence or absence of the disease, taking into account patients with different neuroendocrine tumors.

ACKNOWLEDGMENTS AND FUNDING

This study was supported by the Department of Mathematics and Statistics. Institute of Basic Sciences and Research Institute of the Technical University of Manabí. The authors would like to thank the SOLCA Portoviejo for support and facilitate data and Robin Siteneski for English corrections.

Declaration of competing interest

The authors declare that no financial support or compensation has been received from any individual or corporate entity over the past three years for research or professional service and there is no personal financial holding that could be perceived as constituting a potential conflict of interest.

Authors' ORCID numbers

- Karime Montes Escobar (KME) 0000-0002-9555-0392
- José Luis Vicente Villardon (JLVV) 0000-0003-1416-6813
- Daniel Fabricio Alarcón Cano (DFAC) 0000-0002-9680-1050
- Aline Sitenesky (AS) 0000-0001-6692-7253

Authors' contribution

- Interpretation of data, analysis and writing the manuscript (KME)
- Supervision and writing (JLVV)
- Data collected (DFAC)
- Writing the manuscript and prepared the final draft (AS).
- All authors have read and approved the final version of submitted manuscript.

REFERENCES

1. **Klimstra DS, Modlin IR, Coppola D, Lloyd RV, Suster S.** The pathologic classification of neuroendocrine tumors: a review of nomenclature, grading, and staging systems Pancreas 2010; 39(6):707-12. *doi: 10.1097/MPA.0b013e3181ec124e.*
2. **Zandee WT, de Herder WW.** The evolution of neuroendocrine tumor treatment reflected by ENETS Guidelines. Neuroendocrinol 2018;106(4):357-365. *doi: 10.1159/000486096.*
3. **Rindi G, Wiedenmann B.** Neuroendocrine neoplasia of the gastrointestinal tract revisited: towards precision medicine. Nat Rev Endocrinol 2020;16(10):590-607. *doi: 10.1038/s41574-020-0391-3.*
4. **Rindi G, Klimstra DS, Abedi-Ardekani B, Asa SL, Bosman FT, Brambilla E, Busam KJ, de Krijger RR, Dietel M, El-Naggar AK, Fernandez-Cuesta L, Klöppel G, McCluggage WG, Moch H, Ohgaki H, Rakha EA, Reed NS, Rous BA, Sasano H, Scarpa A, Scoazec JY, Travis WD, Tallini G, Trouillas J, van Krieken JH, Cree IA.** A common classification framework for neuroendocrine neoplasms: an International Agency for Research on Cancer (IARC) and World Health Organization (WHO) expert consensus proposal. Mod Pathol 2018;31(12):1770-1786. *doi:10.1038/s41379-018-0110-y.*
5. **Hijioka S, Hosoda W, Mizuno N, Hara K, Imaoka H, Bhatia V, Mekky MA, Tajika M, Tanaka T, Ishihara M, Yogi T, Tsutumi H, Fujiyoshi T, Sato T, Hieda N, Yoshida T, Okuno N, Shimizu Y, Yatabe Y, Niwa Y, Yamao K.** Does the WHO 2010 classification of pancreatic neuroendocrine neoplasms accurately characterize pancreatic neuroendocrine carcinomas? J Gastroenterol 2015;50(5):564-72. *doi: 10.1007/s00535-014-0987-2.*
6. **Rindi G, Klersy C, Albarello L, Baudin E, Bianchi A, Buchler MW, Caplin M, Couvelard A, Cros J, de Herder WW, Delle Fave G, Doglioni C, Federspiel B, Fischer L, Fusai G, Gavazzi F, Hansen CP, Inzani F, Jann H, Komminoth P, Knigge UP, Landoni L, La Rosa S, Lawlor RT, Luong TV, Marinoni I, Panzuto F, Pape UF, Partelli S, Perren A, Rinzivillo M, Rubini C, Ruszniewski P, Scarpa A, Schmitt A, Schinzari G, Scoazec JY, Sessa F, Solcia E, Spaggiari P, Toumpanakis C, Vanoli A, Wiedenmann B, Zamboni G, Zandee WT, Zerbi A, Falconi M.** Competitive testing of the WHO 2010 versus the WHO 2017 grading of pancreatic neuroendocrine neoplasms: data from a Large International Cohort Study. Neuroendocrinol 2018;107(4):375-386. *doi: 10.1159/000494355.*
7. **Yao JC, Hassan M, Phan A, Dagohoy C, Leary C, Mares JE, Abdalla EK, Fleming JB, Vauthey JN, Rashid A, Evans DB.** One hundred years after "carcinoid": epidemiology of and prognostic factors for neuroendocrine tumors in 35,825 cases in the United States. J Clin Oncol 2008; 26(18):3063-72. *doi:10.1200/JCO.2007.15.4377.*
8. **Oronsky B, Ma PC, Morgensztern D, Carter CA.** Nothing but NET: a review of neuroendocrine tmors and carcinomas. Neoplasia 2017;19(12):991-1002. *doi: 10.1016/j.neo.2017.09.002.*
9. **Chauhan A, Kohn E, Del Rivero J.** Neuroendocrine tumors-less well known, often misunderstood, and rapidly growing in Incidence. JAMA Oncol 2020;6(1):21-22. *doi: 10.1001/jamaoncol.2019.4568.*
10. **Pearman TP, Beaumont JL, Cella D, Neary MP, Yao J.** Health-related quality of life in patients with neuroendocrine tumors: an investigation of treatment type, disease status, and symptom burden. Support Care Cancer 2016;24(9):3695-703. *doi:10.1007/s00520-016-3189-z.*
11. **Kulke MH, Mayer RJ.** Carcinoid tumors. N Engl J Med 1999;340(11):858-68. *doi:10.1056/NEJM199903183401107.*
12. **Corral Cordero F, Cueva Ayala P, Yépez Maldonado J, Tarupi Montenegro W.** Trends in cancer incidence and mortality over three decades in Quito - Ecuador. Colomb Med 2018;49(1):35-41. *doi: 10.25100/cm.v49i1.3785.*
13. **Rindi G, Klöppel G, Couvelard A, Komminoth P, Körner M, Lopes JM, McNicol AM, Nilsson O, Perren A, Scarpa A, Scoazec JY, Wiedenmann B.** TNM staging of midgut and hindgut (neuro) endocrine tumors: a

consensus proposal including a grading system. Virchows Arch 2007;451(4):757-62. *doi:10.1007/s00428-007-0452-1.*

14. **Vicente-Villardón JL, Galindo-Villardón MP, Blázquez-Zaballos A.** Logistic biplots. Multiple correspondence analysis and related methods. London: Chapman & Hall. 2006;503–21.
15. **Gabriel KR.** The biplot graphic display of matrices with application to principal component analysis. Biometrika 1971; 58(3), 453-467. *doi.org/10.1093/biomet/58.3.453.*
16. **Sharov AA, Dudekula DB, Ko MSH**. A web-based tool for principal component and significance analysis of microarray data. Bioinformatics 2005; 21(10), 2548-2549 *doi:10.1093/bioinformatics/bti343.*
17. **Bravata DM, Shojania KG, Olkin I, Raveh A.** CoPlot: a tool for visualizing multivariate data in medicine. Stat Med 2008;27(12):2234-47. *doi1 0.1002/sim.3078.*
18. **Sepúlveda R, Vicente-Villardón JL, Galindo MP.** The Biplot as a diagnostic tool of local dependence in latent class models. A medical application. Stat Med 2008;27(11):1855-69. *doi: 10.1002/sim.3194.*
19. **Demey JR, Vicente-Villardón JL, Galindo-Villardón MP, Zambrano AY**. Identifying molecular markers associated with classification of genotypes by External Logistic Biplots. Bioinformatics 2008; 24(24), 2832-2838. *doi:10.1093/bioinformatics/btn552.*
20. **Gibbs RA, Belmont JW, Hardenbol P, Willis TD, Yu FL, Yang HM, et al.** The international HapMap project. 2003. *doi:10.1038/nature02168.*
21. **Gallego-Alvarez I, Ortas E, Vicente-Villardón JL, Álvarez Etxeberria I**. Institutional constraints, stakeholder pressure and corporate environmental reporting policies. Bus Strateg Environ 2017; 26(6), 807-825. *doi.org/10.1002/bse.1952.*
22. **Cañueto J, Cardeñoso-Álvarez E, García-Hernández JL, Galindo-Villardón P, Vicente-Galindo P, Vicente-Villardón JL, Alonso-López D, De Las Rivas J, Valero J, Moyano-Sanz E, Fernández-López E, Mao JH, Castellanos-Martín A, Román-Curto C, Pérez-Losada J.** MicroRNA (miR)-203 and miR-205 expression patterns identify subgroups of prognosis in cutaneous squamous cell carcinoma. Br J Dermatol 2017;177(1):168-178. *doi: 10.1111/bjd. 15236.*
23. **Hernández-Sánchez JC, Vicente-Villardón JL**. Logistic biplot for nominal data. Adv Data Anal Classif 11. 2017; 11(2), 307-326. *doi.org/10.1007/s11634-016-0249-7.*
24. **Vicente-Villardón, J.L**. MULTBIPLOT: A package for Multivariate Analysis using Biplots. Departamento de Estadística. Universidad de Salmanca. 2010. *(http://biplot.usal.es/ClassicalBiplot/index.html)*.
25. **Vicente-Villardón, J.L**. MultBiplotR: Multivariate Analysis using Biplots. R package version 0.1. 0. *Website http://biplot. usal.es/multbiplot/multbiplot–in–r/ [accessed 20 November 2019].*
26. **Chen TY, Morrison AO, Susa J, Cockerell CJ.** Primary low-grade neuroendocrine carcinoma of the skin: An exceedingly rare entity. J Cutan Pathol 2017;44(11):978-81. *doi: 10.1111/cup.13028.*
27. **Riihimäki M, Hemminki A, Sundquist K, Sundquist J, Hemminki K.** The epidemiology of metastases in neuroendocrine tumors. Int J Cancer 2016; 139(12):2679-2686. *doi:10.1002/ijc.30400.*
28. **Chapman S, Schenk P, Kazan K, Manners, J.** Using biplots to interpret gene expression patterns in plants. Bioinformatics 2002; 18(1), 202-204. *doi.org/10.1093/bioinformatics/18.1.202.*
29. **Gabriel, K. R.** Generalised bilinear regression. Biometrika 1998; 85(3), 689-700. *doi.org/10.1093/biomet/85.3.689*
30. **Gabriel KR, Zamir S**. Lower rank approximation of matrices by least squares with any choice of weights. Technometrics 1979; 21 : 489-498.
31. **Gower JC, Hand DJ.** Biplots 1995; 54. CRC Press.
32. **Jongman, E, & Jongman, S R R** Data analysis in community and landscape ecology. Cambridge University Press, 1995.
33. **Vanoli A, Albarello L, Uncini S, Fassan M, Grillo F, Di Sabatino A, Martino M, Pasquali C, Milanetto AC, Falconi M, Partelli S, Doglioni C, Schiavo-Lena M, Brambilla T, Pietrabissa A, Sessa F, Capella C, Rindi G, La Rosa S, Solcia E, Paulli M.** Neuroendocrine tumors (NETs) of the minor papilla/ampulla: analysis of 16 cases underlines

homology with major ampulla NETs and differences from extra-ampullary duodenal NETs. Am J Surg Pathol 2019;43(6):725-736. *doi:10.1097/PAS.0000000000001234.*

34. **Lloyd R V, Osamura YR, Kloppel G, Rosai J.** WHO classification of tumours of endocrine organs. WHO Press 2017; WHO Classification of Tumours, *4th Edition, Volume 10.*
35. **Taal BG, Visser O.** Epidemiology of neuroendocrine tumours. Neuroendocrinol 2004;80 (Suppl 1):3-7. *doi: 10.1159/000080731.*
36. **Dasari A, Shen C, Halperin D, Zhao B, Zhou S, Xu Y, Shih T, Yao JC.** Trends in the incidence, prevalence, and survival outcomes in patients with neuroendocrine tumors in the United States. JAMA Oncol 2017;3(10):1335-1342. *doi: 10.1001/jamaoncol. 2017.0589.*
37. **Cho MY, Kim JM, Sohn JH, Kim MJ, Kim KM, Kim WH, Kim H, Kook MC, Park DY, Lee JH, Chang H, Jung ES, Kim HK, Jin SY, Choi JH, Gu MJ, Kim S, Kang MS, Cho CH, Park MI, Kang YK, Kim YW, Yoon SO, Bae HI, Joo M, Moon WS, Kang DY, Chang SJ.** Current trends of the incidence and pathological diagnosis of gastroenteropancreatic neuroendocrine tumors (GEP-NETs) in Korea 2000-2009: Multicenter Study. Cancer Res Treat 2012;44(3):157-165. *doi: 10.4143/crt.2012.44.3.157.*
38. **Chauhan A, Yu Q, Ray N, Farooqui Z, Huang B, Durbin EB, Tucker T, Evers M, Arnold S, Anthony LB.** Global burden of neuroendocrine tumors and changing incidence in Kentucky. Oncotarget 2018;9(27):19245-19254. *doi: 10.18632/oncotarget.24983.*
39. **Rorstad O.** Prognostic indicators for carcinoid neuroendocrine tumors of the gastrointestinal tract. J Surg Oncol 2005;89(3):151-160. *doi: 10.1002/jso.20179.*
40. **Rupp AB, Ahmadjee A, Morshedzadeh JH, Ranjan R.** Carcinoid syndrome-induced ventricular tachycardia. Case Rep Cardiol 2016;2016:9142598. *doi: 10.1155/2016/9142598.*
41. **McCormick D.** Carcinoid tumors and syndrome. Gastroenterol Nurs 2002;25(3):105-11. *doi: 10.1097/00001610-200205000-00004.*
42. **Boudreaux JP, Klimstra DS, Hassan MM, Woltering EA, Jensen RT, Goldsmith SJ, Nutting C, Bushnell DL, Caplin ME, Yao JC**. North American Neuroendocrine Tumor Society (NANETS). The NANETS consensus guideline for the diagnosis and management of neuroendocrine tumors: well-differentiated neuroendocrine tumors of the jejunum, ileum, appendix, and cecum. Pancreas 2010;39(6):753-766. *doi:10.1097/MPA.0b013e3181ebb2a5.*
43. **Toth-Fejel S, Pommier RF.** Relationships among delay of diagnosis, extent of disease, and survival in patients with abdominal carcinoid tumors. Am J Surg 2004;187(5):575-579. *doi: 10.1016/j.amjsurg.2004.01.019.*
44. **Beaumont JL, Cella D, Phan AT, Choi S, Liu Z, Yao JC.** Comparison of health-related quality of life in patients with neuroendocrine tumors with quality of life in the general US population. Pancreas 2012;41(3):461-466. *doi: 10.1097/MPA.0b013e3182328045.*
45. **Jedrych J, Pulitzer M.** Primary carcinoid tumor of the skin: a literature review. Int J Surg Pathol 2014;22(2):129-135. *doi: 10.1177/1066896913516672.*
46. **Terada T.** Primary cutaneous neuroendocrine tumor (atypical carcinoid) expressing KIT and PDGFRA with myoepithelial differentiation: a case report with immunohistochemical and molecular genetic studies. Int J Clin Exp Pathol 2013;6(4):802-809.
47. **Koo HS, Sohn YM, Park YK.** Sonographic appearance of a neuroendocrine tumor arising in the axilla: case report and literature review. J Clin Ultrasound 2014;42(1):30-32. *doi: 10.1002/jcu.22024.*
48. **Santos-Juanes J, Fernández-Vega I, Fuentes N, Galache C, Coto-Segura P, Vivanco B, Astudillo A, Martínez-Camblor P.** Merkel cell carcinoma and Merkel cell polyomavirus: a systematic review and meta-analysis. Br J Dermatol 2015;173(1):42-49. *doi: 10.1111/bjd.13870.*
49. **Daoud MA, Mete O, Al Habeeb A, Ghazarian D.** Neuroendocrine carcinoma of the skin--an updated review. Semin Diagn Pathol 2013;30(3):234-244. *doi:10.1053/j.semdp.2013.07.002.*

50. Goto K, Anan T, Fukumoto T, Kimura T, Misago N. Carcinoid-like/labyrinthine pattern in sebaceous neoplasms represents a sebaceous mantle phenotype: immunohistochemical analysis of aberrant vimentin expression and cytokeratin 20-positive Merkel cell distribution. Am J Dermatopathol 2017;39(11):803-810. *doi:10.1097/DAD.0000000000000806.*

51. Leventhal JS, Braverman IM. Skin manifestations of endocrine and neuroendocrine tumors. Semin Oncol 2016;43(3):335-340. *doi: 10.1053/j.seminoncol.2016.02.022.*

Invest Clin 63(1): 32 - 46, 2022 https://doi.org/10.54817/IC.v63n1a03

Influencia de la densidad de energía de ondas de choque focalizadas en el tratamiento de la fascitis plantar.

Ana María Andrés Toribio[1], Ana María González Rebollo[2], Antonio Tristán-Vega[3] y Manuel Garrosa[4]

[1]Servicio de Medicina Física y Rehabilitación, Complejo Asistencial de Zamora, Zamora, España.
[2]Servicio de Medicina Física y Rehabilitación, Hospital Universitario Río Hortega, Valladolid, España.
[3]Laboratorio de Procesado de Imagen, ETSI Telecomunicación, Universidad de Valladolid, Campus Miguel Delibes, Valladolid, España.
[4]Dpto. de Biología Celular, Histología y Farmacología e INCYL (Instituto de Neurociencias de Castilla y León). Universidad de Valladolid. Edificio de Ciencias de Salud, Valladolid, España.

Palabras clave: ondas de choque focalizadas; fascitis plantar; generador piezoeléctrico; rehabilitación.

Resumen. La fascitis plantar (FP) es una patología frecuente e invalidante que puede tratarse con ondas de choque focalizadas. El objetivo principal del estudio fue valorar la eficacia del tratamiento con ondas de choque focalizadas en la FP según la densidad de energía utilizada. Se incluyeron 82 pacientes con diagnóstico clínico de FP que fueron asignados mediante muestreo aleatorio simple a dos grupos de tratamiento: densidad de energía media- alta (0,59mJ/mm^2) y densidad de energía media-baja (0,27mJ/mm^2). Se evaluaron el dolor y la funcionalidad, mediante las escalas EVA (Escala Visual Analógica) y AOFAS (American Orthopedic Foot and Ankle Society Ankle-Hindfoot Scale) respectivamente, al inicio del estudio (consulta base), y al primer, tercer y sexto mes tras el tratamiento. Por último, se evaluó el grado de satisfacción de los pacientes mediante la escala de Roles y Maudsley. Se compararon los resultados de las escalas en las revisiones posteriores al tratamiento, obteniéndose significación estadística para las variables principales del estudio (dolor y funcionalidad) en cada grupo de intervención. Aunque los niveles de dolor y la funcionalidad mejoraron en ambos grupos de estudio, se obtuvo una respuesta analgésica y funcional mayor y más precoz en el grupo tratado con densidad de energía media-alta.

Autor de correspondencia. Ana María Andrés Toribio. Servicio de Medicina Física y Rehabilitación, Complejo Asistencial de Zamora, Zamora, España. Correo electrónico: aandrest@saludcastillayleon.es

Influence of energy density on the effectiveness of the treatment of plantar fasciitis with focused extracorporeal shock waves.

Invest Clin 2022; 63 (1): 32 – 46

Key words: focused extracorporeal shock waves; plantar fasciitis; functionality; energy density.

Abstract. Plantar fasciitis (FP) is a frequent and disabling condition that can be treated with focused extracorporeal shock waves. The main objective of this study was to assess the effectiveness of focused extracorporeal shockwave treatment in FP according to the energy density used. Eighty-two patients with a clinical diagnosis of FP were included and assigned, by simple random sampling, to two treatment groups: medium-high energy density (0.59mJ/mm^2) and low-medium energy density (0.27mJ/mm^2). Pain and functionality were assessed using the VAS (Visual Analogical Scale) and AOFAS (American Orthopedic Foot and Ankle Society Ankle-Hindfoot Scale) scales, respectively, at the start of the study (baseline consultation), and at the first, third and sixth month post-treatment. Finally, the degree of patient satisfaction was evaluated using the Roles and Maudsley score. The results of the scales in the post-treatment reviews were compared, and statistical significance was obtained for the main study variables (pain and functionality) in each intervention group. Although pain levels and functionality improved in both study groups after treatment, a greater and earlier analgesic and functional response was obtained for the medium-high energy density group.

Recibido: 28-07-2021 Aceptado: 18-09-2021

INTRODUCCIÓN

La fascitis plantar (FP) es la causa más común de dolor a nivel de la almohadilla talar; se estima que un 10% de la población general podría verse afectada por esta patología en algún momento de su vida [1]. Su diagnóstico es fundamentalmente clínico y los casos analizados anatomopatológicamente, revelan un predominio del componente degenerativo sobre el inflamatorio. Para enfatizar este hecho, en la literatura se utilizan otras nomenclaturas como: fasciosis plantar, fasciopatía plantar o talalgia. Sin embargo, numerosos estudios, revisiones y guías de práctica clínica abogan por el uso del término clínico "fascitis plantar" (FP), por lo que será el utilizado a lo largo de este artículo [2]. La prevalencia de esta patología en la consulta de Rehabilitación es elevada y afecta con mayor frecuencia a la población entre 40 y 60 años de edad, presentándose de forma bilateral hasta en un tercio de los casos [3].

La etiología de la FP es multifactorial, sin embargo, la causa más frecuente es el estrés biomecánico sobre la fascia plantar, a nivel de su inserción en la tuberosidad

medial del calcáneo. Este componente mecánico, que no sólo es localizado sino un resultado de alteraciones en el sistema aquíleo-calcáneo-plantar, puede desencadenarse por la carga de peso prolongada, la obesidad, la contractura de la musculatura posterior de la pierna, por patrones de deambulación y/o carrera anómalos y por la limitación de la flexión dorsal del tobillo [4].

En la FP el dolor es típicamente más intenso en la mañana, con los primeros pasos y/o después de un descanso prolongado y se agrava por la carga de peso continuada. Inicialmente suele ser intermitente y punzante y progresa hasta hacerse persistente en el talón, dificultando la deambulación. En general, se puede tratar con éxito con medidas conservadoras (antiinflamatorios no esteroideos, fisioterapia manual, terapia física y/o infiltraciones locales con corticoides). Sin embargo, la efectividad de estos tratamientos en la evolución de la FP no se encuentra bien establecida, al tratarse de un cuadro que habitualmente tiende a resolverse en un período variable entre 6 y 18 meses [5-7].

El tratamiento con ondas de choque extracorpóreas, parece ser una alternativa prometedora. Tiene eficacia probada en numerosas entesopatías, que incluyen FP, epicondilalgia y tendinopatía patelar y aquílea [8,9]. En la guía clínica sobre el manejo de la FP publicada por el American College of Foot and Ankle Surgery en el año 2010, el tratamiento con ondas de choque extracorpóreas se recomienda con un grado de evidencia B [10]. Las ondas de choque son ondas acústicas con una presión y duración específicas, capaces de propagarse a través de los tejidos sin perder porcentajes significativos de su energía. Su cadencia es disarrmónica, con un tiempo de subida de señal en nanosegundos y un pico de alta presión. Sus efectos físicos fundamentales son: el efecto primario o directo (fuerzas de tensión y cizallamiento) y el efecto indirecto o secundario (fenómeno de cavitación). Estos efectos físicos causan diferentes reacciones biológicas en la zona de tratamiento [11].

Las ondas de choque inducen una liberación precoz de factores angiogénicos y de crecimiento, que suponen un efecto positivo sobre la neovascularización tendinosa. Estos efectos serían favorables para la resolución de la FP crónica, caracterizada por una hipovascularización local [12].

Existe bibliografía que avala la eficacia del tratamiento con ondas de choque extracorpóreas focalizadas en la reducción del dolor en la FP, pero los datos son heterogéneos en cuanto a: tipo de ondas de choque, generador, número de sesiones, número de disparos por sesión y densidad de energía idónea a utilizar en relación a la efectividad analgésica, lo cual promueve la justificación de este estudio.

Como hipótesis de trabajo se planteó que con la densidad de energía media-alta (0,59mJ/mm^2), se obtendrían resultados clínicos superiores en cuanto a la reducción de dolor e incremento de la funcionalidad. Por otro lado, se buscó evaluar el grado de satisfacción final, tras el tratamiento y seguimiento (6 meses) de los pacientes con FP.

PACIENTES Y MÉTODOS

Considerando la hipótesis y los objetivos previamente marcados, se diseñó un estudio experimental tipo ensayo clínico aleatorizado en grupos paralelos de intervención terapéutica con análisis de superioridad, por intención de tratar y de medidas de eficacia.

El reclutamiento se efectuó a partir de pacientes que acudieron a las consultas externas del Servicio de Medicina Física y Rehabilitación del Hospital Universitario Río Hortega (H.U.R.H.) de Valladolid (España), derivados con diagnóstico de FP desde Atención Primaria o Atención Especializada del Área Oeste en el período de tiempo comprendido desde mayo de 2017 hasta mayo de 2018.

Este trabajo fue aprobado por el Comité Ético de Investigación Clínica (CEIC) del Área de Salud de Valladolid Oeste. Se llevó a cabo de conformidad con todas las leyes y

normativas aplicables, de acuerdo a los principios éticos internacionales, fundamentalmente la Declaración de Helsinki (Fortaleza, Brasil, 2013) y las Normas de Buena Práctica Clínica Epidemiológicas de la ICH (International Conference of Harmonization). Los datos fueron tratados con absoluta confidencialidad, según la Ley Orgánica 15/1999 del Gobierno Español, de 13 de diciembre, de protección de datos de carácter personal. Se obtuvo la firma de consentimiento informado para la participación en el estudio y para la aplicación del tratamiento con ondas de choque focalizadas.

Los criterios de inclusión y exclusión se detallan a continuación:

Criterios de inclusión: edad igual o mayor de 18 años, capacidad cognitiva suficiente para comprender y aceptar los beneficios potenciales y los riesgos de participación en el estudio, diagnóstico clínico de FP (dolor durante los primeros pasos al levantarse de la cama por la mañana y/o tras estar un período de tiempo sentado, dolor a la palpación de la inserción calcánea de la fascia plantar y duración del cuadro igual o superior a 3 meses en el momento de incorporación al estudio), percepción subjetiva de dolor causado por la FP medido por la Escala visual analógica (EVA) [13], igual o mayor que 4, no haber recibido tratamientos previos por este proceso, haber recibido terapia conservadora aislada o combinada entendiéndose como tal: terapia física, fisioterapia, plantillas, férulas nocturnas e infiltraciones con anestésicos locales y/o corticoides). Período de tiempo mínimo tras la aplicación de otros tratamientos: 6 semanas desde la última infiltración, 4 semanas desde la última sesión de electroterapia.

Criterios de exclusión: alteraciones vasculares a nivel local (insuficiencia vascular periférica), enfermedad maligna con o sin metástasis, infección de partes blandas u osteomielitis (aguda, subaguda o crónica) en la zona a tratar, antecedentes de fractura de calcáneo, inmunosupresión, tratamiento anticoagulante activo (por ejemplo: acenocumarol), antecedentes quirúrgicos a nivel del tobillo y/o pie homolateral a la FP, tratamiento previo con ondas de choque, embarazo, radiculopatía lumbosacra o neuropatía periférica compresiva (síndrome del túnel tarsiano), confirmada por electromiografía, alteraciones neurológicas centrales (déficits sensitivos o motores), alteración de reflejos osteotendinosos, ser portador de marcapasos o dispositivos automáticos implantables.

A los pacientes reclutados para el estudio, se les realizó una anamnesis y un examen físico completo por parte del médico rehabilitador, en la consulta base (cb). Para el tratamiento con ondas de choque focalizadas se empleó el Piezoson 100 plus©, un generador piezoeléctrico compacto de ondas de choque de Richard Wolf GmbH de Knittlingen (Alemania), realizado en tecnología de doble capa piezoeléctrica que crea un área focal de gran precisión, la cual permite un tratamiento selectivo y exacto, sin afectar los tejidos o las regiones adyacentes. Según la indicación concreta, este aparato permite seleccionar entre un tratamiento con aplicación de energía a bajo, medio o alto nivel, gracias a la posibilidad de dosificación exacta de la intensidad, como se especificará más adelante.

El protocolo de tratamiento, detallado en la Fig. 1, consistió en la aplicación de 2 sesiones de ondas de choque focalizadas a cada paciente, con un intervalo de tiempo entre ambas de unas 3- 4 semanas. No se utilizó anestesia local. Se situó al paciente en decúbito prono con el pie afectado en ligera flexión plantar (postura de reposo) como se muestra en la Fig. 2. Se aplicaron 1000 disparos por sesión (2000 disparos en total). La frecuencia máxima del generador fue de 4 Hz. La membrana de acoplamiento utilizada en la sonda fue la número 25. Dicha membrana se impregnó con gel conductor para evitar la reflexión y la refracción de la onda ultrasónica por la interposición de aire. Durante el tratamiento la sonda fue desplazada sobre la superficie del talón afectado, incidiendo sobre la región más dolorosa (previamente localizada por palpación).

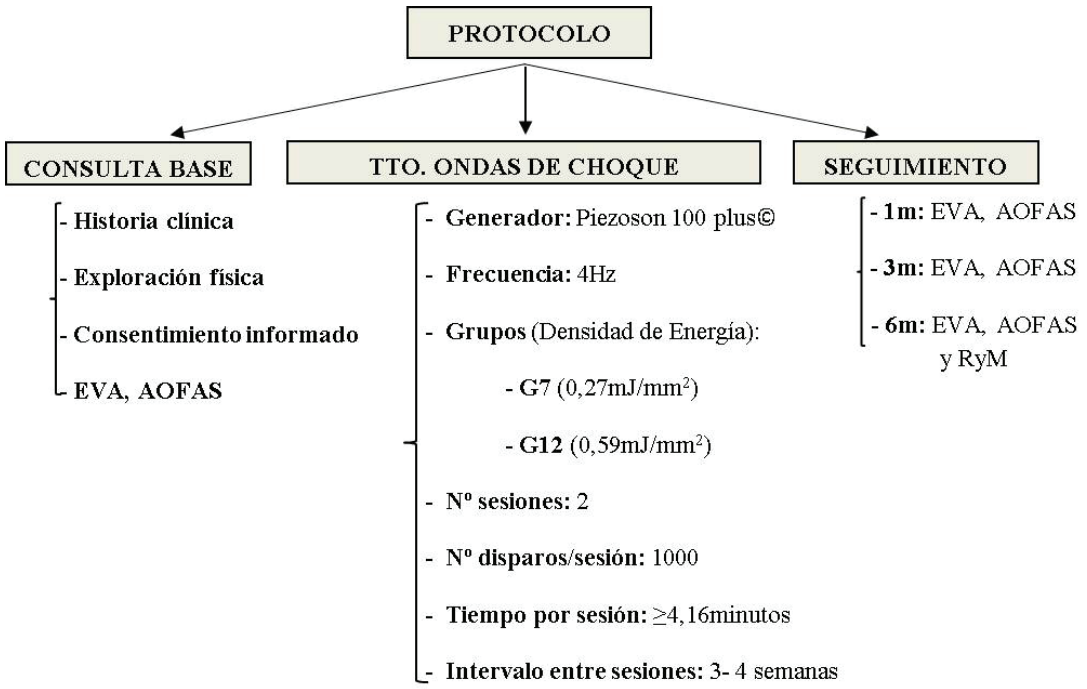

Fig. 1. Protocolo de tratamiento de fascitis plantar con ondas de choque focalizadas.

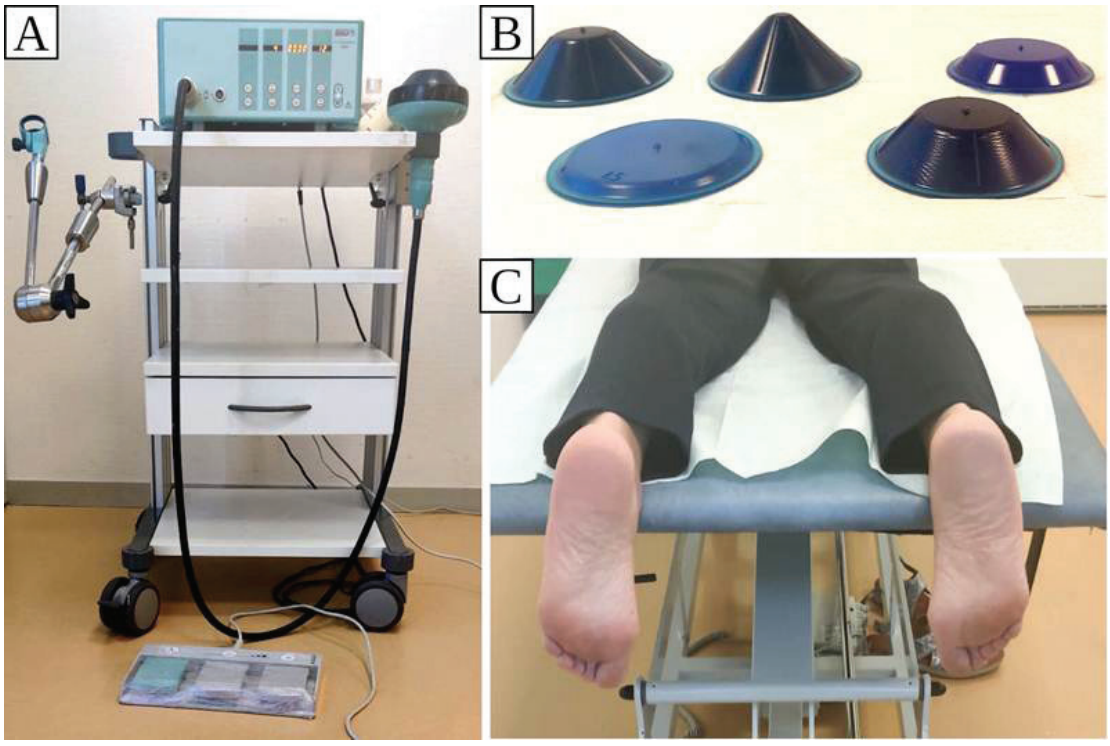

Fig. 2. A. Generador de ondas de choque focalizadas Piezoson 100 plus© (Richard Wolf). B. Almohadillas de acoplamiento. C. Posición del paciente durante el tratamiento con ondas de choque focalizadas para FP.

Posteriormente se realizaron revisiones médicas al primer, tercer y sexto mes después de finalizar la segunda sesión de tratamiento. Se evaluaron el dolor y la funcionalidad mediante las escalas EVA [13] y AOFAS [14], respectivamente; al inicio del estudio y en las tres revisiones post-tratamiento. Por último, se evaluó el grado de satisfacción de los pacientes tras finalizar el seguimiento, mediante la escala Roles y Maudsley (RyM) [15,16].

La escala EVA es una escala de valoración que se divide en 11 puntos, de 0 a 10, el 0 corresponde a la ausencia de dolor y el 10 al máximo dolor que el paciente pudiera imaginarse. Es la escala más utilizada en los trabajos que estudian el efecto de las ondas de choque en la FP [13].

La escala AOFAS incorpora información tanto subjetiva como objetiva. Los pacientes puntúan su dolor, y los facultativos evalúan la alineación del tobillo y del pie afectado para así completar la parte funcional. Las puntuaciones oscilan entre 0 y 100, considerando 100 el tobillo-pie sano. A pesar de no encontrarse validada para la FP, resulta de utilidad para evaluar los niveles articulares: subtalar, talonavicular y calcáneocuboideo [14], que suelen verse afectados en esta patología.

La escala RyM es una escala de valoración funcional autoadministrada, con cuatro categorías de clasificación según el nivel de satisfacción/calidad de vida: excelente, bueno, regular y malo [15]. No ha sido validada para la patología del pie, pero ha sido utilizada en numerosos estudios para evaluar la eficacia de las ondas de choque en la FP [16].

Pese a ser un procedimiento seguro y eficaz, se especificó a cada paciente que durante la aplicación de la técnica, experimentaría una sensación dolorosa que sería variable según el umbral de tolerancia individual. Como posibles efectos secundarios podría agudizarse el dolor post-tratamiento y/o aparecer un leve hematoma en la zona de aplicación.

De los pacientes con FP inicialmente reclutados, se seleccionaron 82 que fueron asignados mediante muestreo aleatorio simple (tabla de números aleatorios) y enmascaramiento ciego para paciente y analizador, a dos grupos de tratamiento que se denominaron: densidad de energía media-alta: G12 (15 varones, 26 mujeres; edad promedio 51,5 años; rango 34 a 67 años) y densidad de energía media-baja: G7 (11 varones, 30 mujeres; edad promedio 51,0 años; rango 28 a 66 años).

Las densidades de energía utilizadas se aplicaron según la clasificación de Rompe [17] y la relación entre estas y la intensidad del generador piezoeléctrico (Piezoson 100 plus©) se exponen en la Tabla 1.

Tabla 1
Relación entre intensidad y densidad de energía del tratamiento con ondas de choque focalizadas por grupos.

Grupo de estudio	Intensidad	Densidad de energía (mJ/mm2)
G7	7	0,27
G12	12	0,59

Se utilizó una densidad de energía terapéutica que fue aplicada de forma indistinta por el clínico, según la aleatorización correspondiente, en la totalidad de la muestra. No existió ningún grupo placebo o que quedase sin recibir tratamiento por no considerarlo una opción éticamente aplicable.

Durante el seguimiento hubo hasta 16 pérdidas, de 7 a 9 por grupo, por considerarse como criterios de eliminación: no completar la intervención (un paciente del G7) y no acudir a alguna o a ninguna de las revisiones posteriores al tratamiento. De esta manera, se realizó el análisis de los datos según se indica en el diagrama de flujo de la Fig. 3.

Para el análisis estadístico descriptivo, la normalidad de las variables cuantitativas fue establecida con la prueba de Kolmogorov-Smirnov. Las variables de distribución

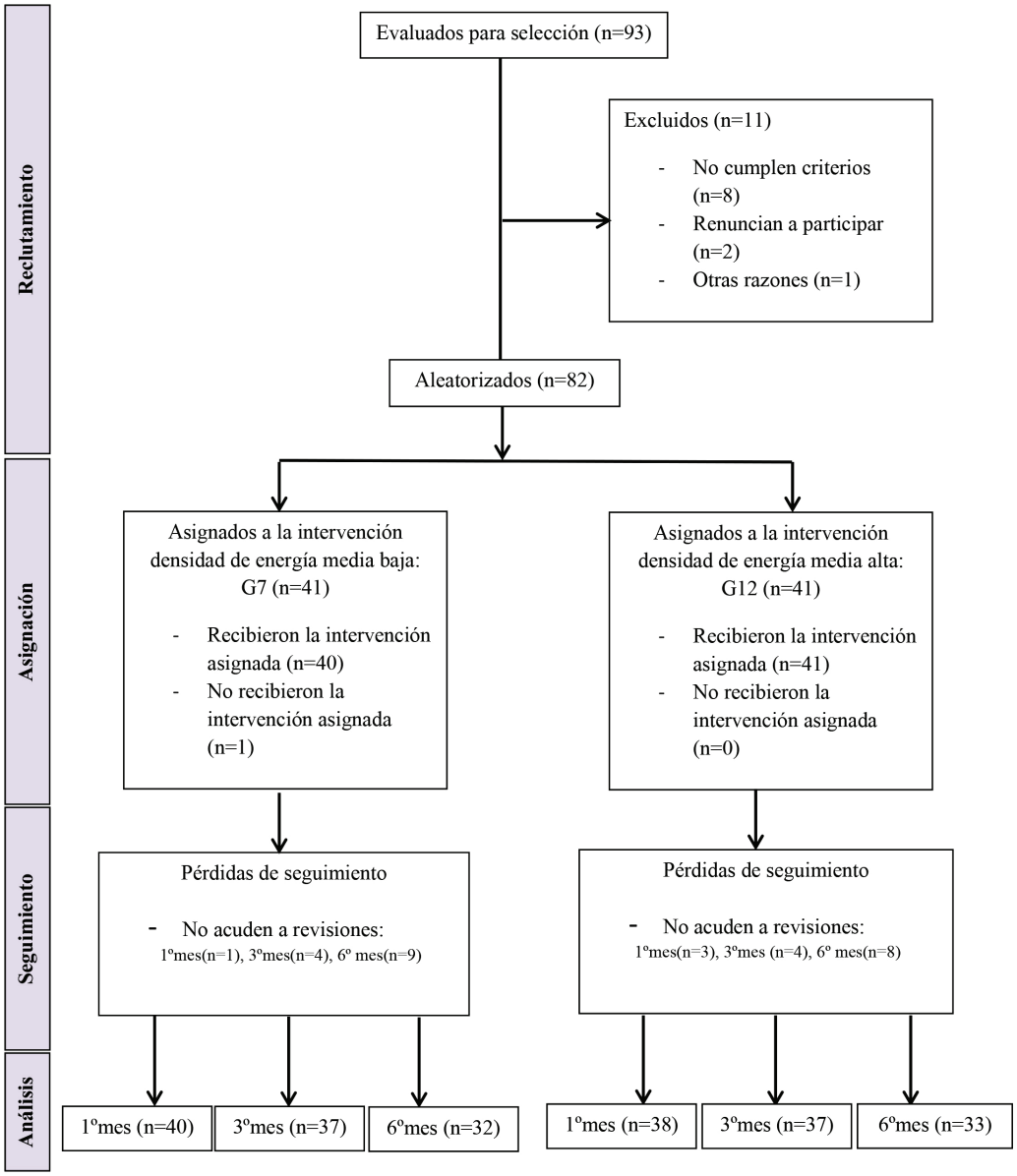

Fig. 3. Diagrama de flujo por fases del ensayo clínico aleatorizado paralelo, de dos grupos (reclutamiento, asignación de la intervención, seguimiento y análisis).

normal fueron descritas como media ± desviación estándar y las de distribución no normal y/o discretas como mediana y rango intercuartílico. Por su parte, las variables cualitativas fueron descritas mediante la tabla de frecuencias absolutas y relativas (porcentajes) de sus categorías. Finalmente, se utilizaron diagramas de cajas para representar las variables cuantitativas. En el análisis bivariante, para estudiar la asociación entre variables cualitativas se utilizó la prueba de Chi cuadrado o razón de verosimilitud (más de 2 categorías). Para estudiar las diferencias entre medias independientes se utilizó la prueba de la t de Student no pareada o la U de Mann-Whitney, dependiendo de las condiciones de aplicación (normalidad), para 2 grupos. Para valorar las diferencias entre

medias relacionadas (basales frente a evolución) se utilizó la prueba t de Student pareada (para variables normales según el test de Kolmogorov-Smirnov) o la de Wilcoxon (para variables no normales). El nivel de significación se estableció, para todas las pruebas, en una $p < 0,05$.

RESULTADOS

Inicialmente se comprobó la ausencia de sesgos por sexo, edad, índice de masa corporal (IMC), profesión de riesgo (entendida como bipedestación prolongada, deambulación prolongada, trabajo de carga de pesos, etcétera), calzado de seguridad, espolón calcáneo, lateralidad, deporte de riesgo (entendido como deporte de impacto sobre el talón) y tratamientos previos para la FP, según Tabla 2.

Además se verificó que ambos grupos (G7 y G12) partían de una situación basal similar en cuanto a dolor y funcionalidad, no existiendo diferencias significativas entre ellos en ninguna de las dos variables de estudio según se muestra en la Fig. 4.

La eficacia del tratamiento con ambas densidades de energía se comprobó mediante la valoración de la significación estadística correspondiente a la comparación entre las tres visitas de control y la consulta basal entre sí, para las escalas EVA y AOFAS (véase Fig. 5). Los datos por grupo y escala fueron analizados de forma independiente. Aunque para ambos grupos de estudio los valores de la escala EVA continuaron mejorando desde la revisión de 3 meses hasta la de 6 meses, la significación estadística por grupo fue diferente. Mientras que la mejoría de EVA en ese período en el G12 obtuvo una $p<0,01$,

Tabla 2
Tabla sociodemográfica por grupos de estudio.

Sesgo		Grupo de Estudio		*p*
		G7(n=41)	G12(n=41)	
Sexo	Hombre	11	15	NS*
	Mujer	30	16	
Edad Media años (rango)		51,0 (28-66)	51,5 (34-67)	NS*
IMC MEDIA		28,4	27,6	NS*
Profesión de Riesgo	Sí	28	28	NS*
	No	13	13	
Calzado de Seguridad	Utiliza	7	9	NS*
	No utiliza	34	32	
Espolón Calcáneo	Presente	21	26	NS*
	Ausente	20	15	
Lateralidad FP	Derecha	17	20	NS*
	Izquierda	24	21	
Deporte de Riesgo	Practica	30	27	NS*
	No practica	11	14	
Tratamientos Previos para FP	Sí	39	39	NS**
	No	2	2	

Test estadístico: t de Student*, Chi cuadrado**; NS no significativo.

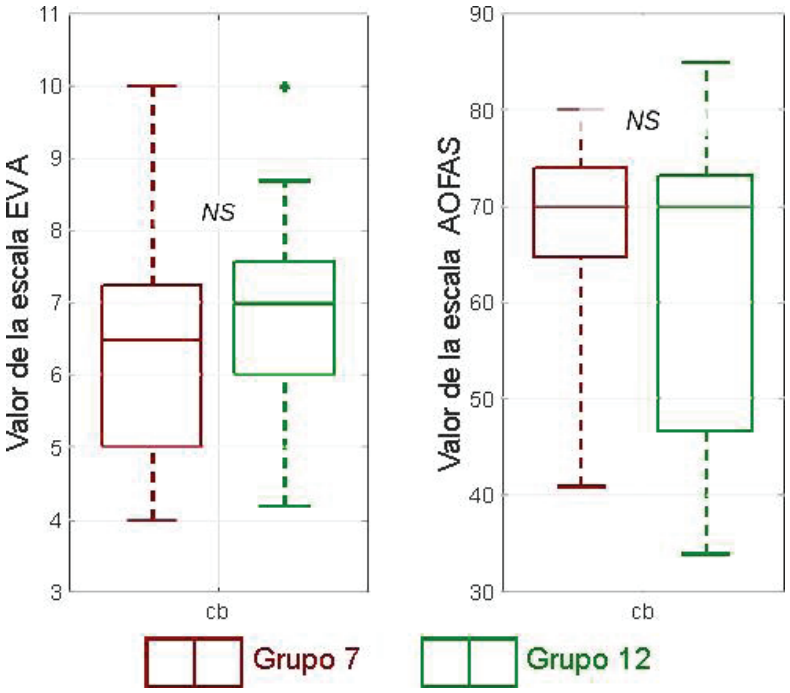

Fig. 4. Evaluación del sesgo en la consulta base (*cb*) según ambas escalas, EVA y AOFAS. Las cajas representan los percentiles 25 y 75 junto con el valor mediano, y las barras los valores extremos de la muestra. Las cruces representan valores fuera de rango.

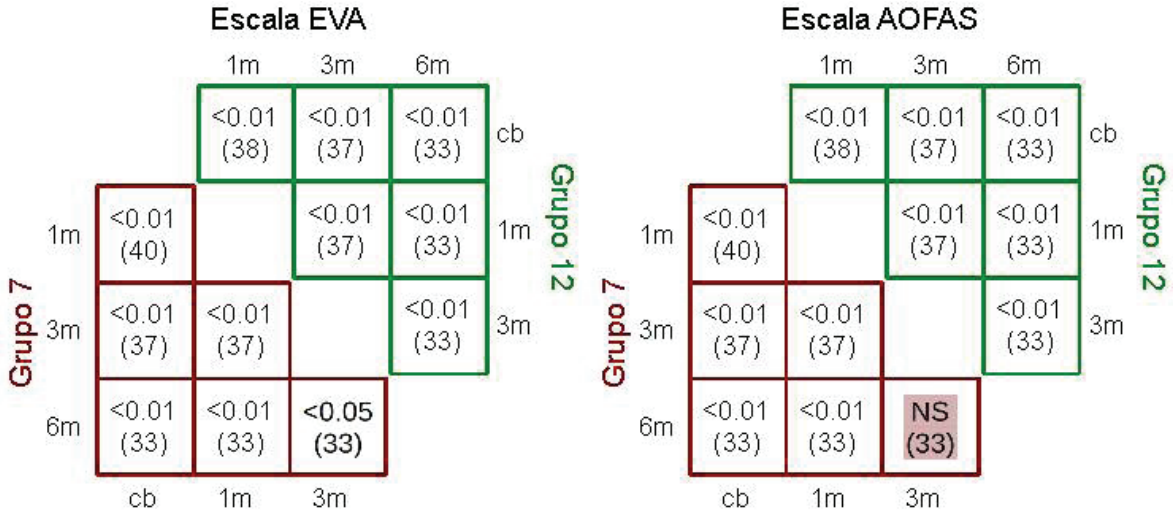

Fig. 5. Comparación de los datos de las escalas EVA y AOFAS correspondientes a cada visita del seguimiento. En cada casilla: *p* asociado a la prueba de la t de Student o U the Man-Whitney comprobado con el test de Kolmogorov-Smirnov; entre paréntesis, tamaño muestral; sombreado en rojo, la ausencia de significación estadística (*NS)*.

la misma variable correspondiente al G7 obtuvo una $p<0,05$. En el caso de la escala AOFAS, desde la revisión de 3 meses hasta la de 6 meses, continuaron mejorando de forma significativa únicamente los pacientes del G12 ($p<0,01$).

La Fig. 6 demuestra que existieron diferencias significativas en la mejoría observada en cada visita de control respecto de la consulta basal dependiendo de la dosis aplicada (G7 o G12), tanto para EVA como para AOFAS. En especial, cabe destacar la diferencia para la primera vista de control según la escala AOFAS que resultó estadísticamente significativa con una $p<0,01$.

Por su parte, la Fig. 7 objetiva que la principal diferencia entre los resultados clínicos obtenidos para G7 o G12 se produjo al término del primer período de revisión (primera visita de control), sin que pueda aseverarse que la evolución para las sucesivas visitas de control (3 y 6 meses) fuera diferente para ambos grupos. Una vez más, la significación estadística alcanzada para la escala AOFAS ($p<0,01$) fue superior a la de EVA ($p<0,05$).

Los resultados obtenidos al sexto mes de seguimiento según la escala RyM se muestran en las Tablas 3 y 4.

DISCUSIÓN

Este ensayo clínico está diseñado para proporcionar resultados relevantes para la práctica clínica futura, con el objetivo de comparar la eficacia de las ondas de choque focalizadas utilizando densidad de energía media-alta y media-baja para el tratamiento de la FP. Nos centramos en el rango de densidad de energía media, descartando la densidad de energía alta, cuya indicación fundamental es el tratamiento de las calcificaciones y pseudoartrosis, y la densidad de energía baja, por su dudoso efecto en la FP según la bibliografía revisada. Analizamos los datos obtenidos de cuestionarios y esca-

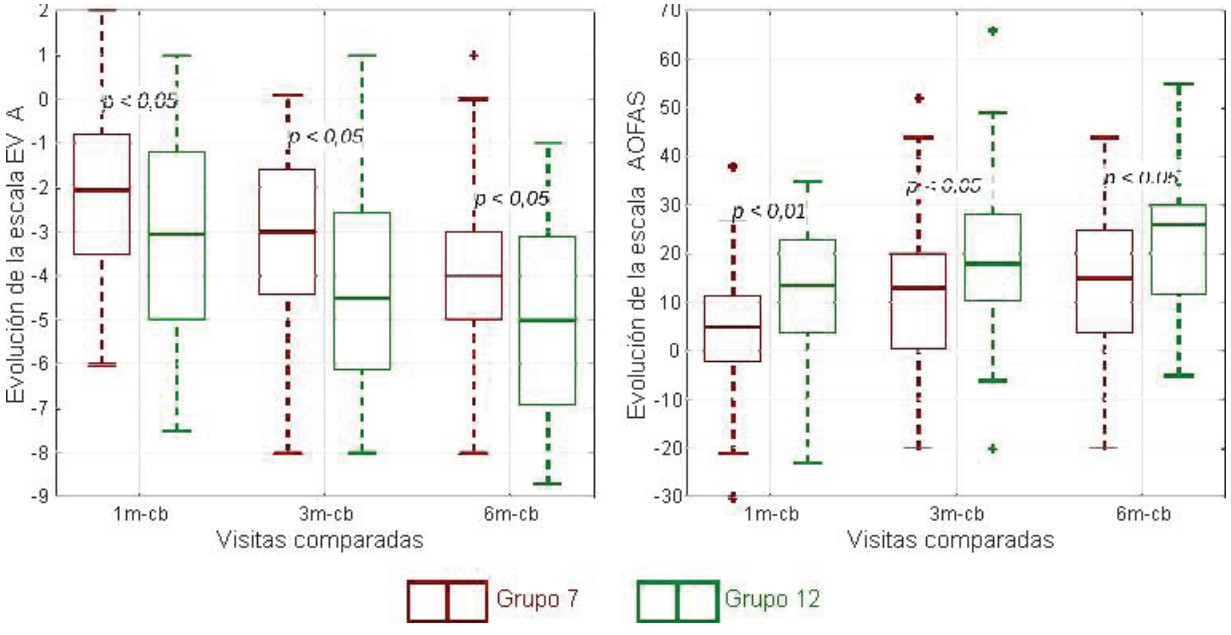

Fig. 6. Evolución diferencial de la puntuación de las escalas EVA y AOFAS por grupos de estudio de cada visita de seguimiento respecto a la consulta base (*cb*). Las cajas representan los percentiles 25 y 75 junto con el valor mediano, y las barras los valores extremos de la muestra. Las cruces representan valores fuera de rango.

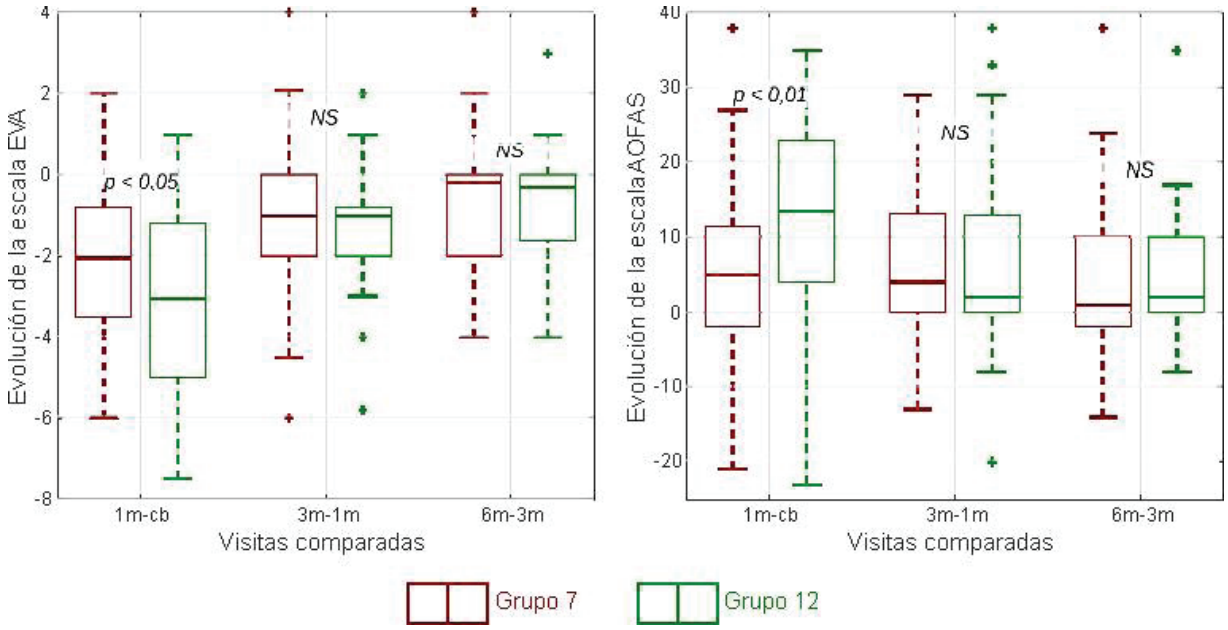

Fig. 7. Evolución diferencial de la puntuación de las escalas EVA y AOFAS por grupos de estudio de cada visita de seguimiento respecto a la consulta previa. Las cajas representan los percentiles 25 y 75 junto con el valor mediano, y las barras los valores extremos de la muestra. Las cruces representan valores fuera de rango.

Tabla 3
Tabla de contingencia de la escala RyM por grupos.

	Excelente	Bueno	Regular	Malo	Total
G7	6	11	13	2	32
G12	9	17	7	0	33
Total	15	28	20	2	65

Tabla 4
Tabla de contingencia escala rym comparativa de las opciones excelente/bueno respecto regular/malo por grupos.

p<0,05*	Excelente/ Bueno	Regular/ Malo	Total
G7	17	15	32
G12	26	7	33
Total	43	22	65

* Test estadístico: Chi cuadrado.

las para valorar dolor, funcionalidad y grado de satisfacción.

La significación estadística obtenida para las diferencias según la escala AOFAS fue en todos los casos mayor que la que se obtiene para EVA. Puesto que la primera incluye tanto valoraciones subjetivas (dolor) como objetivas (funcionalidad). La solidez de las conclusiones que pueden extraerse del correspondiente estudio para AOFAS debería ser, en principio, mayor que para EVA. No obstante, cabe resaltar que los resultados del estudio son completamente consistentes según ambas escalas: en ambos grupos la intervención resulta beneficiosa en la reducción del dolor y mejoría de la funcionalidad del paciente con FP utilizando ambas densidades de energía a largo plazo. Sin embargo, el efecto analgésico es más precoz en el grupo G12 (energía media-alta). Análogamente, la funcionalidad se incrementó en mayor cuantía y con mayor rapidez en ese mismo grupo.

Cabe destacar que en el G12 (energía media-alta), a los 3 y 6 meses se apreció mejoría significativa en ambas escalas estudiadas ($p<0,01$). Sin embargo, en el G7 (energía media-baja), la significación estadística de la escala EVA en ese período fue de $p<0,05$ y la escala AOFAS no demostró ninguna mejoría significativa para este grupo.

En la literatura el generador de ondas de choque focalizadas más utilizado es el electromagnético, como ocurrió en el trabajo de Su-Jin Lee y col. [18] que utilizó un generador EPOS Ultra (Dornier©), donde comparó densidades de energía media (0.16mJ/mm^2) y baja (0.08mJ/mm^2) en la FP. Cada grupo recibió un número de sesiones diferente. Utilizaron dos escalas comunes a nuestra investigación (EVA y RyM) y su seguimiento fue de 3 meses. Como novedad, empleamos la AOFAS para una valoración más completa de la evolución de la FP y aplicamos el mismo protocolo para ambos grupos (2 sesiones, 1000 disparos/sesión) utilizando dos densidades de energía media diferentes (alta y baja); obtuvimos resultados favorables en ambos y durante el seguimiento (6 meses) se observó una mejoría más precoz y mantenida en el tiempo en el grupo tratado con densidad de energía media-alta.

En nuestro estudio, el generador empleado fue el piezoeléctrico y las publicaciones al respecto con este tipo de generador son escasas; entre ellas se encuentra el artículo de Elía Martínez y col. [19] en el que realizaron una comparación del tratamiento con ondas de choque radiales y focalizadas para la FP, no encontrando diferencias significativas entre ambas en el seguimiento a 3 meses. Su protocolo consistió en 3 sesiones de tratamiento de 2000 disparos/sesión con una frecuencia de 4Hz a ritmo de una cada 14 días y la densidad de energía utilizada fue de 0.27mJ/mm^2. En su estudio, compararon las ondas de choque radiales y focalizadas, no compararon las ondas de choque focalizadas en ambos grupos de estudio. En nuestra investigación comparamos dos densidades de energía de las ondas de choque focalizadas para identificar la que resulta más eficaz para el tratamiento de la FP. Según esta misma publicación se desconoce la densidad de energía óptima del tratamiento con ondas de choque focalizadas, aspecto en el que hacemos hincapié en nuestra investigación. Por otra parte el número de disparos fue el doble (2000 disparos/sesión), realizaron una sesión más de tratamiento (3 sesiones) y la densidad de energía de las ondas focalizadas que utilizaron fue media-baja pero el grupo de comparación correspondió a otro tipo de ondas de choque (radiales) y el seguimiento fue a tres meses en lugar de a seis meses como en nuestro caso.

La aplicación de anestesia local y su influencia sobre la eficacia de las ondas de choque es un tema controvertido. Nosotros utilizamos la densidad de energía 0,59mJ/mm^2 sin anestesia local y la tolerancia al tratamiento fue similar con respecto a la de 0,27mJ/mm^2. No se notificaron complicaciones en ningún paciente, más allá de la sensación dolorosa durante la aplicación del mismo.

Un aspecto a destacar de este estudio es que es de tipo prospectivo y que evalúa la mejoría del dolor, así como de la funcionalidad y calidad de vida de los pacientes con FP, aspecto este último de gran importancia por encontrarse gravemente afectado.

Según Córdova y col. [20], en numerosas ocasiones la FP ha sido diagnosticada como espolón calcáneo. Sin embargo, los espolones no confirman un diagnóstico de FP. De hecho, se ha comunicado que el 50% de los pacientes con FP no presentan espolón y el 15% sí lo presentan a pesar de no tener los síntomas [20]. En las radiografías simples del pie, que no suelen ser de gran utilidad, entre 15 y 20% de los pacientes con espolón calcáneo no presenta dolor plantar; tan sólo el 5% de las personas con dolor plantar presenta un espolón. En nuestro estudio los resultados fueron independientes de la presencia o ausencia de espolón calcáneo, ya que esta variable no se tuvo en cuenta en el análisis estadístico debido a la aleatorización de la muestra (véase Tabla 2).

La limitación fundamental de este estudio es el tamaño muestral que se vio reducido por las pérdidas (iniciales: mala tolerancia individual a la aplicación del tratamiento no completando las dos sesiones del protocolo y a largo plazo, por el abandono del seguimiento en consulta), por lo cual nuestros resultados han de ser interpretados de forma prudente.

Otras limitaciones reseñables son: la ausencia de grupo control (placebo) por no considerarse éticamente aplicable, la ausencia de escalas específicas para la valoración de la FP y la subjetividad de las mismas, que dificulta la recogida real de datos.

Existen estudios previos que demuestran la eficacia del tratamiento con ondas de choque focalizadas en la FP utilizando densidades de energía media [3, 21-23]. En general, los protocolos son heterogéneos y las comparaciones se realizan con placebo [24] o con otros tratamientos (infiltraciones con corticoides [4, 21-23], ondas de choque radiales [19], toxina botulínica [16], etc.). Lo novedoso del presente estudio es la comparación de dos densidades de energía y la determinación de la más eficaz para tratar esta patología tan frecuente e incapacitante.

Dados los resultados obtenidos en nuestra muestra, podemos concluir que la densidad de energía media-alta resulta más eficaz en la reducción del dolor y recuperación funcional de los pacientes con FP, por ofrecer una respuesta analgésica mayor y más precoz sin incrementarse la tasa de reacciones adversas asociadas con respecto a la más baja.

Este estudio podría ser un primer paso hacia el consenso para una terapéutica que es ampliamente aplicada a una patología tan frecuente como invalidante. Si bien son necesarios más estudios para poder determinar la eficacia de las ondas de choque en la FP según la densidad de energía aplicada, podemos concluir que la densidad de energía media-alta resulta más eficaz. Por otra parte, sería interesante recopilar datos sociodemográficos de un tamaño muestral mayor y con un seguimiento más a largo plazo, para encontrar la densidad de energía idónea que permitiera tratar de la manera más eficaz y precoz la FP.

Financiamiento

No se dispone de financiamiento por organismos públicos o privados.

Declaración de Conflicto de intereses

No existe conflicto de intereses

Números ORCID de los autores

• Ana María Andrés Toribio (AMAT) 0000-0001-8333-5161

• Ana María González Rebollo (AMGR) 0000-0002-9547-9880

• Antonio Tristán-Vega (AT-V) 0000-0002-4614-2501

• Manuel Garrosa (MG) 0000-0002-4280-5611

Contribución de autoría

• Concepción y diseño del estudio: AMAT, AMGR, MG.

• Reclutamiento de pacientes y adquisición de datos: AMAT, AMGR.

• Análisis y/o interpretación de datos: AT-V, AMAT.

• Redacción del manuscrito: AMAT, AMGR, AT-V, MG.

• Tablas y figuras: AT-V, AMAT.

• Coordinación y revisión crítica del manuscrito: AT-V, AMGR, MG.

• Aprobación de la versión del manuscrito: AMAT, AMGR, AT-V, MG.

REFERENCIAS

1. **Crawford F, Thomson C.** Interventions for treating plantar heel pain. Cochrane Database Syst Rev 2003;3: CD000416.
2. **Dunning J, Butts R, Henry N, Mourad F, Brannon A, Rodriguez H, Young I, Arias-Buría JL, Fernández-de-Las-Peñas C.** Electrical dry needling as an adjunct to exercise, manual therapy and ultrasound for plantar fasciitis: A multi-center randomized clinical trial. PLoS One 2018 Oct 31;13(10):e0205405.
3. **Vaamonde-Lorenzo L, Cuenca González C, Monleón-Llorente L, Chiesa Estomba R, Labrada Rodríguez YH, Castro-Portal A, Archanco Olcese M, Garvin Ocampos L.** Aplicación de ondas de choque focales piezoeléctricas en el tratamiento de la fasciitis plantar. Rev Esp Cir Ortop Traumatol 2019;63(3):227-232.
4. **Chen CM, Lee M, Lin CH, Chang CH, Lin CH.** Comparative efficacy of corticosteroid injection and non-invasive treatments for plantar fasciitis: a systematic review and meta-analysis. Sci Rep 2018;8(1):4033.
5. **Tae Im Yi., Ga Eun Lee, In Seok Seo, Won Seok Huh, Tae Hee Yon, Bo Ra Kim.** Clinical characteristics of the causes of plantar heel pain. Ann Rehabil Med 2011; 35(4):507-513.
6. **Covey CJ, MulderMD.** Plantar fasciitis: how best to treat? J Fam Pract 2013;62(9):466-471.
7. **Goff JD, Crawford R.** Diagnosis and treatment of plantar fasciitis. Am Fam Physician; 84(6):676-682.
8. **Andres BM, Murrell GAC.** Treatment of tendinopathy: what works, what does not, and what is on the horizon. Clin Orthop Relat Res 2008; 466:1539–1554.
9. **Sems A, Dimeff R, Iannotti JP.** Extracorporeal shockwave therapy in the treatment of chronic tendinopathies. J Am Acad Orthop Surg 2006;14(4):195-204.
10. **Thomas JL, Christensen JC, Kravitz SR, Mendicino RW, Schuberth JM, Vanore JV, Weil LS Sr, Zlotoff HJ, Bouché R, Baker J; American College of Foot and Ankle Surgeons Heel Pain Committee.** The diagnosis and treatment of heel pain: a clinical practice guideline-revision 2010. J Foot Ankle Surg 2010;49(3 Suppl):S1-19.
11. **González Rebollo AM.** Introducción a la electroterapia.1ª Ed. Valladolid (España): González Rebollo AM; 2016, p 287-300.
12. **Wang CJ, Wang FS, Yang KD, Weng LH, Hsu CC, Huang CS, Yang LC.** Shock wave therapy induces neovascularization at the tendon-bone junction. A study in rabbits. J Orthop Res 2003;21(6):984-989.
13. **Landorf KB, Radford JA, Hudson S.** Minimal important difference of two commonly used outcome measures for foot problems. J Foot Ankle Res 2010;3:1-7.
14. **Ceccarelli F, Calderazzi F, Pedrazzi G.** Is there a relation between AOFAS Ankle-Hindfoot Score and SF-36 in evaluation of Achilles ruptures treated by percutaneous technique? J Foot Ankle Surg 2014; 53: 16–21.
15. **Roles NC, Maudsley RH.** Radial tunnel syndrome: resistant tennis elbow as a nerve entrapment. J Bone Joint Surg Br 1972;54(3):499–508.
16. **Roca B, Mendoza MA, Roca M.** Comparison of extracorporeal shock wave therapy with botulinum toxin type A in the treatment of plantar fasciitis. Disabil Rehabilitations 2016;38(21):2114-2121.
17. **Rompe JD, Kirkpatrick CJ, Kullmer K, Schwitalle M, Krischek O.** Dose-related effects of shock waves on rabbit tendo Achillis. A sonographic and histological study. J Bone Joint Surg Br 1998;80:546–552.
18. **Su-Jin Lee, Jung-Ho Kang, Ja-Young Kim, Jin-Hong Kim, Seo-Ra Yoon, Kwang-Ik Jung.** Dose-related effect of extracorporeal shock wave therapy for plantar fasciitis. Ann Rehabil Med 2013;37(3):379-388.
19. **Elía Martínez JM, Schmitt J, Tenías Burillo JM, Valero Inigo JC, Sánchez Ponce G, Peñalver Barrios L, García Fenollosa M, Cortés Fabregat A.** Comparación de la terapia de ondas de choque extracorpóreas focales y presión radiales en la fascitis plantar. Rehabilitacion 2020;54:11-18.
20. **Córdova A, López D, Fernández-Lazaro D, Caballero A.** Nueva visión del tratamiento de la fascitis plantar en deportistas: Utili-

dad del entrenamiento funcional mediante el esquí. Invest Clín 2017;58(3), 309-318.

21. **Guevara Serna JA, Acosta Morón JA.** Extracorporeal shockwave therapy versus corticosteroid injection in chronic plantar fasciitis. Rev Colomb Ortop Traumatol 2018;32:43–9.
22. **Lai TW, Ma HL, Lee MS, Chen PM, Ku MC.** Ultrasonography and clinical outcome comparison of extracorporeal shock wave therapy and corticosteroid injections for chronic plantar fasciitis: A randomized controlled trial. J Musculoskelet Neuronal Interact. 2018;18(1):47-54.
23. **Saber N, Diab H, Nassar W, Razaak HA.** Ultrasound guided local steroid injection versus extracorporeal shockwave therapy in the treatment of plantar fasciitis. Alex J Med 2012;48:35–42.
24. **Gollwitzer H, Saxena A, DiDomenico LA, Galli L, Bouché RT, Caminear DS, Fullem B, Vester JC, Horn C, Banke IJ, Burgkart R, Gerdesmeyer L.** Clinically relevant effectiveness of focused extracorporeal shock wave therapy in the treatment of chronic plantar fasciitis: a randomized, controlled multicenter study. J Bone Joint Surg Am 2015;97:701–8.

Invest Clin 63(1): 47 - 56, 2022 https://doi.org/10.54817/IC.v63n1a04

Comparación entre edad cronológica y dental según tres métodos de estimación en una población peruana.

Liz Mónica Perales Quito[1], Andrea Gianella Huaman Ñahuinlla[1], Ximena Alejandra León Ríos[2], Carmen Stefany Caballero García[1] y Marco Andrés Agurto Huerta[1]

[1]Universidad Peruana de Ciencias Aplicadas, Facultad de Ciencias de la Salud, Programa Académico de Odontología. Lima, Perú.
[2]Universidad Peruana de Ciencias Aplicadas, Facultad de Ciencias de la Salud, Programa Académico de Odontología. Lima, Perú. Grupo de Investigación CTS 367. Plan Andaluz de Investigación. Andalucía, España.

Palabras clave: determinación de la edad por los dientes; radiografía panorámica; crecimiento y desarrollo; niños; adolescente.

Resumen. Las técnicas de estimación de edad dental tienen gran importancia en la evaluación odontológica, específicamente en el área de ortodoncia, académica y forense. El objetivo de este estudio fue comparar la edad dental según los métodos de Demirjian, Nolla y Cameriere con la edad cronológica en una población peruana. El diseño del estudio es de tipo observacional, descriptivo, de corte transversal y retrospectivo; tuvo una población total de 578 radiografías panorámicas de sujetos de 6 a 14 años, en las cuales se calculó la diferencia de medias de un estudio previo y, finalmente, fueron seleccionadas 193 de forma aleatoria. Se compararon la edad cronológica (EC) y la edad dental (ED) según los métodos de Nolla, Demirjian y Cameriere, utilizando las Pruebas de Rangos de Wilcoxon y Kruskall Wallis. Las medias de la EC fueron de 8,77±2,34 y 8,90±2,04 años para el género femenino y masculino, respectivamente. Las diferencias de medias de la EC y ED, de acuerdo con los métodos Nolla, Demirjian y Cameriere, fue de -0,38, 0,96 y -0,29 años, respectivamente, para la muestra total de estudio. Se encontró una correlación positiva para los tres métodos estudiados; sin embargo, el método de Demirjian mostró una diferencia estadísticamente significativa con una subestimación de -0,91 años en la muestra total. Asimismo, el método de Cameriere fue el que tuvo más cercanía a la edad cronológica.

Autor de correspondencia: Andrea Gianella Huaman Ñahuinlla. Programa Académico de Odontología. Facultad de Ciencias de la Salud. Universidad Peruana de Ciencias Aplicadas. Lima (Perú) Teléfono: +51 980100304. E-mail: giannella.huaman@gmail.com

Comparison between chronological and dental ages according to three estimation methods in a Peruvian population.

Invest Clin 2022; 63 (1): 47 – 56

Key words: age determination by teeth; panoramic radiography; growth and development; child; adolescent.

Abstract. Dental age estimation techniques have great importance in dental evaluation, specifically in the orthodontic, academic, and forensic areas. The aim of this study was to compare the dental age according to the Demirjian, Nolla and Cameriere methods with the chronological age in a Peruvian population. This is an observational, descriptive, retrospective and cross-sectional study, which had a total population of 578 panoramic radiographs of subjects aged 6 to 14 years, where the difference in means from a previous study was calculated, and 193 subjects were finally randomly selected. The chronological ages (CA) and dental ages (DA) were compared using the Wilcoxon and Kruskall Wallis Range Tests. The means were 8.77 ± 2.34 and 8.90 ± 2.04 years of the CA for the female and male genders, respectively. The difference in means of the CA and DA according to the Nolla, Demirjian and Cameriere methods were -0.38, 0.96 and -0.21 years, respectively, for the total study sample. A positive correlation was found for the three methods studied; however, the Demirjian method showed a statistically significant difference with an underestimation of -0.91 years in the total sample. Also, the method of Cameriere was the closest to the chronological age.

Recibido: 20-05-2021 Aceptado: 09-09-2021

INTRODUCCIÓN

La edad cronológica se basa en la edad de un individuo, la cual es medida desde su nacimiento; esta determina el desarrollo y la maduración somática, además de ser predictible mediante diferentes métodos como la edad ósea, dental y morfológica [1]. Estas técnicas tienen gran importancia en la evaluación médica, odontológica en pacientes de ortodoncia y con fines académicos o forenses [2-4]. Esta edad cronológica en niños puede presentar diferencias en sus estimaciones de la edad dental, debido a procesos prematuros o tardíos, evoluciones irregulares, factores genéticos, ambientales, nutricional, género, status socioeconómico, malos hábitos que alteran el desarrollo dental en relación a su cronología, entre otros aspectos [5-7].

Actualmente, se dispone de varios métodos para estimar la edad dental entre los cuales cabe mencionar a Demirjian, Nolla, Haavikko, Willems, Cameriere, y, así determinar si la madurez dental de un individuo está dentro de su grupo de edad cronológica [2, 8, 9]. De ellos, Demirjian y Nolla son los métodos más representativos en la práctica clínica y académica por su fácil evaluación observacional basado en estadios de maduración dental y llevadas a tablas de conversión

según el género [10, 11]. Un estudio realizado en una población de Alemania comparó los métodos de Cameriere y Demirjian obteniendo como resultado que el método de Demirjian es más preciso que el método de Cameriere en niños y niñas de 6 a 14 años [12]. Un estudio del 2007, realizado en una población peruana comparó el efecto de la nutrición en el desarrollo de maduración dental, usando los métodos de Demirjian y Cameriere; se encontró que el método de Demirjian sobrestimó 1 año más en ambos sexos, mientras que el método de Cameriere tendió a subestimar a la edad cronológica [6].

En virtud de lo anterior, el objetivo de este estudio fue comparar la edad dental según los métodos de Nolla, Demirjian y Cameriere de origen americano, franco-canadiense e italiano y observar si son aplicables en una población peruana. No hay estudios en Perú que comparen las edades dentales usando los métodos Nolla, Demirjian y Cameriere, las cuales son aplicadas en diferentes poblaciones con distintas estimaciones de edades dentales para identificar la cercanía a la edad cronológica. Por otro lado, Cameriere es un método de desarrollo reciente que es aplicado en distintas poblaciones más no ha sido usado recientemente en una población peruana. El mismo es hallado mediante la aplicación una fórmula de medición [13, 14].

MÉTODOS

El diseño del estudio es observacional, descriptivo, de corte transversal y retrospectivo. Para la realización de esta investigación se solicitó la aprobación del Comité de Ética de Investigación de la Facultad de Ciencias de la Salud (CEI: 027-05-19). En todos los aspectos, este estudio cumplió con los estándares éticos actualmente requeridos por el Comité de Investigación y Ensayos Clínicos, según la Declaración de Helsinki 1964 (revisada en Fortaleza, Brasil, 2013).

Se obtuvo la base de datos de 578 radiografías de niños de 6 a 14 años atendidos en un centro universitario de salud del distrito de Chorrillos, Lima-Perú. El cálculo de tamaño de muestra fue realizado en el programa Epidat 4.2 (Xunta de Galicia/OPS) en base a un estudio previo [15]. Se utilizó una diferencia de medias de 1.15 y las desviaciones estándar de 1.99 y 2.37, correspondiente a la edad dental según Uberlaker y Demirjian respectivamente; asimismo, una razón entre tamaños muestrales de 1:1, un nivel de confianza de 95% y una potencia de 80%; finalmente, se analizaron 193 radiografías panorámicas. Estas fueron tomadas por un equipo de rayos X (Planmeca Promax 3D 2016 - Helsinki), la cual permite una visualización de mejor resolución en la pantalla de la computadora. Se realizó un muestreo aleatorio según los criterios de inclusión, los cuales fueron: radiografías panorámicas nítidas que presentaban todas las piezas dentales desde la 31 a la 37. Las radiografías panorámicas con presencia de traumas, defectos óseos, alteraciones de desarrollo, lesiones cariosas profundas, presencia de síndromes y tratamientos ortodónticos fueron excluidas.

La capacitación para la aplicación de los métodos de Nolla [10], Demirjian [11] y Cameriere [14] fue realizada por un especialista en Radiología Oral y Maxilofacial. Posteriormente, se seleccionaron 20 radiografías de forma aleatoria y se analizó la concordancia entre el interexaminador 1 y 2 con el experto mediante el Coeficiente Kappa de Cohen, encontrándose coeficientes de concordancia de "muy bueno" (0.9975 - 1). Asimismo, el Coeficiente de correlación Intraclase dio un resultado positivo (0.94984 - 0.98851).

Las variables principales del estudio fueron la edad cronológica y la edad dental. La edad cronológica (EC) se calculó restando la fecha de nacimiento del día en que se realizó la radiografía, mediante una conversión de la edad calendario a edad decimal [16]. El total de las radiografías panorámicas fueron divididas en 6 grupos de acuerdo con las edades cronológicas (de 6 a 14.9 años). La edad dental (ED) fue estimada en las radiografías por los métodos Nolla, Demirjian y Cameriere. La ED según Nolla y Demirjian, fueron medidas

en relación sus estadios de mineralización, mostrando valores numéricos y reemplazados en tablas específicas según el sexo. La ED según Cameriere fue medida en el visor Romexis. Se calculó la distancia de las superficies internas de los ápices abiertos (Ai) y la longitud del diente (Li); estos datos se normalizan mediante xi (xi=Ai/Li). La fórmula de Cameriere es:

Edad = 8.971 + 0.375 · G + 1.631 · X5 + 0.674 · N0 – 1.034 · s – 0.176 · S · N0 [14].

Siendo N0, el número de piezas dentales con desarrollo completo de la raíz y ápices cerrados, S es la suma de número de piezas con ápices abiertos, G es género (1 para niños y 0 para niñas) y X5 es la distancia (A5) sobre la longitud (L5) del segundo premolar.

Los datos fueron analizados mediante el programa Stata v.15.1 para Windows. Cada uno de los 9 grupos fueron evaluados individualmente con la prueba de Shapiro Wilk y homogeneidad de varianzas, no encontrándose normalidad en los valores de las edades. Las diferencias entre la EC y ED estimada fueron comparadas en base al año y sexo. Se utilizó la Prueba de Kruskal-Wallis para analizar los resultados de la muestra. En el análisis no estratificado por edad y sexo de los tres métodos se usó la prueba de rangos de Wilcoxon, un valor de $p<0,05$ se consideró estadísticamente significativo. Asimismo, se realizó el coeficiente de correlación de Spearman para evaluar la relación entre la edad cronológica y la edad dental estimada.

RESULTADOS

Se evaluaron un total de 200 radiografías Panorámicas, de las cuales se eliminaron 7 por no cumplir la edad requerida para esta investigación quedando un total de 193 muestras. Se encontraron diferencias estadísticamente significativas entre la edad dental y la edad cronológica, según Demirjian.

En la Tabla 1, se observa la distribución por edad y sexo de las radiografías de los niños incluidos en el estudio. La muestra estuvo constituida por 48,70% (94) sexo femenino y 51,29% (99) sexo masculino. El rango de edad de 7-7,9 representó el mayor porcentaje del total de la con 29,7% del sexo femenino y 24,3% del sexo masculino; el rango de 12-14,9 fue el que ocupó un menor porcentaje de la muestra 11,7% y 11,1%, respectivamente. Además, se comparó la edad cronológica con la edad dental, según las técnicas empleadas en el estudio. Se determinó la media de la edad cronológica y la edad dental de las técnicas Nolla, Demirjian y Cameriere, según el sexo. En los grupos de sexo femenino y masculino se encontraron diferencias estadísticamente significativas para los rangos de edad.

En la Tabla 2, se muestra la diferencia de medias entre la edad cronológica y la edad dental estimada por los diferentes métodos empleados. Se encontró que en el rango de edad de 6 a 6,9 años la técnica Demirjian presentó una diferencia de medias de -1,41 (IC al 95%, LI: -1,58, LS: -1,24), así como en el rango de 12 a 14,9 años la misma técnica mostró -1,34 (IC al 95%, LI: 0.52, LS: 1,38). Asimismo, la técnica Cameriere mostró en los rangos de edad de 8 a 8,9 una diferencia de medias de 0.23 (IC al 95%, LI: -0,03, LS: 0,49) y con la técnica Nolla, en el mismo rango, se observó un valor de 0,33 (IC al 95%, LI: 0.03, LS: 0.64).

En la Tabla 3, se muestra la comparación de la edad cronológica con la edad dental, en el total de radiografías panorámicas, según la técnica Nolla, Demirjian y Cameriere. Se encontró que la diferencia de edad dental con la edad cronológica (ED-EC) de la técnica de Demirjian, Nolla y Cameriere fueron de 0,91, -0,38 y -0,29 años respectivamente, la cual mostró que Demirjian sobreestimó (+0,91) la edad cronológica en comparación con Cameriere y Nolla. Asimismo, se hallaron diferencias estadísticamente significativas entre la comparación de la edad

Tabla 1
Comparación entre Edad Dental con la Edad Cronológica según los rangos de edad mediante tres métodos de estimación.

		Femenino			Masculino		
Rango	Método	Media	D.E	p*	Media	D.E	p*
6-6,9	EC	6,55	0,32[a]	<0,001	6,40	0,29[a]	<0,001
	Nolla	5,93	0,70[ab]		6,31	0,48[ac]	
	Demirjian	7,67	0,45[c]		7,85	0,38[b]	
	Cameriere	6,61	0,60[b]		6,81	0,38[ad]	
7-7,9	EC	7,41	0,30[ac]	<0,001	7,51	0,29[a]	<0,001
	Nolla	7,03	0,84[ab]		7,13	0,77[a]	
	Demirjian	8,14	0,55[d]		8,18	0,45[b]	
	Cameriere	7,36	0,69[bc]		7,34	0,36[a]	
8-8,9	EC	8,40	0,24	0,059	8,53	0,29[a]	<0,001
	Nolla	8,00	0,92		8,08	0,84[a]	
	Demirjian	8,85	0,92		8,99	0,79[b]	
	Cameriere	8,14	0,81		8,11	0,68[a]	
9-9,9	EC	9,54	0,34[ad]	<0,001	9,37	0,19[a]	<0,001
	Nolla	8,91	0,91[b]		8,93	0,59[bc]	
	Demirjian	10,60	1,32[c]		10,55	1,15[bd]	
	Cameriere	9,43	0,72[ad]		9,13	0,73[ab]	
10-11,9	EC	10,79	0,71[a]	0,028	11,11	0,67[a]	0,002
	Nolla	10,36	2,41[a]		9,63	1,2[b]	
	Demirjian	11,54	1,79[b]		11,47	1,83[a]	
	Cameriere	10,15	1,31[a]		9,91	0,78[ab]	
12-14,9	EC	12,04	0,73	0,062	13,05	0,57[a]	<0,001
	Nolla	13,18	2,48		12,82	1,47[a]	
	Demirjian	13,99	1,77		14,78	1,26[ab]	
	Cameriere	12,37	0,97		11,80	11,80[ac]	

*Prueba de Kruskal-Wallis, Nivel de significancia estadística (p<0,05); EC: Edad cronológica; ED: Edad dental; DE: Desviación estándar; IC: Intervalo de confianza. Las letras distintas denotan diferencias estadísticamente significativas, prueba post hoc de Kruskal Wall.

cronológica y la edad dental con la técnica Demirjian (p<0,05).

Finalmente, la Fig. 1 muestra el diagrama de dispersión positiva de la edad dental de los métodos Nolla, Demirjian y Cameriere respecto a la edad cronológica; se observa que el método de Cameriere tiene una distribución lineal en relación con la EC. Por otro lado, el método de Demirjian muestra una distribución más dispersa a la EC.

DISCUSIÓN

El estudio tuvo como objetivo determinar el método más preciso para estimar la edad dental respecto a la edad cronológica en una población peruana. Los resultados establecen que existe una correlación positiva para cada uno de los métodos; sin embargo, al comparar las medias de la edad cronológica (EC) con la edad dental (ED) se evidenció

Tabla 2
Diferencia de media entre la edad cronológica y la edad dental estimada por los diferentes métodos estudiados.

Rango	n	Método	EC-ED(DE)	IC máx	IC mín
6-6,9	33	Nolla	0,22 (0,61)	0,00	0,44
		Demirjian	-1,41 (0,48)	-1,58	-1,24
		Cameriere	-0,38 (0,49)	-0,55	-0,21
7-7,9	52	Nolla	0,17 (0,82)	-0,06	0,40
		Demirjian	-0,86 (0,60)	-1,03	-0,70
		Cameriere	-0,06 (0,66)	-0,24	0,12
8-8,9	37	Nolla	0,33 (0,91)	0,03	0,64
		Demirjian	-0,60 (0,97)	-0,93	-0,28
		Cameriere	0,23 (0,79)	-0,03	0,49
9-9,9	24	Nolla	0,26 (1,32)	-0,29	0,82
		Demirjian	-1,39 (1,59)	-2,06	-0,71
		Cameriere	0,13 (0,68)	-0,15	0,41
10-11,9	25	Nolla	0,89 (1,93)	0,09	1,68
		Demirjian	-0,58 (1,77)	-1,31	0,15
		Cameriere	0,89 (1,14)	0,42	1,35
12-14,9	22	Nolla	0,05 (1,80)	-0,74	0,84
		Demirjian	-1,34 (1,42)	-1,96	-0,70
		Cameriere	0,96 (0,97)	0,52	1,38

EC: Edad cronológica, ED: Edad dental, DE: Desviación estándar.

IC: Intervalo de confianza.

Tabla 3
Comparación de la edad cronológica y edad dental, según los métodos de Demirjian, Nolla y Cameriere en una población peruana.

	Edad Cronológica (EC)	Edad Dental (ED)		
Método	Media ±D.E	Media ±D.E	ED-EC	p*
Demirjian	8,84±2,18	9,75±2,38	0,91	0,001
Nolla	8,84±2,18	8,46±2,37	-0,38	0,057
Cameriere	8,84±2,18	8,55±1,82	-0,29	0,788

*Prueba de rangos de Wilcoxon, Nivel de significancia estadística (p<0,05).

que el método de Demirjian presentó mayor sobreestimación a la edad cronológica.

Existen diferentes métodos para estimar la edad dental tales como Nolla, Demirjian, Haavikko, Willems, Cameriere, entre otros que son contrastadas con la edad cronológica. Por un lado, Demirjian y Nolla son los más conocidos nacional e internacionalmente y han mostrado buenos resultados al predecir la edad cronológica. Además, estos son usados comúnmente en la práctica clínica y forense. Por otro lado, Cameriere es un método de estimación reciente [14], pero que ha sido aplicado a diversas poblaciones por su precisión y confiabilidad. Por las razones expuestas estos métodos han sido escogidos

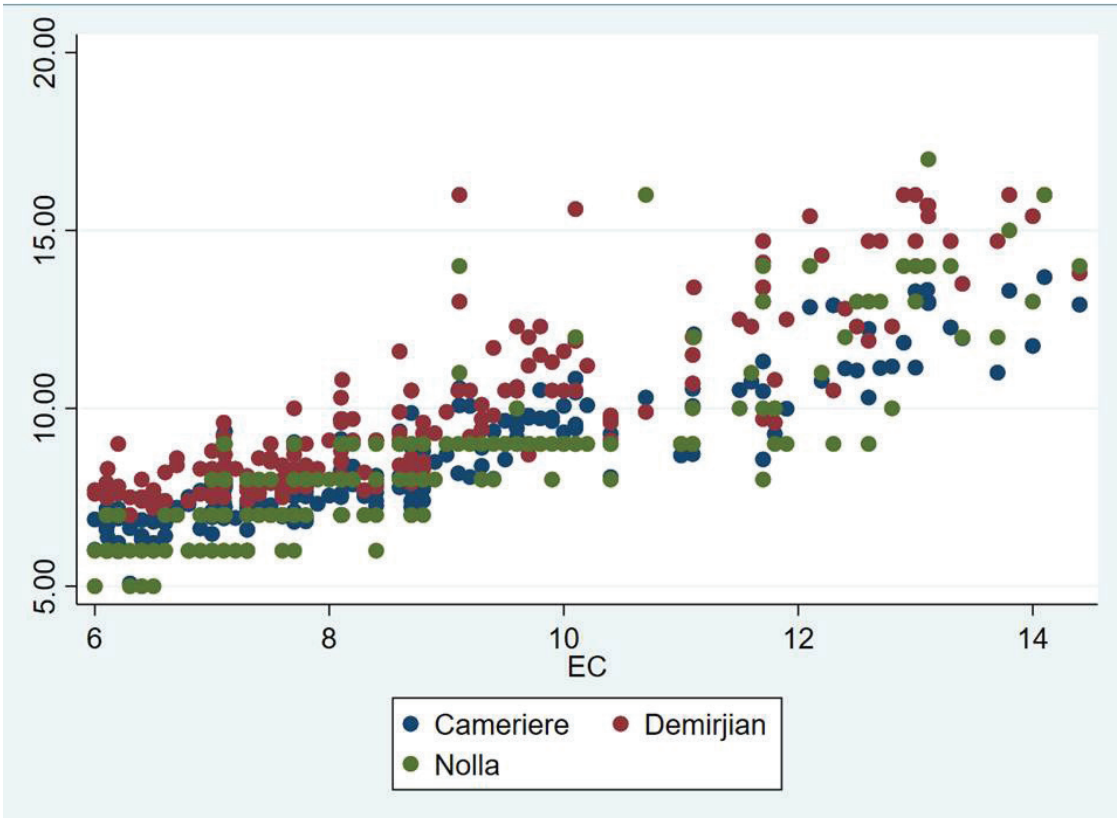

Fig. 1. Distribución de la Edad cronológica y la Edad dental, según los métodos de Demirjian, Nolla y Cameriere en una población peruana.

para ejecutar el presente estudio [2, 4, 17, 18]. El instrumento que se usa para las técnicas de estimación dental es mayormente la radiografía panorámica, por su disponibilidad, bajo costo, rápida toma de la imagen y poca distorsión de la imagen, en contraste con la radiografía intraoral, tomografía o resonancia magnética por su dificultad en tomar una imagen radiográfica en niños, la distorsión al momento de tomar la misma y por los pocos estudios que existen utilizando este tipo de pruebas diagnóstico [19].

En cuanto al método Nolla, los resultados del presente estudio mostraron una subestimación por -0,38 años para el total de la muestra, en comparación con otros estudios que mostraron mayor subestimación en ambos géneros en poblaciones de España [20, 21], Croacia [13] e India [8]. En cuanto a los países latinoamericanos, existe una subestimación menor tanto para Brasil, México como para este estudio. Esto se podría deber al mayor mestizaje presente en estas regiones en comparación al continente europeo y asiático.

Al analizar el método de Demirjian, se encontraron diferencias estadísticamente significativas al comparar la EC con ED con una sobreestimación de 0,91 años, lo cual se evidencia en estudios anteriores [20, 15]. Asimismo, en un estudio realizado en Perú, los resultados para la población masculina y femenina fue la sobreestimación de 1 año a más de la ED en comparación a la EC [15]; sin embargo, un estudio realizado en Alemania [12] mostró que el método de Demirjian fue preciso al comparar la ED con la EC.

Para el método de Cameriere, el resultado del presente estudio subestimó la edad dental por -0,29 años; este resultado es similar a otro estudio realizado en Perú [6]. Asi-

mismo, diversos autores como Ozveren [22], Javadinejad [17] y Pongo da Luz [13] mostraron una estimación de edad precisa y exacta en comparación a otros métodos. Sin embargo, en estudios recientes se puede observar que Cameriere sobreestima en grupos de edad menores (6-11 años) y subestima la edad en rangos mayores (12-14 años) [12, 24]. Esto se debe a que en estas edades las piezas dentarias se encuentran cerca de su maduración y presenta una difícil medición de las paredes internas del ápice. En cuanto al género masculino se observa un resultado de sobreestimación y subestimación dependiendo de la población. Mientras que en el género femenino se presentó subestimación de la edad cronológica.

La subestimación y la sobreestimación es debido a que existen muchos factores que pueden alterar el desarrollo y erupción de piezas dentales, tales como el origen étnico. Se ha observado en diversos estudios que los diferentes métodos tienden a inclinarse o alejarse de poblaciones específicas al momento de predecir la ED, por sus usos en una muestra diferente a la población original [13, 25]. Asimismo, factores como la desnutrición [9] generan a un impacto negativo en el desarrollo esquelético y formación dental, puesto a que altera la proliferación celular para la transformación del folículo dental relacionado con el proceso de mineralización donde proteínas y enzimas activan o desactivan las funciones de mineralización dental, ósea y capacidad de erupción; sin embargo, una buena nutrición tienen cambios positivos en cuanto a su desarrollo y crecimiento, estado de salud y calidad de vida [6, 9, 26].

Con respecto al género femenino, el desarrollo es más rápido debido a los cambios hormonales en la pubertad durante la cual muestran una maduración dental acelerada en comparación con el género masculino; por lo tanto, existe una diferencia en cuanto su comparación de la edad dental con la cronológica [23, 27]. Asimismo, los factores biológicos como bajo peso al nacer o niños nacidos prematuramente, influyen en el desarrollo intrauterino de las piezas dentales y su posterior desarrollo en la primera infancia [28].

Estos factores pueden producir una variación de las edades en una pequeña o mayor diferencia a los resultados de estimaciones de la ED y así no acercarse a la EC [29]. Además, el método de Demirjian tiene una muestra original francesa-canadiense, por lo cual presenta características fenotípicas y genotípicas diferentes a la muestra de esta investigación. Según Liversidge y otros [18], la sobreestimación en diferentes estudios se debe a una distribución normal, donde la media es pobre en los extremos de edad, por lo cual el uso de estos métodos no es factible en muestras pequeñas o rangos de edad insuficientes. Asimismo, Liversidge y col. [25] realizaron un estudio en el 2015 donde estimó la edad dental de una población europea, encontrando diferencias estadísticamente significativas; concluyó que se debe realizar con frecuencia las estimaciones dentales por los diferentes cambios que pueden presentar una población.

Por lo antes expuesto, el método de Cameriere mostró una subestimación de -0,29 años acercándose a la EC y mostrando ser un buen método para análisis forense y clínico de individuos con edades desconocidas, al ser un tipo de método por medición y fórmula hay un margen de error menor para la predicción de la EC. Finalmente, se recomienda el uso de una muestra extensa con grupos de edad amplios e iguales para obtener resultados más precisos, confiables y replicables en una población.

Financiamiento

La investigación fue financiada por la Universidad Peruana de Ciencias Aplicadas (UPC), Código "EXPOST-UPC".

Declaración de conflicto de intereses

No existe conflicto de intereses.

Número ORCID y Contribución de autores

- LMPQ: 0000-0002-0916-9043. Recolección de datos, ejecución del análisis estadístico, redacción del borrador original.
- AGHÑ: 0000-0001-6304-5036. Recolección de datos, ejecución del análisis estadístico, redacción del borrador original.
- XALR: 0000-0002-3494-331X. Análisis e interpretación de los datos, redacción del manuscrito final.
- SCG: 0000-0001-8672-9369. Supervisión de la investigación, análisis e interpretación de los datos, redacción del manuscrito final.
- MAAH: 0000-0002-3192-7509. Conceptualización de la investigación, supervisión de la recolección de datos y capacitación para la aplicación de los métodos de estimación.

REFERENCIAS

1. **Pizano M, Quezada M, Del Castillo C, Orejuela F**. Estimación de la edad de acuerdo al método de Demirjian en niños de 4 a 16 años de la Ciudad de Puebla, México. Rev Estomatol Herediana. 2016; 26(3):139-146. *Doi: 10.20453/reh.v26i3.2957*.
2. **Apaydin B, Yasar F.** Accuracy of the demirjian, willems and cameriere methods of estimating dental age on turkish children. Niger J Clin Pract 2018; 21:257-263. *Doi: 10.4103/1119-3077.226966*.
3. **Aguirre E, Del Castillo C, Orejuela F, León R, Quezada M**. Estimación de la edad de acuerdo al método de Demirjian en niños de 5 a 16 años de la ciudad de Guayaquil, Ecuador. Rev Estomatol Herediana. 2017; 27(4):235-241. *Doi: 10.20453/reh.v27i4.3215.*
4. **Martínez V, Ortega A**. Comparación de los métodos de Nolla, Demirjian y Moorrees en la estimación de la edad dental con fines forenses. Rev Odontol Mexicana 2017; 21(3): 155-164. *Doi: 10.1016/j.rodmex.2017.09.002*.
5. **Lewis A, Garn S.** The relationship between tooth formation and other maturational factors. Angle Ortho. 1960; 30(2)70-77.
6. **Cameriere R, Flores C, Mauricio F, Ferrante L**. Effects of nutrition on timing of mineralization in teeth in a Peruvian sample by the Cameriere and Demirjian methods. Ann Hum Biol 2007; 34(5): 547–556. *Doi: 10.1080/03014460701556296.*
7. **Marques M, Ribeiro R, Pereira D, Rabelo S, Francesquini L, Daruge E**. Age estimation by measurements of developing teeth: accuracy of Cameriere's method on a Brazilian sample. J Forensic Sci 2011; 56(6):1616-1619. *Doi: 10.1111/j.1556-4029.2011.01860.x*
8. **Mohammed R, Sanghvi P, Perumalla K, Srinivasaraju D, Srinivas J, Kalyan U, Rasool SK.** Accuracy of four dental age estimation methods in southern Indian children. J Clin Diagn Res 2015; 9(1): 1-8. *Doi: 10.7860/JCDR/2015/10141.5495*.
9. **Ayodeji T, Yengopal V, Schepartz L**. The Demirjian versus the Willems method for dental age estimation in different populations: a meta-analysis of published studies. PLoS ONE 2017; 12(11): 1-23. *Doi: 10.1371/journal.pone.0186682*.
10. **Nolla C**. The development of the permanent teeth. J Dent Child 1960; 27(3): 254-266.
11. **Demirjian A, Goldstein H, Tanner JM.** A new system of dental age assesment. Ann Hum Biol 1973; 45(2):211-227.
12. **Wolf T, Briseño-Marroquín B, Callaway A, Patyna M, Müller V, Willershausen I, Ehlers V, Willershausen B.** Dental age assessment in 6- to 14-year old German children: comparison of Cameriere and Demirjian methods. BMC Oral Health 2016; 16 (120): 1-8. *Doi: 10.1186/s12903-016-0315-8.*
13. **Pongo da Luz L, Anzulović D, Benedicto E, Galic I, Brkić H, Biazevic M.** Accuracy of four dental age estimation methodologies in Brazilian and Croatian children. Sci Justice 2019; 59(4): 442-447. *Doi: 10.1016/j.scijus.2019.02.005*.
14. **Cameriere R, Ferrante L, Cingolani M.** Age estimation in children by measurement of open apices in teeth. Int J Legal Med 2006; 120: 49–52. *Doi: 10.1007/s00414-005-0047-9.*

15. **Pachas A, Suárez D, Evaristo T**. Estimación de la edad cronológica a través de los métodos de Demirjian y Ubelaker en niños peruanos. Int J Dent Sci 2019; 21(2): 95-103. *Doi: 10.15517/ijds.v0i0.36828.*
16. **Eveleth P, Tanner J.** Worldwide variation in human growth, 2nd ed. Cambridge: Cambridge University Press, 1990. 405.
17. **Javadinejad S, Sekhavati H, Ghafari R.** A comparison of the accuracy of four age estimation methods based on panoramic radiography of developing teeth. J Dent Res Dent Clin Dent Prospects 2015; 9(2): 72-78. *Doi: 10.15171/joddd.2015.015*
18. **Liversidge H, Smith B, Maber M.** Bias and accuracy of age estimation using developing teeth in 946 children. Am J Phys Anthropol 2010; 143(4): 545-554. *Doi: 10.1002/ajpa.21349.*
19. **Bjørk M, Kvaal SI**. CT and MR imaging used in age estimation: a systematic review. J Forensic Odontostomatol 2018; 36(1): 14-25.
20. **Melo M, Ata-Ali J**. Accuracy of the estimation of dental age in comparison with chronological age in a Spanish sample of 2641 living subjects using the Demirjian and Nolla Methods. Forensic Sci Int 2017; 270-276. *Doi: 10.1016/j.forsciint.2016.10.001*
21. **Paz M, Rojo R, Mourelle M, Dieguez M, Prados-Frutos J**. Evaluation of the accuracy of the Nolla method for the estimation of dental age of children between 4-14 years old in Spain: A radiographic study. Forensic Sci Int 2019; 301: 318-325. *Doi: 10.1016/j.forsciint.2019.05.057.*
22. **Ozveren N, Serindere G, Meric P, Cameriere R**. A comparison of the accuracy of Willems' and Cameriere's methods based on panoramic radiography. Forensic Sci Int 2019; 302: 1-7. *Doi: 10.1016/j.forsciint.2019.109912.*
23. **Alshihri A, Kruger E, Tennant M.** Dental age assessment of Western Saudi children and adolescents. Saudi Dent J 2015; 27(3): 131-136. *Doi: 10.1016/j.sdentj.2015.01.002.*
24. **Nigro L, Haltenhoff R, Lascala C, Velandia L, Cameriere R**. Age estimation: Cameriere's open apices methodology accuracy on a southeast Brazilian sample. J Forensic Leg Med 2018; 58:164-168. *Doi: 10.1016/j.jflm.2018.06.006.*
25. **Liversidge H.** Controversies in age estimation from developing teeth. Ann Hum Biol 2015;1(1): 1-10. *Doi: 10.3109/03014460.2015.1044468.*
26. **Vaillard E, Huitzil E, Moyaho M, Ortega A, Castillo L**. Efectos de la desnutrición infantil en la erupción dental. Rev Tamé 2015; 3 (9): 289-296.
27. **Dhongde P, Chandak S, Atulkar M, Moon A.** Assesment of growth status: Nolla's dental age v/s chronological age. Int J Oral Health Med Res 2017;3(5):15-17.
28. **Manjunatha B, Soni N**. Estimation of age from development and eruption of teeth. J Forensic Dent Sci 2014; 6(2):73-76. *Doi: 10.4103/0975-1475.132526.*
29. **Liversidge H.** Interpreting group differences using Demirjian's dental maturity method. Forensic Sci Int 2010; 201(1-3): 95-101. *Doi: 10.1016/j.forsciint.2010.02.032.*

Invest Clin 63(1): 57 - 69, 2022 https://doi.org/10.54817/IC.v63n1a05

A new approach of immunotherapy against *Crotalus* snakes envenoming: ostrich *(Struthio camelus)* egg yolk antibodies (IgY-technology).

Carlos Bello[1], Fátima Torrico[1], Juan C. Jiménez[1,2], Mariana V. Cepeda[1], Miguel A. López[1] and Alexis Rodríguez-Acosta[1,3]

[1]Biotecfar C.A, Facultad de Farmacia, Universidad Central de Venezuela, Caracas, República Bolivariana de Venezuela.
[2]Instituto de Inmunología, Facultad de Medicina, Universidad Central de Venezuela, Caracas, República Bolivariana de Venezuela.
[3]Laboratorio de Inmunoquímica y Ultraestructura, Instituto Anatómico, Universidad Central de Venezuela, Caracas, República Bolivariana de Venezuela.

Key words: antivenom; *Crotalus* snakes; ostrich egg yolk; IgY; *Struthio camelus*; venom.

Abstract. Crotalid envenomation is a neglected collective health problem involving many countries in America, which need secure and inexpensive snake anti-venom treatments. Here, high antibody titers (IgY) were raised in the Ostrich (*Struthio camelus*) egg yolk by immunizing with the venom of Venezuelan venomous *Crotalus* snakes. Ostriches were immunized with a pool of venoms from common rattlesnake (*Crotalus durissus cumanensis*), Uracoan rattlesnake (*Crotalus vegrandis*), Guayana rattlesnake (*Crotalus durissus ruruima*) and black rattlesnake (*Crotalus pifanorum*). The anti-snake venom antibodies were prepared from egg yolk by the water dilution method, enriched by the addition of caprylic acid (CA) and precipitation with ammonium sulfate at 30% (W/V). The purity and molecular mass of the final product was satisfactory, yielding a single ~ 175 kDa band in SDS-PAGE gels ran under non-reducing conditions. In the immunoblot analysis, specific binding of the antivenom was observed with most venom proteins. The LD_{50} was 16.5 g/mouse (825 μg/kg body weight). High titers of IgY against Crot/pool venom were shown by ELISA. The median effective dose (ED_{50}) was 19.66 mg/2LD_{50}. IgY antibodies neutralized efficiently the *Crot*/pool venom lethality. As far as we know, this is the first anti-snake venom produced in ostriches, which could make this technology an affordable alternative for low-income countries, since it is likely to produce

Corresponding author: Alexis Rodríguez-Acosta. Instituto Anatómico, Ciudad Universitaria de Caracas, Universidad Central de Venezuela, Caracas 1041. Email: rodriguezacosta1946@yahoo.es

about 2-4 g of IgY per ostrich egg. Hence, almost 400 g of IgY can be purified from only one ostrich during a year. In addition, there are enormous differences in the cost of investment in the maintenance of horses, from the points of view of infrastructure, feeding and veterinary care, in which the cost can reach USD 100 per animal per day, compared to a maintenance cost of USD 146 per month per producing bird. These results are encouraging and could easily be extrapolated to the manufacturing of other antivenoms and antitoxins as well, as they could be applied to the manufacturing of potential diagnostic tools.

Un nuevo enfoque de inmunoterapia contra el envenenamiento de serpientes *Crotalus:* anticuerpos de yema de huevo de avestruz *(Struthio camelus)* (tecnología IgY).

Invest Clin 2022; 63 (1): 57 – 69

Palabras clave: antiveneno; avestruz *Crotalus*; IgY; *Struthio camelus*; veneno.

Resumen. El envenenamiento por crotálidos es un problema de salud colectiva desatendido, que involucra a muchos países del continente americano, los cuales necesitan tratamientos seguros y económicos. En este trabajo, se obtuvieron títulos altos de anticuerpos (IgY) producidos en yema de huevo de avestruz (*Struthio camelus*) mediante la inmunización con el veneno de serpientes venezolanas del genero *Crotalus*. Se inmunizaron avestruces con una colección de veneno de serpientes de cascabel común (*Crotalus durissus cumanensis*), cascabel de Uracoa (*Crotalus vegrandis*), cascabel de Guayana (*Crotalus durissus ruruima*) y cascabel negra (*Crotalus pifanorum*). Los anticuerpos anti-veneno de serpiente se prepararon a partir de yema de huevo por el método de dilución en agua, enriquecidos mediante la adición de ácido caprílico (CA), seguido de una precipitación con sulfato de amonio al 30% (P/V). La pureza y masa molecular de los anticuerpos (IgY) se definieron mediante ensayos de SDS-PAGE nativos y las masas moleculares se establecieron electroforéticamente, obteniéndose una única banda de IgY de ~ 175 kDa. El análisis de inmunotransferencia mostró la unión específica del antiveneno con la mayoría de las proteínas del veneno. La DL_{50} fue de 16,5 μg/ratón (825 μg / kg de peso corporal); Se mostraron títulos altos de IgY contra el veneno de Crot / pool mediante ELISA. La dosis mediana efectiva (DE_{50}) fue de 19,66 mg/2 LD_{50}. Los anticuerpos IgY neutralizaron eficazmente la letalidad del veneno de Crot / pool. Hasta donde sabemos, se trata del primer antídoto de serpiente producido en avestruces, lo que podría abaratar la producción de este tratamiento en países del tercer mundo. Ya que es probable que se obtengan alrededor de 2-4 g de IgY por huevo de avestruz. Por lo tanto, se podrían purificar casi 400 g de IgY de un solo avestruz durante un año. Asimismo, debido a las enormes diferencias en el costo de inversión en el manteni-

miento de los caballos desde el punto de vista de infraestructura, alimentación y atención veterinaria, en los que el costo puede llegar a los 100 USD por día, frente a los 146 USD por mes de mantenimiento de la producción de aves. Estos resultados abren un campo terapéutico, para la fabricación de otros antivenenos contra un amplio espectro de toxinas y también como probables herramientas de diagnóstico.

Received: 03-08-2021 Accepted: 04-11-2021

INTRODUCTION

Venomous snakebite is a worldwide problem, especially in tropical and subtropical geographical regions. There are more than five million snakebite accidents annually worldwide; the members of the Viperidae family [1] produce the most common snakebites that take place in the American continent (~ 98%).

Traditional antivenom production is based on purified antibodies extracted from hyperimmunized horses' plasma [2]. In recent years, several authors report that bird's (mainly chicken) antibodies produced against snake venoms, presented venom effective neutralization activities [2,3]. However, despite their potential considering their body size and egg-laying advantages, ostriches (*Struthio camelus*) have not been previously tested for snake anti-venom production. Clinical assays will be need to assess their security as an antidote to human victims of ophitoxemia and further experimentation addressing IgY-based antivenoms safety and effectiveness is required.

MATERIALS AND METHODS

Reagents

Polyvalent anti-ophidic serum (PAOS) (Biotecfar C.A, Universidad Central de Venezuela, Pharmacy Faculty, Caracas, República Bolivariana de Venezuela). Sodium chloride, sodium citrate, sodium azide, tris, hydrochloric acid, sodium hydroxide, Coomassie blue, acrylamide, bis-acrylamide, ammonium per-sulphate, glacial acetic acid, temed, glycerol, sodium bicarbonate, caprylic acid (Sigma-Aldrich, Missouri, USA). Saran wrap (S.C. Johnson & Son, Inc, USA). Complete Freund's and incomplete Freund's adjuvants (GIBCO, USA). Antibody goat anti-avian (included anti-ostrich) (Laboratories ABCAM, USA). Peroxidase substrate (TMB) (Vector Lab, USA). 30 kDa cassette filtration unit (Vivaflow 50 R, Sartorius, Germany). Filter (Sartorious Laboratories, Germany). Microtitration plates (Corning® ELISA microplates, USA). Automatic ELISA reader (Bio-Tek Laboratories, USA). Mini-Protean II system (Bio-Rad Laboratories, USA). Trans Blot SD system (Bio-Rad Laboratories, USA). Molecular mass standards for SDS-PAGE were from Bio-Rad Laboratories Ltd (California, USA).

Ostriches

Two female healthy adult ostriches (*Struthio camelus*) were obtained from a local ostrich farm (Villa de Cura town, Aragua state, República Bolivariana de Venezuela). They were housed under standard environment (humidity, lighting and temperature) and fed *ad libitum* with standard ostrich diet and potable water (Fig. 1).

Venom

A pool of venoms from common rattlesnake (*Crotalus durissus cumanensis*) (0.15 mg/mL), Uracoan rattlesnake (*Crotalus vegrandis*) (0.03 mg/mL), Guayana rat-

Fig. 1. (A) Ostriches at bird's farm, Villa de Cura, Aragua state, Venezuela. (B) *Crotalus durissus cumanensis*. (C) *Crotalus ruruima*. (D) *Crotalus pifanorum*. (E) *Crotalus vegrandis* (1).

tlesnake (*Crotalus durissus ruruima*) (0.02 mg/mL) and black rattlesnake (*Crotalus pifanorum*) (0.012mg/mL) were obtained by milking the snakes and then crystallized under vacuum in a desiccator containing $CaCl_2$ as a desiccant and maintained at 4°C until use (Fig. 1).

Ethical statement

Skilled staff prepared all the experimental methods relating to the use of live animals. These methods were permitted by the Institute of Anatomy Ethical Committee of the Universidad Central de Venezuela under assurance number (Protocol N° 190619) and followed the norms obtained from the Guidelines for the Care and Use of Laboratory Animals, published by the USA National Institute of Health [4].

Immunization procedure

Two female ostriches were injected intramuscularly intro the bird's anterior thigh muscles on day 0 with the *Crot*/pool of the Venezuelan rattlesnake venoms (1μg/kg body weight) emulsified with an equivalent volume of complete Freund's adjuvant. The primary booster dose was administered two weeks later in an incomplete Freund's adjuvant. Successively, the second and third boosters emulsified with an equivalent volume of incomplete Freund's adjuvant were administered at 45-day intervals in order to sustain high antibody titers. Blood was collected through the wing vein, arranged to obtain the serum. Sera were separated by centrifugation (1500 G for 15 min). Preimmune serum and egg yolk replicas collected from ostriches were used as negative controls. They were stored in a freezer at −20°C, until used.

Purification of antibodies from egg yolk

Isolation of IgY from egg yolk was performed with a modified method [5]. Briefly, once the egg shell was opened, the yolk was softly detached from the white of the egg, washing it with abundant distilled water, until all the white egg disappeared. Then, the yolk was punctured with a syringe and all its contents were extracted and mixed completely with a five-fold dilution with PBS pH 7.4 and slow addition of caprylic acid (CA), then the pH was adjusted to 5.0 with 10 M

hydrochloric acid. Concisely, the CA was slowly added dropwise at an approximate rate of 0.6 mL/min, until a final concentration of 6% (v/v) was obtained.

After the first step of the process, the sample was filtered through a 15 μm and then 0.45 μm filter.

The preparation was kept to room temperature, and afterward ammonium sulfate at 30% (W/V) concentration was added, keeping it under constant stirring for one hour at room temperature and then filtered through a 2-μm filter. In order to eliminate the ammonium sulfate, a tangential filtration process was applied using a cassette of 30 kDa. The sample was resuspended in saline solution and kept under stirring for one hour- Subsequently, filtered through a 2-μm filter to remove remaining solids and a diafiltration process was started until eight diafiltration volumes were completed. When the ammonium sulfate was removed, the washed sediment was dissolved in 200 mL saline pH 6.3.

Sodium dodecyl sulfate-polyacrylamide gel electrophoresis (SDS-PAGE) of IgY

Purified IgY under non-reduced and reduced conditions were electrophoresed with a MINIPROTEAN II (BioRad, USA) chamber. SDS-PAGE was performed using 12% gels. Wide range molecular weight markers (Bio-Rad) were run in parallel and gels were stained with Comassie blue (National Diagnostic, USA).

Determination of antibody titers by an indirect ELISA

The immunoglobulins titers in serum and egg yolk of immunized ostriches were tested by enzyme-linked immunosorbent assay (ELISA). Titer was considered as the concentration of an antibody, as determined by finding the highest dilution at which it was still able to cause recognition of the antigen. The uncomplicated way to do this is as follows: selecting the highest responding serum and another that shows low response. Do readings for serial dilutions as we have done (Fig. 3). Looking for one dilution were both sera are in the steepest part of the curve, are clearly different (generally a 1:1000 – 1:4000 dilutions will do it) and the OD450nm of the most responding serum is nearly 1.0. Then it is possible to define the titer as the OD450nm for each serum at the dilution obtained before.

All ELISA incubations were carried out at 24-26°C. Briefly, aliquots (100 μL) of the *Crot*/pool venom (1 μg/mL PBS) were pipetted into the wells of the micro-titration plates in overlay phosphate buffer saline (PBS) pH 7.4 that were protected with saran wrap and stored overnight at 4°C. The wells content was aspirated, and washed three times with washing buffer (PBS, pH 7.4 containing 0.05% Tween-20), the wells were then overflowed with blocking buffer (skimmed milk 2% in PBS-T) and left for one hour. After the aspiration of blocking buffer, the ostrich sera or purified IgY immunoglobulins samples were diluted properly in blocking buffer and 100 μL added to the wells before incubating at 37°C for one hour. Later, the plates were washed three times with washing buffer and incubated with goat anti-avian (included anti-ostrich) IgY peroxidase (1:10.000) at 37°C for one hour. The contents of the wells were subsequently aspirated, the wells washed three times with PBS-0.05% Tween 20 (PBS-TW), and 100 μL of peroxidase substrate (TMB)(Vector Lab, USA) was added to each well. The plates were maintained in the dark, at room temperature for 20 min for the progress of dye. The reaction was stopped with 50 μL of sulfuric acid 1 M. The absorbance of solutions at X = 450 nm was determined after the addition of substrate by an automatic ELISA reader.

Immunoblot analysis

Recognition of IgY antibodies was performed by western blot according to the modified method [6] (n=3). Briefly, to determine the specificity of the immunoglobulins against *Crot*/pool snake venoms, the anti-

bodies were tested with a total of six venoms *Crotalus durissus cumanensis*, *Crotalus vegrandis, Crotalus durissus ruruima,* and *Crotalus pifanorum* venoms.

These venoms were electrophoresed on a 10% SDS gel using a Mini-Protean II system at 150V (Bio-Rad PowerPac Basic) for one hour. Then, were transferred onto a 0.2 μm nitrocellulose membrane (Millipore) using a Trans Blot SD system at 100 mA for one hour. After blocking the membrane for one hour at room temperature with 5% skimmed dry milk in PBS buffer pH 7.4 containing 0.05% (w/v) Tween 20, the nitrocellulose membrane was incubated under stirring for one hour with anti-*Crot*/pool ostrich IgY antivenom diluted to 1:1000 in PBS-Tween 20. After the rinses, the secondary antibody goat anti-avian IgY (coupled to horseradish peroxidase) diluted 1:20000 in PBS-Tween 20 was complemented. Finally, blots electrophoretic bands identified by *Crot*/pool ostrich IgY antivenom were colorimetric visualized using the peroxidase substrate (TMB), and the image was analyzed.

Lethality Dose (LD_{50})

Five groups of five NIH female mice (*Mus musculus*) for *Crot*/pool venom were maintained in plastic boxes (Tecniplast, Italy) and observed throughout the quarantine period and experiments. The endpoint of lethality of the mice was established after 48 hr. The venom was suspended in 0.85% saline at the maximum test dose per mouse. Serial dilutions of 2-fold using saline solution were prepared to obtain four extra concentrations. All solutions throughout the experiment were kept at 0°C and warmed to 37°C before being injected into mice. The lethal toxicity was determined by injecting 0.2 mL of venom (containing dosages ranging between 38.0 to 11.6 μg/mouse) into the peritoneum of 18–20 g female NIH mice. The injections were dispensed using a 1-mL syringe fitted with a 25-gauge, 0.5-inch needle. Saline as normal controls were used. The lethal dose fifty (LD_{50}) was calculated following the Spearman-Kärber (n = 3 ± SD) method [7]. The estimated LD_{50} was then used for testing median effective dose fifty (ED_{50}/2 LD_{50}).

Antivenom neutralization test: median effective dose fifty (ED_{50}/2 LD_{50}) assays of yielded antibodies (anti-Crot/pool ostrich IgY antivenom neutralizing lethal toxic activity of Crot/pool venom)

The median effective dose value (ED_{50}) of the *anti-Crot/pool* ostrich IgY antivenom from ostrich egg yolk was measured for analysis of quantitative and categorical data, with the aid of the Prism 8 program (Graphpad, USA). Five groups of five female NIH mice (18–20 g) were confronted with a combination of serial dilutions of a certain amount of anti-*Crot*/pool venoms (1.488, 1.395, 1.321, 1.145, 0.843), containing constant concentration of *Crot*/pool venom (33 µg). 2LD_{50}: (LD_{50}=16.5 μg/mouse x 2 = 33 μg venom/20 g mouse). The Ostrich IgY anti-*Crot*/pool venom/ *Crot*/pool venom combinations were pre-incubated for 30 min at 37°C, then was intravenously injected into mice for each dose. Negative control mice were injected with two LD_{50} of venom alone. The neutralizing potency reproduces the ratio of mL of anti-*Crot*/pool venom /mg of *Crot*/pool venom or mg of antivenom/mg of venom. The control group was also injected with venom pre-incubated with normal ostrich serum.

RESULTS

Immune response

Two female ostriches were immunized as described in Materials and Methods. Detectable specific IgY anti-venom responses were not observed in sera until 15 days from the initial dose, by the time of the first booster-dose. This secondary response was sustained thereafter by successive booster injections given at 45-days pauses.

IgY purification

At a pH of 5-6 most of the immunoglobulins were recovered and the caprylic acid

precipitation leads to a maximum recovery of IgY, with minimum contaminating proteins. After ammonium sulfate purification, the obtained sample under reduction conditions gave two mains electrophoretic IgY bands of ~65 and ~20 kDa. Otherwise, under non-reducing conditions a IgY single band of ~175 kDa was observed (Fig. 2). The average recovery of IgY from a single egg yolk was ~ 3800 mg (N=5).

Immune-specific recognition of crotalic venom pool by IgY

The anti- *Crot*/pool venom-specific activity of IgY in partially purified preparations was assayed by a home-designed indirect ELISA as described in Materials and Methods. The purification procedure resulted in venom-specific IgY recognition of *Crot*/pool venoms (Fig. 3). Microtiter plates with pre-immune serum showed no binding.

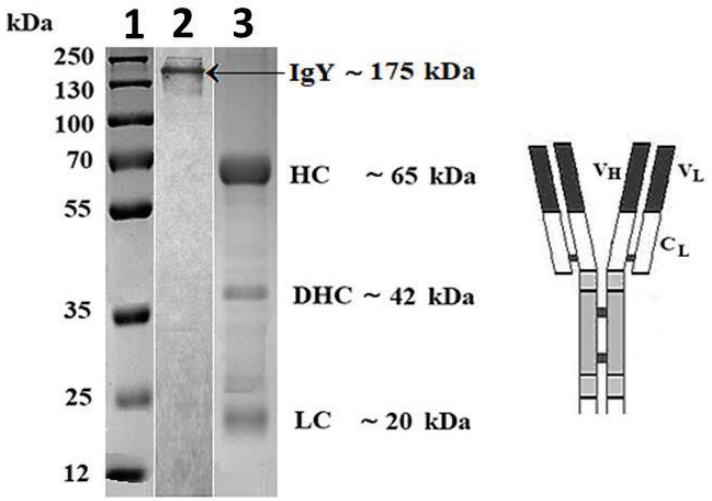

Fig. 2. IgY tested under native and reduction conditions. (**1**) Molecular mass markers. (**2**) IgY (native conditions); (**3**) Under reducing conditions HC: Heavy chain; DHC: Detritus heavy chain; LC: Light chain; VH: Variable fraction of heavy chain; VL: Portion variable light chain; CL: Constant fraction of light chain.

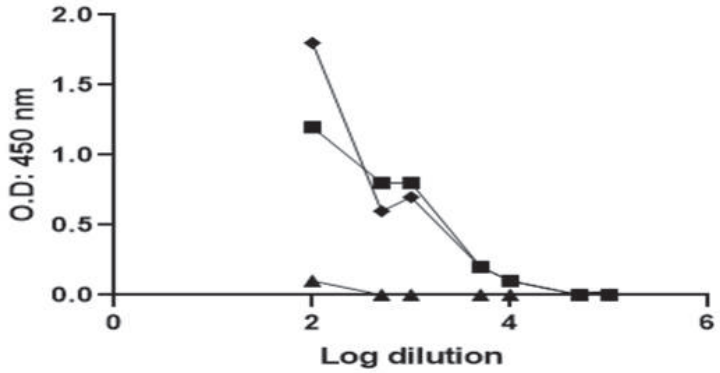

Fig. 3. ELISA immuno-specific recognition of IgY. The anti- *Crot*/pool venom-specific activity of IgY showed that final product (rhombus) and final product dialyzed (square) resulted in the venom-specific IgY recognition of *Crot*/pool venoms. The pre-immune serum (triangle) was negative.

Specificity of Crot/pool antivenom (IgY) to *Crotalus* venoms via Western blot

The identity of the *Crot*/pool venom proteins was confirmed with the *Crot*/pool antivenom (IgY) by Western-blot, identifying most of the fraction venoms used in the present work (Fig. 4). As a reference, the polyvalent antivenom of equine origin produced by BIOTECFAR C.A (Caracas, Venezuela) was used.

Antivenom effective dose (ED_{50})

In order to estimate the ED_{50} of the final *Crot*/pool antivenom (IgY), different amounts of this antivenom were preincubated with $2LD_{50}$ (33 μg) of a *Crot*/venom pool, as described in Materials and Methods. An ED_{50} of 19.66 mg was calculated for the *Crot*/pool antivenom, as the minimum amount of purified IgY preparation able to protect 50% of the mice population. There were no survivals in the control group (Table 1, Fig. 5).

DISCUSSION

Snakebite accidents, categorized as a neglected tropical disease by the World Health Organization (WHO) is responsible for nearly 50.000 deaths annually, mostly in Third World countries [8].

In the current work specific anti-*Crotalus* snake venoms antibodies were obtained by an immunization schedule in female ostriches *(Struthio camelus)*. The eggs from bird species have demonstrated being a desirable basis for the production of antibodies, without invasive methods, which present a predominant class of IgY immunoglobulin [3, 9,10]. This IgY has been used in diagnosis, research, and immunotherapy [11-13]. Furthermore, bird's immunoglobulins production poses several benefits over mammalian antibodies with respect to the antigenic specificity and low manufacturing expenses [3,12]. It was possible to obtain about 2-4 g of IgY per ostrich egg. Hence, almost 400 g of IgY can be purified from only one ostrich per year. For that reason, ostrich eggs could represent an exceptional source of immunoglobulins for antivenom production.

A great amount of cross-reactive and neutralizing antibodies (IgY) were produced in the egg yolk of ostriches (*Struthio camelus*) by immunizing with the venom of four *Crotalus* (*Crot*/pool) using a simple and

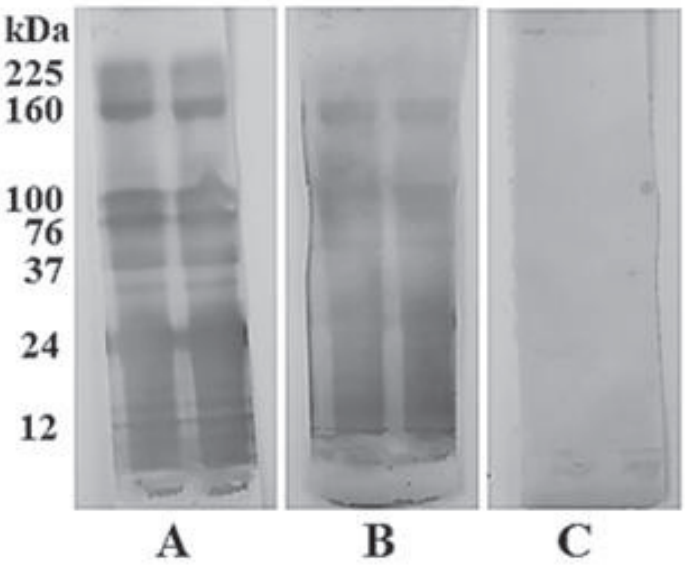

Fig. 4. Western blot. (A) *Crot*/pool venom+ PAOS (Biotecfar C.A, Venezuela); (B) *Crot*/pool venom+ immunized ostrich IgY; (C) Negative control (Non-immunized ostrich IgY+PBS).

Table 1
Determination of the survive percentage of mice after the injection of $2LD_{50}$ of *Crot*/pool venom with different concentrations of ostrich IgY. Evaluation of the neutralizing capacity of anti-crotalic IgY antibodies.

LD50 16.5 (μg/mouse)												
Concentration (mg/mL)	Vol. (mL) Mx	Amount of proteins (mg)	Vol. (mL) Venom	Amount of injected venom (μg)	Vol. (mL) Saline solution	Final Vol. (mL)	Inoculated animals	Dead	Alive	Accumulated Deaths	Accumulated Alive	% survival
18.6	1.655	30.78	0.330	33	0.015	2	5	0	5	0	13	100.00
	1.335	24.83			0	1.5	5	1	4	1	8	88.89
	1.125	20.93			0.375	1.5	5	2	3	3	4	57.14
	0.750	13.95	0.165		0.750	1.5	5	4	1	7	1	12.50
	0.375	6.98			1.125	1.5	5	5	0	12	0	0.00
	0.190	3.53			1.310	1.5	5	5	0			

LD_{50}: Lethal dose fifty; Vol: Volume.

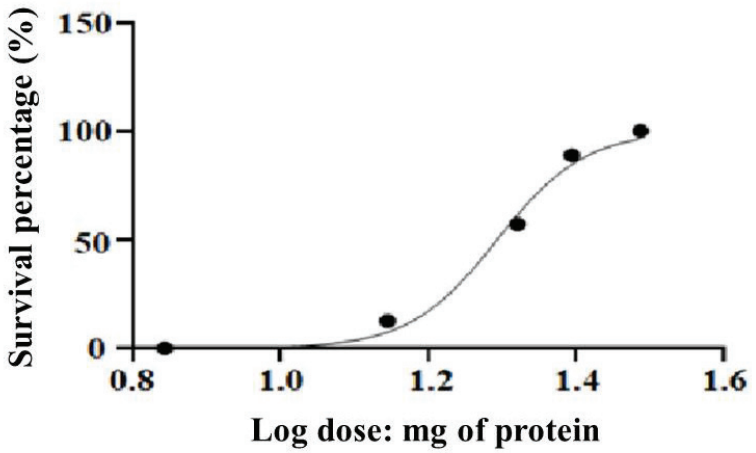

Fig.5. Curve of Log doses of mg of protein with the percentage of survival animals. An ED_{50} of 19.66 mg *Crot/* pool antivenom (IgY) was calculated from the represented data as the mass of IgY that was able to protect at least 50% of the mice population against a $2LD_{50}$ (33 μg) challenge of *Crot/*pool venom. In the control group there were no survivals. (%): percentage. (Log): logarithm.

inexpensive method. Knowledge of venom variations permits the selection of suitable specimens for production of more effective antivenoms and biological substances.

The anti- *Crot/*pool venom immunoglobulins were carried out from egg yolk by the McLaren RD et *al*. [5] method and given a single pure electrophoretic IgY band of 174 kDa (native conditions) and 65/20 kDa (under reduced conditions) in the SDS-PAGE.

Neutralization experiments demonstrated a high neutralization capacity of the anti- *Crot/*pool preparation, as a preincubated mixture of both purified antivenom (19.66 mg) with two LD_{50} dose of *Crot/*pool venom (33 μg) protected 50% of the mice.

It has been showed since the early nineties (1990) that chicken egg yolk and their IgY immunoglobulins were able to neutralize scorpion and rattlesnake venoms, confirmed by *in vivo* experiments performed in rodents [13]. Comparing hens with ostriches, the ostrich is one of the most primitive living avian suggesting that the diverse features of the bird Ig genes appeared very early during the divergence of the avian species and are thus common by most, if not all, bird's species [14].

Antibodies are competent of explicitly recognizing a wide diversity of antigens with different affinities. Affinity, simultaneously with avidity is closely related to sensitivity, which is an experimentally measurable value in terms of antibody titer. Affinity is the concentration of the antigen that is needed to occupy the binding sites, of half of the antibody molecules present in an antibody solution, while avidity is the universal summation of the affinities of various antibodies (bivalent, multivalent and of different isotypes) fixed to all places to all available epitopes, considering conformational and valence aspects of the antibody [15]. Authors [3] have developed successful anti-coral snake venom IgY antibodies, which were carried out in chicken egg yolks and their neutralizing action was similarly presented in mice by *in vivo* counteraction experiments. These antivenom immunoglobulins neutralized the toxic and lethal consequences of venom and, accordingly, could function to treat coral snake envenomed victims. Similarly, authors [16] have also produced hen antibodies against *Scolopendra gigantea* toxins with high neutralization titers and antivenom for the treatment of scolopendrism [17].

The present experimental work refers to the production of anti-(*Crot*/pool) antivenom in ostrich egg yolk and its ability in deactivating the lethal consequences of the above mentioned *Crotalus* venoms. Immunization of ostriches with *Crot*/pool venom provoked a characteristic primary humoral response of low antibody titer in the ostrich sera and the egg yolks at 15 days, followed for a higher secondary response. The immunoglobulins titres amplified after the second booster and the intensities were sustained by continuing boosters. Ostrich eggs kept at 5°C during a year exhibited no substantial reduction in the antibody titers.

The caprylic acid [18, 19] method showed that under controlled pH conditions, at a constricted pH range of 5.3–6.3 and low ionic strength of acidified water simplified the separation of IgY, after the yolk lipids aggregation, producing a clear IgY enriched supernatant, which was confirmed by SDS-PAGE analysis. This technique has been used for experimental purposes [18], but actually is used in the production of horse antivenoms [19], with novel fractionation approaches for antivenom production with the purpose of achieving antivenoms of higher purity, which would stimulate less allergic reactions in snake bitten patients treated with this product.

In the current work, it has been established by an immunoblot and/or ELISA assays that the anti-(*Crot*/pool) antivenom IgY recognized and responded to *Crot*/pool venom proteins. Immunoblot analysis revealed not only the specific binding of the antivenom but also dose-dependent blocking of antivenom by venom proteins.

The outcomes of inhibition studies show a specific neutralizing capacity of venom activity in the experimental anti-(*Crot*/pool) IgY antivenom. This ending activity was regularly dose dependent, presenting ample inhibition at a concentration of $2LD_{50}$ (33μg) of *Crot*/pool venom, being indicative of specific binding of the IgY antibodies to venom proteins to which they were developed and their capacity to block the lethal effects of *Crot*/pool venoms. These types of immuno-neutralization help reverse toxicity and define the kinetics of toxins and antibodies.

Until now, traditional treatment of snakebite accidents is based on the use of antivenoms from horse's origin. Nevertheless, equine serum in theory could activate complement cascade and initiate acute hypersensitivity reactions in patients formerly sensitized to horse serum proteins [20]. The immunoglobulin IgY has the capacity of eliminating this possible side effect since it does not react as the mammalian IgG performs and it does not activate the mammalian complement factors [9]. For that reason, the horse serum mammalian IgG activating mammalian complement factors [20] does not permit physicians to give out much larger doses of horse antivenom.

Regarding recent developments of chicken antivenoms, Latin American authors [17] have characterized IgY antivenoms capable of neutralizing the lethal activity of *B. alternatus* snake venom, at a preclinical level. An antivenom, as an alternative to the conventional antivenom production with egg yolk antibodies (IgY-technology) was proposed. Similarly, to the results presented in the current work, antivenom efficacy assays were carried out by them and after successive immunizations, levels of specific IgY reached a maximum that was maintained throughout the observation period; IgY antivenoms obtained after several immunizations neutralized 35.65 μg of *B. alternatus* venom per mg of antivenom. Other authors [21] proposed that birds were excellent hosts for the production of neutralization antibodies at low cost. These antibodies could be applied in the development of diagnostic kits or as an alternative for snakebite envenomation handling in the immediate future.

In conclusion, the specificity and specific activity of the antibody were scrutinized by western blotting and confirmed the presence of highly specific antibodies to *Crot*/

pool venoms in the treated ostrich egg yolk. Ostrich's antivenom can represent an excellent alternative for producing high amounts of antivenoms at very low costs [22]. Thus, they could be a very good option to treat these accidents in countries with low economic resources where the ophitoxemia is a collective health problem. Therefore, the cleanliness, efficiency, and simplicity of producing antivenoms in ostriches, and the inability of these antibodies (IgY) to bind to the human complement formulates an interesting alternative to other antivenoms produced in mammals. These findings point out that ostrich egg antibody can be helpful as a therapeutic instrument to treat snakebites in humans, cattle and domestic animals.

In addition, these results open a therapeutic field, for the manufacturing of other antivenoms against the broad spectrum of toxins and also as a probable diagnostic tool.

ACKNOWLEDGEMENTS

The authors are grateful to Lic. Rosa Gutierrez Sánchez and her husband Juan C. Da Silva, owners of the ostrich's farm "Inversiones en Avestruces Rosa Gutierrez F.P" for their generous help, managing the animal's upkeep. We would like to thank the helpful commentaries from two anonymous referees, which allowed us to improve the manuscript.

Declaration of conflict of interest

The authors pronounce that they have no known competing financial interests or personal associations that could give the idea to influence the work described in this work.

Funding

This work was funded by Biotecfar C.A (Grant Ostrich #1), Facultad de Farmacia, Universidad Central de Venezuela, Caracas, República Bolivariana de Venezuela.

Authors' ORCID numbers

- Carlos Bello (CB) 0000-0002- 5689-9284
- Fática Torrico (FT): 0000-0003-3388-8299
- Mariana Cepeda (MC): 0000-00025396-8483
- Miguel A. López (MAL): 0000-0002-6162-711X
- Alexis Rodriguez-Acosta (ARA): 0000-0003-1234-7522
- Juan Carlos Jimenez (JCJ): 0000-0002-1554-4292

Authors' contribution

MAL, FT and ARA envisioned and planned research; CB, JCJ, MVC and ARA carried out experiments; CB, FT, JCJ and ARA analysed data; CB, FT, JCJ and ARA elucidated results of experiments; CB and ARA drafted manuscript; MAL, CB, FT, JCJ and ARA edited and revised manuscript; MAL, CB, FT, JCJ, MVC and ARA accepted final version of manuscript.

REFERENCES

1. **Rengifo C, Rodríguez-Acosta A.** Serpientes, Veneno y Tratamiento Médico en Venezuela. Caracas: Universidad Central de Venezuela, 2019; 1-272.
2. **Aguilar I, Sánchez EE, Girón ME, Estrella A, Guerrero B. Rodríguez-Acosta A**. Coral snake antivenom produced in chickens (*Gallus domesticus*). Rev Inst Med Trop Sao Paulo 2014; 56: 61-66.
3. **Almeida CM, Kanashiro MM, Rangel-Filho FB, Mata MF, Kipnis TL, da Silva WD.** Development of snake antivenom antibodies in chickens and their purification from yolk. Vet Rec 1998; 143: 579–584.
4. **NIH**, Principles of laboratory animal care. National Institute of Health of United States of America, Pub. 85-23, Maryland; 1985; 1–112.

5. **McLaren RD, Prosser CG, Grieve RC, Borissenko M**. The use of caprylic acid for the extraction of the immunoglobulin fraction from egg yolk of chickens immunised with ovine alpha-lactalbumin. J Immunol Methods 1994; 177:175-184.
6. **Towbin H, Stachelin T, Gordon J.** Electrophoretic transfer of proteins from polyacrylamide gels to nitrocellulose sheets: procedure and some applications. Proc. Natl Acad Sci USA 1979; 76: 4350–4354.
7. **Spearman- Kärber R**. Alternative methods of analysis for quantal responses. In: Finney D, editor. Statistical method in biological assay. London, Charles Griffin; 1978; 1– 78.
8. **Bagcchi S.** Experts call for snakebite to be re-established as a neglected tropical disease. BMJ. 2015; 351: h5313.
9. **Larsson A, Balow RM, Lindahl TL, Forsberg PO.** Chicken antibodies: taking advantage of evolution. A Rev Poultry Sci 1993; 72: 1807-1812.
10. **Adachi K, Handharyani E, Sari DK, Takama K, Fukuda K, Endo I, Yamamoto R, Sawa M, Tanaka M, Konishi I, Tsukamoto Y.** Development of neutralization antibodies against highly pathogenic H5N1 avian influenza virus using ostrich (*Struthio camelus*) yolk. Mol Med Rep 2008;1:203–209.
11. **Larsson A, Mellstedt H.** Chicken antibodies: a tool to avoid interference by human anti-mouse antibodies in ELISA after *in vivo* treatment with murine monoclonal antibodies. Hybridoma 1992; 11: 33–39.
12. **Schade R, Calzado EG, Sarmiento R, Chacana PA, Porankiewicz-Asplund J, Terzolo HR**. Chicken egg yolk antibodies (IgY-technology): a review of progress in production and use in research and human and veterinary medicine. Altern Lab Anim 2005;33:129-154.
13. **Thallay BS, Carroll SB**. Rattle snake and scorpion antivenoms from the egg yolks of immunized hens. Biotechniques (NY) 1990; 8: 934–938.
14. **Huang T, Zhang M, Wei Z, Wang P, Sun Y, Hu X, Ren L, Meng Q, Zhang R, Guo Y, Hammarstrom L, Li N, Zhao Y.** Analysis of immunoglobulin transcripts in the ostrich (*Struthio camelus*), a primitive avian species. PLoS ONE 2012; 7: e34346.
15. **Morimoto J, Sarkar M, Kenrick S, Kodadek T.** Dextran as a generally applicable multivalent scaffold for improving immunoglobulin-binding affinities of peptide and peptidomimetic ligands. Bioconjug Chem 2014; 25:1479-1491.
16. **Parrilla P, Navarrete LF, Girón M.E, Aguilar I, Rodríguez-Acosta A.** Use of chicken egg yolk-derived immunoglobulin against *Scolopendra* venom as an alternative to treat scolopendrism. Rev Cient FCV-LUZ 2008; 18: 385-392.
17. **Leiva CL, Cangelosi A, Mariconda V, Farace M, Geoghegan P, Brero L, Fernández-Miyakawa M, Chacana P**. IgY-based antivenom against *Bothrops alternatus*: Production and neutralization efficacy. Toxicon 2019; 163: 84-92.
18. **Dos Santos MC, D'imperio-Lima MR, Furtado GC, Colletto GM, Kipnis TL, Dias da Silva W.** Purification of F(ab')2 anti-snake venom by caprylic acid: a fast method for obtaining IgG fragments with large neutralization activity, purity and yield. Toxicon 1989; 27: 297-303.
19. **Rojas G, Jimenez JM, Gutierrez JM**. Caprylic acid fractionation of hyper immune horse plasma: description of a simple procedure for antivenom production. Toxicon 1994; 32: 351-363.
20. **Sutherland SK.** Serum reactions. An analysis of commercial antivenoms and the possible role of anticomplementary activity in *de-novo* reactions to antivenoms and antitoxins. Med J Aust. 1977; 1: 613–615.
21. **Lee CH, Liu CI, Leu SJ, Lee YC, Chiang JR, Chiang LC, Mao YC, Tsai BY, Hung CS, Chen CC, Yang YY**. Chicken antibodies against venom proteins of *Trimeresurus stejnegeri* in Taiwan. J Venom Anim Toxins Incl Trop Dis 2020; 26: e20200056.
22. **Carbajo E**. Produccion de avestruces: Una industria ya establecida. Rev Cien Vet 2007; 23: 3-5.

Invest Clin 63(1): 70 - 80, 2022 https://doi.org/10.54817/IC.v63n1a06

Efficacy of ultra-mini percutaneous nephrolithotomy and retrograde intrarenal surgery in the treatment of 2-3 cm lower calyceal stones.

Ya-Wei Guan, Xing Ai, Zhi-Hui Li, Guo-Hui Zhang, Zhuo-Min Jia and Jing-Fei Teng

Department of Urologic Surgery, The Third Medical Center, Chinese PLA (People's Liberation Army) General Hospital, Beijing, China.

Key words: ultra-mini percutaneous nephrolithotomy; retrograde intrarenal surgery; kidney stone; efficacy.

Abstract. We aimed to compare the efficacy and safety of ultra-mini percutaneous nephrolithotomy (UMP) and retrograde intrarenal surgery (RIRS) for the management of lower calyceal stones. A group of 136 patients with a single lower calyceal stone (2-3 cm in diameter) was divided into the UMP or RIRS groups. The average operation time in the RIRS group was significantly longer than that in the UMP group, and the intraoperative blood loss in the former was markedly less than that in the latter. Besides, in the RIRS group, the decreased value of postoperative Hb was obviously lower, the postoperative hospital stay was evidently shorter, and the total hospitalization expenses were markedly less than those in UMP group were. Moreover, the success rate of the first-stage lithotripsy in the UMP group was notably higher than that in RIRS group. The RIRS group had an obviously lower VAS score but a markedly higher BCS score than the UMP group six hours after surgery. At 24 h after operation, the levels of serum CRP, TNF-α and IL-6 in patients in both groups were remarkably increased, and they were evidently lower in the RIRS group than those in the UMP group were. Three days after surgery, the levels of serum CRP, TNF-α and IL-6 were notably lower in the UMP group than those in RIRS group were. RIRS and UMP are safe and effective in the treatment of 2-3 cm lower calyceal stones. The first-stage UMP is characterized by a high stone-free rate (SFR), short operation time and low postoperative infection risk, while RIRS is associated with less blood loss and low total expenses.

Corresponding Author: Xing Ai, Department of Urologic Surgery, The Third Medical Center, Chinese PLA (People's Liberation Army) General Hospital, No. 5 Nanmencang, Dongcheng District, Beijing, China. Tel: +86010-84008022; Email: aixing0007@163.com

Eficacia de la nefrolitotomía percutánea ultramini y la cirugía intrarrenal retrógrada en el tratamiento de cálculos caliceales inferiores de 2-3 cm.

Invest Clin 2022; 63 (1): 70 – 80

Palabras clave: ultra-mini nefrolitotomía percutánea; cirugía intrarrenal retrógrada; cálculo renal; eficacia.

Resumen. Nuestro objetivo fue comparar la eficacia y seguridad de la nefrolitotomía percutánea ultramini (UMP) y la cirugía intrarrenal retrógrada (CRIR) en el manejo quirúrgico de los cálculos caliceales inferiores. Un grupo de 136 pacientes con un solo cálculo calicial inferior (2-3 cm de diámetro) se dividió en un grupo UMP o un grupo CRIR. El tiempo de operación promedio en el grupo CRIR fue significativamente más largo que en el grupo UMP, y la pérdida de sangre intraoperatoria en el primero fue marcadamente menor que en el segundo. Además, en el grupo CRIR, el valor disminuido de la Hb postoperatoria fue obviamente menor, la estancia hospitalaria postoperatoria fue evidentemente más corta y los gastos totales de hospitalización fueron notablemente menores que los del grupo UMP. Además, la tasa de éxito de la litotricia de primera etapa en el grupo UMP fue notablemente más alta que en el grupo CRIR. El grupo CRIR tuvo una puntuación VAS obviamente más baja pero una puntuación BCS marcadamente más alta que el grupo UMP a seos horas después de la operación. A las 24 h después de la operación, los niveles séricos de PCR, TNF-α e IL-6 en los pacientes de ambos grupos aumentaron notablemente y fueron evidentemente más bajos en el grupo CRIR que en el grupo UMP. Tres días después de la operación, los niveles séricos de PCR, TNF-α e IL-6 fueron notablemente más bajos en el grupo UMP que en el grupo CRIR. Los procedimientos CRIR y el UMP son seguros y eficaces en el tratamiento de cálculos caliciales inferiores de 2-3 cm. El UMP de primera etapa se caracteriza por tener una tasa libre de cálculo (SFR) alta, un tiempo de operación corto y un riesgo de infección posoperatorio bajo, y el RIRS se caracteriza por una menor pérdida de sangre y gastos totales bajos.

Received: 07-05-2021 Accepted: 22-09-2021

INTRODUCTION

Urinary calculi are widely prevalent worldwide. The incidence rate of urinary calculus in North America, Europe and Asia is 7～13%, 5～9% and 1～5% respectively. In southern China, the incidence rate of renal calculus can reach 28%, which is the most common urinary disease in young adults. About 83.2% of renal calculus present in 21～50 years-old-people. The lower calyx stone is a common type of kidney stone, accounting for 36% of those [1,2]. Percutaneous nephrolithotomy (PCNL) and retrograde nephrolithotomy (RIRS) are the main surgical methods for treatment of lower calyceal calculi. Although the stone-free rate (SFR) of standard channel and microchannel PCNL

is high, the trauma caused by PCNL is obviously greater than that caused by RIRS [3]. RIRS is considered to be the gold standard for the treatment of lower calyceal stones, but it has been discovered in clinical application that because of the bending angle, lower calyceal stones are often in the blind area of vision and cannot be taken out. Furthermore, as the supporting lithotripsy tool is only 200 μm holmium laser and the ureter is thin, the lithotripsy efficiency is low, the stone-free rate is low, and the operation time is long [4,5]. Ultra-mini percutaneous nephrolithotomy (UMP) causes smaller traumas compared with traditional standard channel and microchannel PCNL (mPCNL), and UMP has a higher lithotripsy efficiency, a higher stone-free rate, and more advantages in treating 1-2 cm stones than the RIRS, so increasingly more attention is being paid to UMP [6-8]. However, there remains a controversy over surgical methods for 2-3 cm lower calyceal stones.

In this study, the efficacy and safety of RIRS and UMP in the treatment of 2-3 cm lower calyceal stones were compared, so as to provide a strong basis for the surgical methods for 2-3 cm lower calyceal stones.

MATERIALS AND METHODS

Research objects

Methods: The clinical data of 136 patients with a single lower calyceal stone (2-3 cm in diameter) were collected. These patients were admitted to our hospital from March 2018 to December 2019, and had indications for RIRS and UMP treatment. According to the random number table method, the patients were randomly divided into two groups, 68 patients in each group were treated with UMP and RIRS, respectively. The inclusion criteria included: (1) patients aged 18-71 years old; (2) the diameter of lower calyceal calculi was 2-3cm; (3) those with no fever or pyuria before operation; (4) those with Visual Analog Scale (VAS) pain score ≤3 points; (5) those with stable blood pressure and blood glucose; (6) those whose examination results of bleeding time and coagulation time were normal after they stopped oral anticoagulants such as aspirin or warfarin for two weeks; (7) those with no congenital malformations or urinary obstructions that need to be treated with an emergency operation. The exclusion criteria were as follows: (1) patients with lower calyceal stones <2 cm or >3 cm, (2) those complicated with stones in the renal pelvis, middle and upper renal calyx, ureter or other parts, (3) those with severe hydronephrosis, (4) those complicated with severe abnormal heart, liver or kidney functions, or (5) those with severe coagulation disorder or bleeding tendency. Among the 136 patients, there were 88 males and 48 females aged 35-77 years old, with an average age of 52.68±9.49 years old. No statistically significant differences were found in the baseline data between the two groups, which were comparable (Table 1, $p>0.05$). All the subjects signed an informed consent in accordance with the Helsinki Declaration. This study was approved by the Ethics Committee of the Chinese PLA General Hospital.

Treatment methods

RIRS: Before operation, a F6 double J stent was used routinely for two weeks. Then, the patient was placed in lithotomy position under general anesthesia, and the double-J tube was removed under rigid ureteroscope. Guided by a zebra guide wire, it was observed whether there was distortion, stenosis or calculus of the ureter in the renal pelvis under the ureteroscope. Later, the zebra guide wire was indwelt and the rigid ureteroscope was removed. Next, a soft ureteroscope sheath was placed along the zebra guide wire, and a soft ureteroscope was inserted along the sheath, which was pushed up to the ureteropelvic junction to enter the renal pelvis. First, the upper calyx and the middle and lower calyces of the kidney were observed in succession. After the stones

Table 1
Demographics and general clinical data of all studied patients.

Parameters	RIRS group n=68	UMP group n=68	*p*-value
Gender (Male/Female)	41/27	47/21	0.370
Age (years)	51.41±9.35	53.03±9.68	0.323
BMI (kg/m^2)	23.25±3.54	23.79±3.29	0.359
Stone location			0.732
Left kidney	32 (47.1%)	35 (51.5%)	
Right kidney	36 (52.9%)	33 (48.5%)	
Stone diameter (cm)	2.60±1.61	2.51±1.47	0.734
Degree of hydronephrosis			0.500
Mild	58 (85.3%)	54 (79.4%)	
Moderate	10 (14.7%)	14 (20.6%)	
Preoperative use of double J tube	12 (17.6%)	6 (8.8%)	0.310
Stone CT value (Hu)	823.65±646.72	983.39±704.73	0.171
Systemic disease			
Hypertension	15 (22.1%)	18 (26.5%)	0.690
Coronary heart disease	4 (5.9%)	7 (10.3%)	0.531
Diabetes mellitus	9 (13.2%)	6 (8.8%)	0.585

Notes: RIRS: Retrograde intrarenal surgery; UMP: Ultra-mini percutaneous nephrolithotomy; BMI: Body Mass Index.

were found, the scope was retreated into the sheath, and a 200 μm holmium laser fiber was inserted to powder the stones from the periphery to the center in the "worm-eaten" form with 8-15 W power. Then the larger stones were taken out through a stone-taking basket, and careful checking was performed to ensure that there was no residual stones ≥3 mm. Besides, the zebra guide wire was indwelt, and the F6 double-J stent catheter was placed under the guidance of the guide wire.

UMP: Under general anesthesia, the patients were firstly placed in the lithotomy position. Next, a F5 ureteral catheter was retrogradely indwelt under a cystoscope to establish an artificial hydronephrosis by continuous water injection at the tail end. Then the patients were placed in the prone position, and a 16G puncture needle was utilized to puncture the target renal calyx under the location of color Doppler ultrasound. The smooth outflow of urine indicated a successful puncture. Subsequently, a J stent metal guide wire at the head end was indwelt, and it was observed from a color Doppler ultrasound that the tail end of the wire reached the kidney collecting system. Later, a 4 mm incision was made on the skin at the puncture site, and the channel was dilated using F10 and F14 fascia dilators in turn along the guide wire. After that, the F13 UMP

sheath was pushed along the guide wire, and the UMP nephroscope was inserted to observe the renal collecting system and look for stones. Thereafter, lithotripsy was carried out using a 200 μm holmium laser under the lithotripsy power of 10-20 w, during which stones were broken into fragments <3 mm. After flushing in the ureteral catheter combined with the inner wall of the outer sheath, the stone fragments were washed out using the endoscope sheath through the vortex formed at the head end of the endoscope. At the end of lithotripsy, nephrostomy fistula and double-J stent catheters were not indwelt.

Observational indicators

The operation time, intraoperative blood loss, postoperative hospital stay, total hospitalization expenses, incidence rate of postoperative complications and other indicators were compared between the two groups of patients. Hemoglobin (Hb) was determined one day before and one day after operation, and the decreased value of Hb was evaluated by comparing the preoperative and the postoperative Hb levels. The pain of patients was evaluated using the VAS scale (0-10 points), in which 0 point = no pain at all, 1-3 points = tolerable slight pain, and for those with ≥4 points, pethidine hydrochloride (1 mg/kg) was intramuscularly injected for analgesia at an interval of more than four hours. The complications of patients were recorded according to the modified Clavien classification system. In the meantime, the Bruggrmann comfort scale (BCS) was also recorded. Five ml fasting venous blood was collected before operation, 24 hours after operation and three days after operation. The serum levels of CRP, IL-6 and TNF in the two groups were compared and analyzed by ELISA.

The early postoperative lithotripsy and the SFR were evaluated based on the kidney ureter bladder (KUB) on the first day after operation. According to the diameter of residual stones, the next treatment plan was decided. Physical vibration lithotripsy was used to treat residual stones whose diameter was ≦ 4 mm; the patients with residual stone diameter ≥ 5mm were treated with extracorporeal shock ultrasonic lithotripsy. Double-J catheters were taken out 2-4 weeks after operation. In the follow-up, renal CT plain scan was performed to re-evaluate the SFR 3-4 weeks after operation. Standards for stone-free state were as follows: There was no residual stone or the diameter of the residual stone was ≤2 mm, and the stone was asymptomatic, non-obstructive and non-infectious [9].

Statistical methods

SPSS 22.0 was adopted for statistical analysis. Measurement data were expressed as mean ± standard deviation ($\bar{x}\pm s$). Intergroup comparisons and pairwise intragroup comparisons were conducted by the *t* test. Count data were expressed as percentage (%) and compared using the χ^2 test or Fisher's Exact Test. $p<0.05$ represented that the difference was statistically significant.

RESULTS

Operation of the two groups of patients

The average operation time in RIRS group was significantly longer than that in UMP group [(50.4±9.8) min *vs.* (42.4±8.3) min, $p<0.001$], and the intraoperative blood loss in the former was markedly less than that in the latter [(7.2±2.7) mL *vs.* (17.5±4.6) mL, $p<0.001$]. Besides, in RIRS group, the decreased value of postoperative Hb [(5.0±3.4) g/L *vs.* (7.9±3.7) g/L, $p=0.003$] was obviously lower, the postoperative hospital stay [(2.6±1.4) days *vs.* (3.8±1.6) days, $p=0.006$] was evidently shorter, and the total hospitalization expenses [(17,300±1,300) Yuan *vs.* (24,700±1,800) Yuan, $p<0.001$] were notably less than those in UMP group. Moreover, the success rate of the first-stage lithotripsy in UMP group [94.1% (64/68)] was higher than that in RIRS group [77.9%

(53/68)], showing a statistically significant difference (p=0.012).

The RIRS group had an obviously lower VAS pain score [(2.8±0.8) points *vs.* (4.6±1.1) points, p=0.011] but a markedly higher BCS score [(2.5±0.8) points *vs.* (1.8±0.7) points, p=0.026] than the UMP group 6 h after operation. However, there were no statistically significant differences in VAS score [(1.5±0.7) points *vs.* (1.9±0.7) points, p=0.258] and BCS score [(3.4±0.6) points *vs.* (2.9±0.5) points, p=0.317)] at 24 h after operation between the two groups of patients (p>0.317) (Table 2).

Incidence rate of related surgical complications of the two groups of patients

The incidence rate of the complications of patients was recorded according to the modified Clavien complication classification system. No complications of grade 3 or above occurred in both groups, and there were no patients needing blood transfusion due to massive hemorrhage or sharp decrease in Hb in the two groups. Six patients in RIRS group and four patients in UMP group had fever, with the body temperature of <38.5°C and blood routine showed only a slight increase in white blood cell count, and no bacteria were detected in blood and urine culture. The patient only received physical cooling treatment. Fourteen patients in the RIRS group and 19 patients in the UMP group had postoperative pain with the VAS score >6 points, and they were treated with analgesic drugs. Besides, nausea and discomfort occurred in three patients and one patient in the two groups, respectively, and they underwent treatment with antiemetic drugs. There were two patients and cero patient had low serum sodium in the two groups, respectively, and they were supplemented with sodium. Moreover, the urinary tract infection rate of the UMP group was significantly lower than that of the RIRS group (P<0.05). The examinations showed that the two patients with urinary tract infection in the UMP group had blood leukocytes >10×10^9/L and urine leukocytes >90/μL. After the application of antibacterial drugs

Table 2
Comparison of surgery parameters and postoperative vas, bcs scores of patients in the two studied groups.

Parameters	RIRS group n=68	UMP group n=68	p-value
Operation time (min)	50.4±9.8	42.4±8.3	0.001
Blood loss (mL)	7.2±2.7	17.5±4.6	0.001
Postoperative Hb decrease (g/L)	5.0±3.4	7.9±3.7	0.003
Postoperative hospital stay time (day)	2.6±1.4	3.8±1.6	0.006
Hospitalization expenses (ten thousands yuan)	1.73±0.13	2.47±0.18	0.001
VAS score (points)			
6 h postoperative	2.8±0.8	4.6±1.1	0.011
24 h postoperative	1.5±0.7	1.9±0.7	0.258
BCS score (points)			
6 h postoperative	2.5±0.8	1.8±0.7	0.026
24 h postoperative	3.4±0.6	2.9±0.5	0.317

Notes: RIRS: Retrograde intrarenal surgery; UMP: Ultra-mini percutaneous nephrolithotomy; VAS: Visual analogue scale; BCS: Bruggrmann comfort scale.

for three days, the blood and urine routine returned to normal in reexaminations. In addition, there were three patients and one patient suffered from hypertension in the RIRS and UMP groups, respectively, and they took oral nicardipine tablets. All complications returned to normal after symptomatic treatment. No complications such as impairment of renal function, serious urinary system injury and urinary sepsis occurred in any patient after operation. There was significant difference in the incidence of urinary tract infection between the two groups($p<0.05$), and there was no significant difference in the risk of fever, pain, nausea and vomiting, electrolyte disorder, hypertension, blood transfusion and complications above grade 3 ($p>0.05$). (Table 3).

Expression levels of serum inflammatory factors in patients before and after treatment

Immediately before operation, there were no statistically significant differences in the levels of serum C-reactive protein (CRP), tumor necrosis factor-alpha (TNF-α) and interleukin-6 (IL-6) between the two groups ($p>0.05$). At 24 h after operation, the levels of serum CRP, TNF-α and IL-6 in the two groups of patients were remarkably increased, and they were evidently lower in RIRS group than those in UMP group ($p<0.001$). At 3 days after operation, the levels of serum CRP, TNF-α and IL-6 in the two groups of patients remarkably declined compared with those at one day after operation, and they were notably lower in UMP group than those in RIRS group ($p<0.05$) (Table 4).

Postoperative follow-up results of patients

In the UMP group, KUB was reexamined on the first day after operation, and it was found that the diameter of residual stones was ≤4 mm in four cases, and physical vibration lithotripsy was given one week after operation. On the first day after operation, the KUB showed that 15 patients had residual stones, and two patients had residual stones ≥5 mm in diameter in RIRS group. On the third day after operation, they were given extracorporeal shock wave lithotripsy as an auxiliary treatment combined with stone removal using the lithotripter. In RIRS group, there were 11 cases of small residual stones (stone diameter ≤4 mm) after operation, all of which were treated by physical vibration *in vitro*. No UMP or RIRS treatment were

Table 3
Comparison of postoperative complications of patients in the two studied groups.

Parameters	RIRS group n=68	UMP group n=68	p-value
Clavien grade 1			
Fever, >38.5°C	6 (8.8%)	4 (5.9%)	0.744
Pain, VAS score>6 points	14 (20.6%)	19 (27.9%)	0.424
Nausea / vomiting	3 (4.4%)	1 (1.5%)	0.619
Transient electrolyte disturbance	2 (2.9%)	0 (0%)	0.496
Clavien grade 2			
Hypertension	3 (4.4%)	1 (1.5%)	0.619
Urinary system infection	13 (19.1%)	2 (2.9%)	0.003
Blood transfusion	0 (0%)	0 (0%)	1.000
Clavien grade 3	0 (0%)	0 (0%)	1.000

Notes: RIRS: Retrograde intrarenal surgery; UMP: Ultra-mini percutaneous nephrolithotomy.

Table 4
Comparison of inflammatory factors of patients in the two studied groups.

	RIRS group n=68	UMP group n=68	*p*-value
CRP (mg/L)			
Immediate postoperative	4.21 ± 1.57	4.11 ± 1.33	0.689
1 day postoperative	25.68 ± 4.59	18.52 ± 5.28	0.001
3 days postoperative	19.83 ± 2.42	15.61 ± 2.74	0.001
TNF-α (pg/mL)			
Immediate postoperative	1.97 ± 0.79	1.88 ± 0.73	0.491
1 day postoperative	12.35 ± 2.54	9.84 ± 3.16	0.001
3 days postoperative	9.76 ± 1.31	7.79 ± 1.39	0.017
IL-6 (pg/mL)			
Immediate postoperative	5.85 ± 1.78	5.96 ± 1.91	0.729
1 day postoperative	28.74 ± 2.02	22.28 ± 2.12	0.001
3 days postoperative	23.58 ± 1.37	20.16 ± 1.72	0.003

Notes: RIRS: Retrograde intrarenal surgery; UMP: Ultra-mini percutaneous nephrolithotomy; CRP: C-reactive protein; TNF: Tumor Necrosis Factor; IL: Interleukin.

performed in both groups. At 3-4 weeks after operation, renal CT was applied for re-examinations to evaluate the SFR, which was 97.1% (66/68) in UMP group and 91.2% (62/68) in RIRS group, with no statistically significant difference (p=0.274).

DISCUSSION

Kidney stones are the most common type of urinary calculi, and 36% of them are lower calyceal stones [10]. Lower calyceal stones are often surgically treated, and RIRS and PCNL are the main surgical methods at present. Through PCNL, SFR can reach more than 90%, so it has become the first choice to treat kidney stones with a diameter greater than 2 cm [11]. However, PCNL will inevitably damage renal parenchyma and surrounding tissue structures, and easily lead to serious complications [12]. The traditional standard PCNL puncture channel is F22-26, the microchannel percutaneous nephrolithotomy (mPCNL) puncture channel is generally F16-20, and the UMP puncture channel is only F12-14, so the trauma caused by UMP is smaller, with less blood loss and faster postoperative recovery. However, UMP requires higher precision of puncture and expansion. In addition, UMP is generally only suitable for 1-2 cm medium stones because of the thinner channel, and as the stones in the upper ureter, upper calyx and middle calyx can be treated by RIRS, UPM is the most suitable for treating 1-2 cm lower calyceal stones, and the lower calyx is the least accessible part in RIRS [13, 14].

However, it is difficult to treat lower calyceal stones with a diameter greater than 2 cm. Studies in other countries have shown that ureteroscopic holmium laser lithotripsy can achieve the same SFR as mPCNL with a low incidence rate of complications in the treatment of kidney stones with a diameter greater than 2 cm [15]. Aboumarzouk *et al.* [16] used ureteroscopy to treat lower calyceal stones with an average diameter of 3 cm. The SFR in the first stage was 75%, while that in the second stage was nearly 90%. Koyuncu *et al.* [17] used ureteroscopy and percutaneous nephroscopy to treat lower

calyceal stones with a diameter greater than 2 cm. The SFR was as high as 90% one month after operation. Compared with that in the PCNL group in the same period, the SFR was as high as 90.6% one month after operation, displaying no statistically significant difference. Zeng *et al.* [18] applied UMP to treat lower calyceal stones with a diameter smaller than 25 mm, and the channel size was F12-14. The SFR could reach 95.8% three months after operation, and the incidence rate of postoperative complications, especially the blood loss, was significantly reduced, suggesting that UMP has a good application prospect in the treatment of kidney stones. The results of this study showed that compared with those in UMP, the average operation time was obviously prolonged, the postoperative hospital stay was markedly shortened, and the total hospitalization expenses were remarkably reduced in the RIRS group. However, the loss of Hb after operation in the UMP group was only (7.9±3.7) g/L due to the thinner operation channel, which was higher than that in RIRS group (5.0±3.4) g/L, but it notably declined in comparison with that after PCNL (9.6 g/L on average) reported in the literature [19], indicating that the effect of UMP in reducing blood loss is satisfactory. In addition, there were no statistically significant differences in the VAS score and BCS score between the two groups of patients 24 h after operation, and the pain did not increase because of the puncture, implying that UMP has a slight impact on patients due to the small puncture channel.

The incidence rate of systemic inflammatory response syndromes after endoscopic stone surgery was 8.6-11.4%, and without timely treatment, the syndromes in some patients will develop into urinary sepsis and even cause death. It is reported that excessive intrapelvic pressure [>30 mmHg (1 mmHg=0. 133 kPa)] and long accumulation time (>50 s) can evidently increase the incidence rates of postoperative fever and urinary sepsis [20, 21]. The results of this study manifested that the postoperative fever rate was 8.8% in the RIRS group and 5.9% in the UMP group. Besides, the level of inflammatory factors in the UMP group was also markedly lower than that in the RIRS group. This may be due to the fact that negative pressure suction was utilized during UMP, which reduced the pressure in the renal pelvis and the risk of infection.

SFR is an important indicator for evaluating the effectiveness of lithotripsy. According to a report, the included angle between the infundibulum of the lower calyx and pelvis affects the SFR of RIRS in treating lower calyceal stones. The smaller the included angle is, the lower the SFR will be [22]. In the treatment of lower calyceal stones using UMP, the lower calyx can be directly punctured, thus avoiding this effect. The results of this study illustrated that the SFR after the first-stage surgery in UMP group was significantly higher than that in RIRS group. It is believed that if the stone hardness is high and bleeding during operation affects the visual field, the operation time will be too long. Besides, if there is urinary tract infection before operation, secondary surgery or postoperative assisted lithotripsy should be considered, and the double-J stent catheter can be indwelt after operation, which is beneficial to both the first-stage RIRS and the postoperative lithotripsy.

This study was a retrospective study. The number of enrolled patients was limited, the follow-up time was short, the follow-up content was not comprehensive, and the long-term prognosis of patients was not analyzed. In the future, long-term follow-up multi-center studies with large sample sizes are needed to verify the conclusions of this study.

As a conclusion, RIRS and UMP are safe and effective in the treatment of 2-3 cm lower calyceal stones. The first-stage UMP is characterized by a high SFR, short operation time and low postoperative infection risk, while RIRS is featured with less blood loss and low total expenses.

Funding

None.

Declaration of conflict of interest

No conflict of interest.

Authors' ORCID numbers

- Yawei Guan: 0000-0001-7960-3135
- Xing Ai: 0000-0001-9043-4918
- Zhihui Li: 0000-0002-6282-1475
- Guohui Zhang: 0000-0003-1050-247X
- Zhuomin Jia: 0000-0002-1474-0128
- Jingfei Teng: 0000-0001-5294-3914

Authorship contribution

- YG, XA , ZL: planning, results and final editing.
- YG ,XA: writing of the paper.
- ZL, GZ, ZJ, JT: data collection and analyses.
- All authors approved the final version of the manuscript.

REFERENCES

1. **Shabana W, Oquendo F, Hodhod A, Ahmed A, Alaref A, Trigo S, Hadi RA, Nour HH, Kotb A, Shahrour W, Elmansy H.** Miniaturized ambulatory percutaneous nephrolithotomy versus flexible ureteroscopy in the management of lower calyceal renal stones 10-20mm: A propensity score matching analysis. Urology 2021; S0090-4295(21)00463-5.
2. **Choudhury S, Talukdar P, Mandal TK, Majhi TK.** Supine versus prone PCNL in lower calyceal stone: Comparative study in a tertiary care center. Urologia 2021; 88(2):148-152.
3. **Sari S, Ozok HU, Topaloglu H, Cakici MC, Ozdemir H, Karakoyunlu AN, Senturk AB, Ersoy H.** The association of a number of anatomical factors with the success of retrograde intrarenal surgery in lower calyceal stones. Urol J 2017; 14(4):4008-4014.
4. **Chen Q, Cao Y, Xia L, Zhong H, Du Z, Xuan H, Lu M.** The retrospective experience of day-surgery semi tubeless ultra-mini percutaneous nephrolithotomy. Transl Androl Urol 2021; 10(2):654-661.
5. **Jones P, Rai BP, Aboumarzouk O, Somani BK.** Treatment options and outcomes for lower pole stone management: are we there yet? Ann Transl Med 2016; 4(3):61.
6. **Yilmazel FK, Cinislioglu AE, Karabulut I, Yilmaz AH, Ozkaya F, Adanur S.** Ultra-mini flexible percutaneous nephrolithotomy in the treatment of moderate-size kidney stones: a new instrument, a preliminary prospective study. Urolithiasis 2021 Aug;49(4):345-350. *doi: 10.1007/s00240-020-01225-3. Epub 2020 Nov 10.*
7. **Knoll T.** Super-, perfect-, ultra-, micro-, mini-, ...: does anybody benefit from miniaturized percutaneous nephrolithotomy? World J Urol 2018; 36(2):319-320.
8. **Kallidonis P, Tsaturyan A, Lattarulo M, Liatsikos E.** Minimally invasive percutaneous nephrolithotomy (PCNL): Techniques and outcomes. Turk J Urol 2020; (Supp. 1):S58-S63.
9. **Huang JS, Xie J, Huang XJ, Yuan Q, Jiang HT, Xiao KF.** Flexible ureteroscopy and laser lithotripsy for renal stones 2 cm or greater: A single institutional experience. Medicine (Baltimore) 2020; 99(43):e22704.
10. **Viljoen A, Chaudhry R, Bycroft J.** Renal stones. Ann Clin Biochem 2019; 56(1):15-27.
11. **Morgan MS, Pearle MS.** Medical management of renal stones. BMJ 2016; 352:i52.
12. **Wollin DA, Preminger GM.** Percutaneous nephrolithotomy: complications and how to deal with them. Urolithiasis 2018; 46(1):87-97.
13. **Yili L, Yongzhi L, Ning L, Dongwei X, Chunlai L, Suomin L, Ping W.** Flexible ureteroscopy and holmium laser lithotripsy for treatment of upper urinary tract calculi in patients with autosomal dominant polycystic kidney disease. Urol Res 2012; 40(1):87-91.

14. **Jones P, Elmussareh M, Aboumarzouk OM, Mucksavage P, Somani BK.** Role of minimally invasive (Micro and Ultra-mini) PCNL for adult urinary stone disease in the modern rra: evidence from a systematic review. Curr Urol Rep 2018; 19(4):27.
15. **Li Z, Lai C, Shah AK, Xie W, Liu C, Huang L, Li K, Yu H, Xu K.** Comparative analysis of retrograde intrarenal surgery and modified ultra-mini percutaneous nephrolithotomy in management of lower pole renal stones (1.5-3.5 cm). BMC Urol 2020; 20(1):27.
16. **Aboumarzouk OM, Monga M, Kata SG, Traxer O, Somani BK.** Flexible ureteroscopy and laser lithotripsy for stones >2 cm: a systematic review and meta-analysis. J Endourol 2012; 26(10):1257-1263.
17. **Koyuncu H, Yencilek F, Kalkan M, Bastug Y, Yencilek E, Ozdemir AT.** Intrarenal surgery vs percutaneous nephrolithotomy in the management of lower pole stones greater than 2 cm. Int Braz J Urol 2015; 41(2):245-251.
18. **Zeng G, Wan S, Zhao Z, Zhu J, Tuerxun A, Song C, Zhong L, Liu M, Xu K, Li H, Jiang Z, Khadgi S, Pal SK, Liu J, Zhang G, Liu Y, Wu W, Chen W, Sarica K.** Super-mini percutaneous nephrolithotomy (SMP): a new concept in technique and instrumentation. BJU Int 2016; 117(4):655-661.
19. **Ather MH, Sulaiman MN.** Flexible ureteroscopy versus miniaturized percutaneous nephrolithotomy for renal stones of 1-2 cm. Fac Rev 2020; 9:29.
20. **Zhang H, Hong TY, Li G, Jiang N, Hu C, Cui X, Chu C, Zhao JL.** Comparison of the efficacy of ultra-mini PCNL, flexible ureteroscopy, and shock wave lithotripsy on the treatment of 1-2 cm lower pole renal calculi. Urol Int 2019; 102(2):153-159.
21. **He Z, Tang F, Lei H, Chen Y, Zeng G.** Risk factors for systemic inflammatory response syndrome after percutaneous nephrolithotomy. Prog Urol 2018; 28(12):582-587.
22. **Tokas T, Skolarikos A, Herrmann T, Nagele U.** Pressure matters 2: intrarenal pressure ranges during upper-tract endourological procedures. World J Urol 2019; 37(1):133-142.

Invest Clin 63(1): 81 - 91, 2022 https://doi.org/10.54817/IC.v63n1a07

Clinical significance of methyl-CpG binding protein 2 in postherpetic neuralgia: an observational study.

Zhijian Wang[1], Wei Shen[1], Mengye Zhu[1], Mu Xu[1], Mizhen Qiu[1], Daying Zhang[1] and Shibiao Chen[2]

[1]Department of Pain, the First Affiliated Hospital of Nanchang University, Nanchang, China.

[2]Department of Anesthesiology, the First Affiliated Hospital of Nanchang University, Nanchang, China.

Key words: MECP2; postherpetic neuralgia; inflammatory factors; quality of life.

Abstract. The present study was aimed to investigate the clinical significance of methyl-CpG binding protein 2 (MECP2) in patients with postherpetic neuralgia (PHN). This prospective case control study enrolled 319 cases of PHN patients from April 2017~December 2019. The patients' sleep quality and quality of life were evaluated using the Pittsburgh sleep quality score and the SF-36 scale, respectively. The serum levels of MECP2, CRP, IL-6 and TNF-α were tested using enzyme linked immunosorbent assay (ELISA). The pain condition of the patients was evaluated using the visual analogue scale (VAS). The levels of MECP2 were significantly increased in PHN patients compared with the patients without PHN. Serum MECP2 levels were the highest in patients with severe pain, and were the lowest in patients with mild pain. Similarly, the frequency of severe pain in patients with low expression of MECP2 was significantly lower than the patients with higher MECP2 expression. Besides, serum levels of inflammatory factors CRP, IL-6 and TNF-α were markedly increased in PHN patients, which were also increased with the increase of the severity of pain. CRP, IL-6 and TNF-α were positively correlated with serum levels of MECP2 in PHN patients. Before the study, patients with lower MECP2 levels showed a significantly higher SF-36 score and lower Pittsburgh and VAS scores than patients with higher levels of MECP2. However, after one month, no significant difference was found between the patients. ROC curve showed MECP2 had the potential as a diagnostic biomarker for PHN. In conclusion, higher serum MECP2 levels are associated with a more severe pain condition and increased release of inflammatory factors.

Corresponding Author: Shibiao Chen, Department of Anesthesiology, the First Affiliated Hospital of Nanchang University, Nanchang 330006, China. Tel.: 86-0791-88692578. Email: sbiao_ch0211@126.com

Importancia clínica de la proteína 2 de unión a metil-CpG (MECP2) en la neuralgia posherpética: un estudio observacional.

Invest Clin 2022; 63 (1): 81 – 91

Palabras clave: MECP2; neuralgia posherpética; factores inflamatorios; calidad de vida.

Resumen. El objetivo de este estudio fue investigar la importancia clínica de la MECP2 en pacientes con neuralgia posherpética (NPH). Este estudio observacional prospectivo incluyó 319 pacientes con NPH entre abril de 2017 y diciembre de 2019. La calidad del sueño y la calidad de vida de los pacientes se evaluaron con la escala de calidad del sueño de Pittsburgh y la escala SF - 36, respectivamente. Los niveles séricos de MECP2, PCR, IL-6 y TNF-α fueron determinados por ELISA. Se utilizó la escala visual analógica (EVA) para evaluar la intensidad del dolor. Los niveles de MECP2 en pacientes con NPH aumentaron significativamente en comparación con los pacientes sin NPH. El nivel sérico de MECP2 fue más alto en pacientes con dolor grave y el más bajo en pacientes con dolor leve. Además, la incidencia de dolor grave en pacientes con baja expresión de MECP2 fue significativamente menor que en pacientes con alta expresión de MECP2. Además, los niveles séricos de PCR, IL-6 y TNF-α aumentaron significativamente en pacientes con NPH, y se incrementaron con el aumento del grado de dolor. Los niveles séricos de PCR, IL-6 y TNF-α en pacientes con NPH se correlacionaron positivamente con los niveles séricos de MECP2. Antes del estudio, los pacientes con niveles más bajos de MECP2 tenían puntuaciones significativamente más altas de SF - 36, y puntuaciones más bajas de Pittsburgh y EVA que los pacientes con niveles más altos de MECP2. Sin embargo, no se encontraron diferencias significativas entre los pacientes un mes después. Las curvas ROC mostraron que la MECP2 podría ser un biomarcador de diagnóstico para la NPH. En general, los niveles séricos más altos de la MECP2 se asociaron con condiciones de dolor más graves y un aumento de la liberación de factores inflamatorios.

Received: 11-08-2021 Accepted: 30-10-2021

INTRODUCTION

Postherpetic neuralgia (PHN) is a common complication after an acute episode of herpes zoster, with an estimated incidence of 5∼20% in herpes zoster patients, especially in elderly patients [1-3]. Studies report that PHN can last for months to years, seriously affecting people's quality of life [4]. There are many risk factors to influence the incidence of PHN [5]. Generally, the PHN is thought to be due to the immune/inflammatory response by the reactivation and migration of varicella zoster virus [6,7]. Since pain is the most common symptom of PHN, both inflammation and pain related factors are of great significance in PHN investigation.

Methyl-CpG binding protein 2 (MECP2), a kind of protein that can bind methylated DNA, is thought to play important roles in nervous system diseases like seizure [8], and is also associated with pain [9]. It is found that the deficiency of MECP2 in forebrain excitatory neurons could lead to cortical hyperexcitation and seizures [10]. However, overexpression of MECP2 resulted in higher susceptibility

toward seizures [11]. Furthermore, MECP2 is found to be elevated in several pain and inflammation conditions [12, 13]. Generally, an increased MECP2 level is accompanied with nerve injury, like dorsal root ganglia injury and increased pain sensitivity [14]. However, up to now, there is no study focusing on the role of MECP2 in PHN.

In the present study, we performed a prospective observational research to investigate the clinical significance of MECP2 in PHN patients. This study might provide a new research target and biomarker for PHN.

MATERIAL AND METHODS

Patients

This prospective observational study enrolled 319 patients with and without postherpetic neuropathy from April 2017～December 2019. The diagnosis of herpes zoster was established according to the Chinese Consensus of Herpes Zoster [15]. The diagnosis of PHN was determined according to the Chinese expert consensus on diagnosis and treatment of postherpetic neuralgia [16]. Briefly, the herpes zoster diagnostic criteria were defined as patients with irregular erythema occurred in a certain nerve distribution area, followed by a majority or cluster of millet to mung bean sized herpes, which quickly turned into blisters and was accompanied by neuralgia. The diagnostic criteria of PHN were defined as after the skin lesions of herpes zoster subsided, the patient developed local pain, pruritus and paresthesia for more than one month. The inclusion criteria were: 1) all patients were diagnosed as PHN according to the above criteria and didn't receive any treatment before; 2) the patients showed abnormal pain and touch feeling distributed by innervation area and sometimes showed skin pigmentation; 3) the pain types were as sharp pain or persistent burning pain, or tight bundle pain; and 4) patients showed other discomfort on lesion position after nerve injury, including itching, tight feeling and ant feeling. The following patients were excluded: 1) patients with severe inflammation diseases, such as pneumonia; 2) patients with fractures or other severe system diseases like myocardial infarction or stroke within three months before the study; 3) patients with other neuralgia like intercostal neuralgia, cephalalgia nervosa, post-stroke neuralgia, etc. All patients received routine strategy therapy including anti-pain treatment like treatment with pregabalin (150 mg×2/d for 14 d) or carbamazepine (100 mg/d for 14 d), and the grade of pain was recorded by the patients in awake state. Additionally, serum samples and medical records were collected from the 319 herpes zoster patients whose skin lesions of herpes zoster subsided without PHN. The inclusion of herpes zoster patients without PHN was according to the above diagnostic criteria of herpes zoster as well as the above inclusion criteria. All participants signed a written informed consent. The ethic approval was obtained from the Ethic Committee of the First Affiliated Hospital of Nanchang University and a written informed consent was obtained from all patients.

Measurement of MECP2 and inflammatory factors

Blood samples of all PHN patients were collected at the day they came to the outpatient department. The samples were collected in tubes without anticoagulant and were centrifuged at 12000 g for 20 min. The serum levels of MECP2, CRP, IL-6 and TNF-α were tested using commercially available enzyme linked immunosorbent assay (ELISA) kits according to the manufacturer's instructions. The kits used were MECP2 (MYBioSource, cat. No. MBS2515729), CRP (BOSTER Bio, cat. No. EK1316), IL-6 (BOSTER Bio, cat. No. EK0410) and TNF-α (BOSTER Bio, cat. No. EK0525).

Data collection

The pain condition of patients was evaluated at the time of diagnosis using the visual analogue scale (VAS). The severity of the pain condition of PHN patients were defined as: mild

VAS 1~3, moderate VAS 4~6, or severe VAS 7~10. Patient's demographic data including age, sex, BMI, complications, and clinical characteristics including disease course, rash types and sites of skin involvement, were collected. The patients' sleep quality and quality of life were evaluated using the Pittsburgh sleep quality score and the SF-36 scale before the study and after one month of treatment, respectively.

Statistical analysis

All data distributed normally were expressed by means ± SD. The distribution of the data was analyzed by Kolmogorov-Smirnov method. Comparison between the two groups was conducted by t test and comparison among three or more groups was performed using one-way analysis of variance (ANOVA) followed by Tukey post hoc test. Rates were compared by Chi square test. ROC curve was used for diagnostic value of MECP2 in PHN patients. All calculation was performed using SPSS 18.0 (SPSS Inc., Chicago, USA) and GraphPad 6.0 (GraphPad Software, San Diego, CA, USA).

RESULTS

MECP2 was upregulated in PHN patients

The basic clinical characteristics of all patients are listed in Table 1. There were no significant differences in age, sex, BMI and complications between the PHN patients and the controls. The mean VAS score of all PHN patients was 3.38±2.26. Serum levels of MECP2 were determined in PHN patients and the herpes zoster patients without PHN. It was found that the levels of MECP2 were significantly increased in PHN patients when compared with the non-PHN patients ($P<0.05$, Fig. 1).

Table 1
Basic characteristics of all participants.

Variables	PHN, n=319	non-PHN, n=319	P value
Age, y	58.32±8.71	58.71±8.88	0.571
Sex, male (%)	179 (56.11)	170 (53.29)	0.689
BMI, kg/m^2	25.33±3.81	25.34±3.79	0.985
Complications, n (%)			0.848
Diabetes	33 (10.34)	38 (11.91)	
Hypertension	56 (17.55)	47 (14.73)	
Current smoker	112 (35.11)	108 (33.86)	
Disease course (PHN), Mon	4.40±1.12	-	
Sites of skin involvement, n (%)			0.908
Lumbosacral nerve area	154 (48.28)	161 (50.47)	
Intercostal nerve area	61 (19.12)	52 (16.30)	
Trigeminal nerve area	43 (13.48)	37 (11.60)	
Brachial plexus area	25 (7.84)	30 (9.40)	
Perineal nerve area			
VAS score	3.38±2.26	-	
Distribution of VAS score, n (%)			
Mild	152 (47.65)	-	
Moderate	98 (30.72)	-	
Severe	69 (21.63)	-	

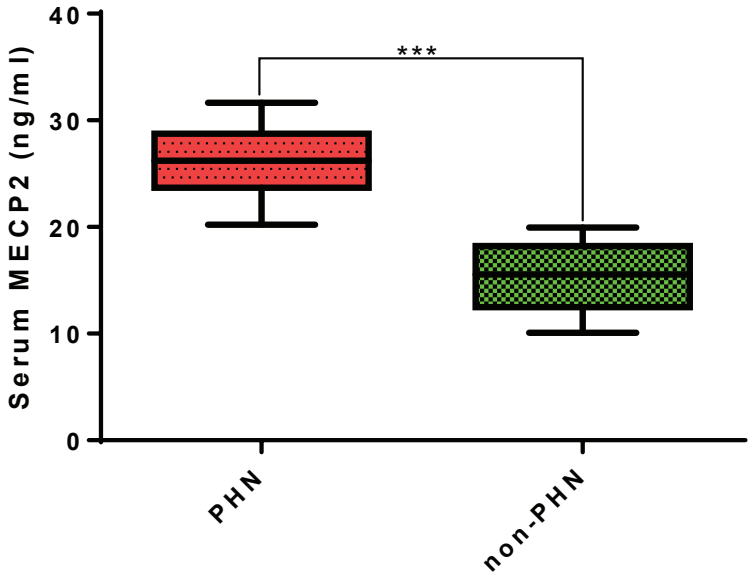

Fig. 1. Serum levels of MECP2 in PHN patients and the non-PHN.

MECP2 was positively correlated with pain severity of PHN patients

Then, levels of MECP2 were detected in PHN patients with different pain severities. As shown in Fig. 2, serum MECP2 levels were the highest in patients with severe pain, and were the lowest in patients with mild pain, and the difference was significant between the groups ($P<0.05$). The patients were then further divided into high MECP2 expression group and low MECP2 expression group according to the mean serum levels in PHN patients (45.83 ng/mL). It was found that the frequency of severe pain in patients with low expression of MECP2 was significantly lower than the patients with higher MECP2 expression ($P<0.05$, Table 2). Notably, patients with mild pain were found to be markedly decreased in patients with higher MECP2 than patients with higher MECP2 ($P<0.05$).

Relationship between MECP2 and inflammatory factors in PHN patients

To further investigate the role of MECP2 in PHN, the serum levels of inflammatory factors CRP, IL-6 and TNF-α were determined. It was found all these factors were markedly increased in PHN patients compared with the no-PHN patients ($P<0.05$, Fig. 3), and serum levels of CRP, IL-6 and TNF-α increased with the severity of pain in PHN patients ($P<0.05$), except for the difference of TNF-α between severe and moderate pain. The Pearson's correlation test showed that CRP, IL-6 and TNF-α were positively correlated with serum levels of MECP2 in PHN patients ($P<0.05$, Table 3).

Association between MECP2 and quality of life of PHN patients

The Pittsburgh sleep quality score and the SF-36 scale, as well as the VAS score were then evaluated before the study and after one month of treatment. It was found that before study, patients with lower MECP2 levels showed significantly higher SF-36 score and lower Pittsburgh and VAS scores than patients with higher MECP2 ($P<0.05$, Table 4). However, after one month, no significant differences were found between the patients.

Diagnostic value of MECP2 in PHN

Finally, we determined the diagnostic value of MECP2 for PHN in herpes zoster

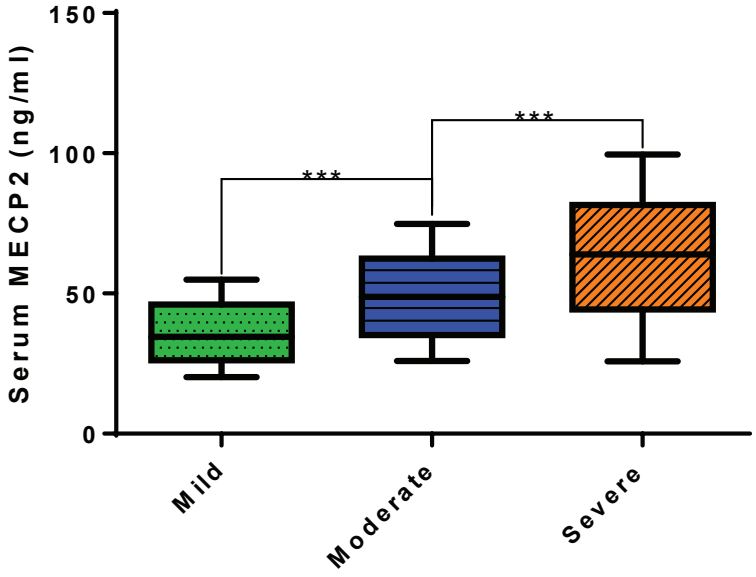

Fig. 2. Serum levels of MECP2 in patients with different pain severity.

Table 2
Pain severity in PHN patients with different expression of MECP2.

Variables	Low MECP2, n=173	High MECP2, n=146	P value
VAS distribution, n (%)			<0.0001
Mild	113 (65.32)	39 (26.71)	
Moderate	43 (24.86)	55 (37.67)	
Severe	17 (9.83)	52 (35.62)	

patients. It was found that MECP2 has the potential as a biomarker for PHN diagnosis, with a ROC curve ACU, cutoff value 33.56 ng/mL, sensitivity 70.5%, specificity 65.5% (Fig. 4).

DISCUSSION

Postherpetic neuralgia is a common complication after treatment of herpes zoster and may decrease the patients' quality of life. Since the prevention of PHN is an effective method to reduce the patients' pain after herpes zoster, biomarkers for diagnosis and prediction of PHN are also important. In the present study, we demonstrated that serum MECP2 was up-regulated in PHN patients and higher MECP2 was associated with a more severe pain condition, higher levels of inflammatory factors, and lower quality of life before treatment.

Rzeszotarska have reported that MECP2 is a factor associated with both inflammatory factors and pain [12]. Generally, most studies found that increased MECP2 is associated with increased pain sensitivity and increased pro-inflammatory factors. It was found in the mouse chronic pain model, that MECP2 was increased in S1 glutamate (GluS1) neurons and increased MECP2 was associated with increased neuronal activity and knockdown of MECP2 diminished the offspring pain sensitization, which was increased by overexpressing MECP2. In 2,4,6-trinitrobenzenesulfonic acid-induced- pelvic inflammation pain in a rat model, MECP2 was also

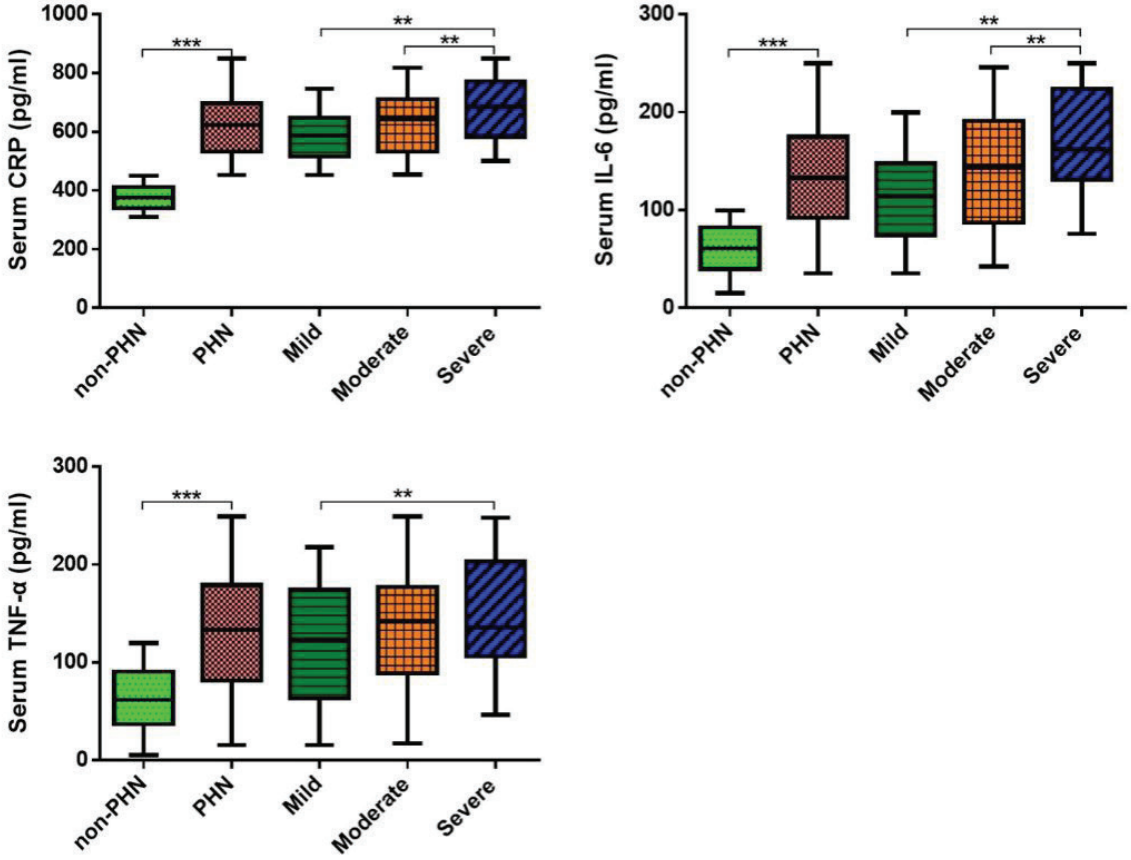

Fig. 3. Serum levels of CRP, IL-6 and TNF-α in non-PHN patients and PHN patients with different pain severity.

Table 3
Correlation between MECP2 and inflammatory factors in PHN patients.

Factors	Pearson' correlation	P value
CRP	0.495	<0.001
IL-6	0.471	<0.001
TNF-α	0.354	<0.001

found to be overexpressed in neurons and the increased MECP2 was accompanied with increased cAMP response element-binding protein [13]. In chronic constriction injury, global DNA methylation and MeCP2 expression were both increased in the rats' spinal cord, which could be decreased by intrathecal 5-azacytidine [17]. Besides, the deficiency of MECP2 resulted in an increase in neutrophil infiltration and anti-inflammatory factor IL-10, as well as decreased level of TNF-α [18]. The inhibition of MECP2 was also found to alleviate inflammation, while overexpression of MECP2 promoted inflammation response in different kinds of cells [19-21]. However, several studies also found positive results, demonstrating overexpression of MECP2 led to decreased acute mechanical pain, thermal pain in acute pain transduction and overexpression improved neuropathic pain [22]. In Rett syndrome, mutation and duplication of MECP2 both induce decreased pain sensitivity [9]. Besides, MECP2 deficiency might also exacerbate neuroinflammatory setting and autoreactive response during an autoimmune challenge [23]. In the present study, we observed that serum MECP2 was up-regulated in PHN patients and was associated with

Table 4
Association between MECP2 and quality of life of PHN patients.

Variables		Low MECP2, n=173	High MECP2, n=146	*P* value
VAS	Before	3.38±2.26	5.40±2.54	<0.0001
	After 1 month	1.99±0.63	2.11±0.65	0.0958
SF-36	Before	63.87±7.87	62.01±8.39	0.0422
	After 1 month	73.13±7.45	73.12±7.00	0.9902
Pittsburgh score	Before	12.30±2.47	13.78±2.78	<0.0001
	After 1 month	7.80±4.55	7.63±4.14	0.7293

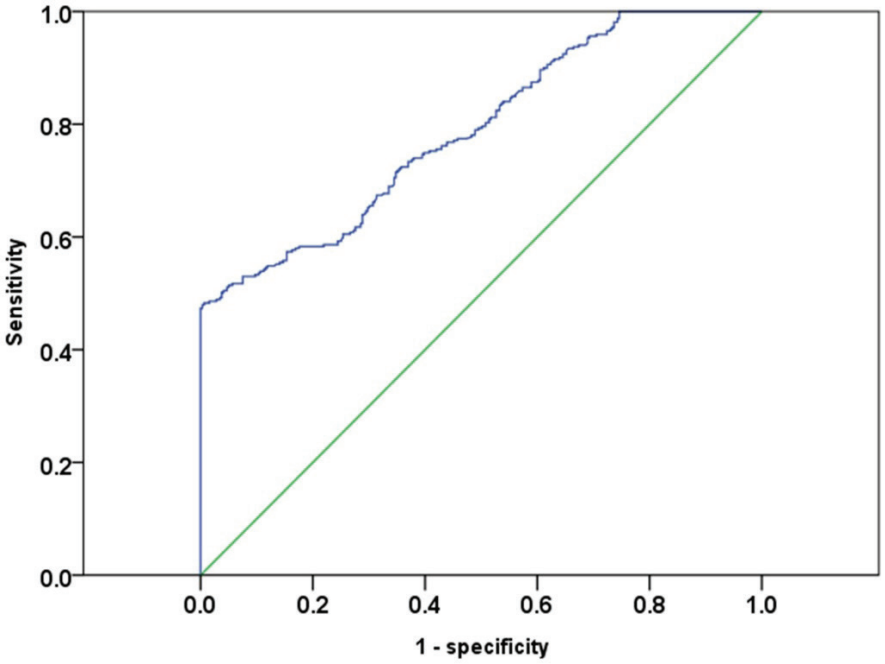

Fig. 4. ROC curve for diagnostic value of MECP2 in PHN.

patients' release of inflammatory factors and pain condition, which was consistent with most of the above researches. Since the relationship between MECP2 and pain remains controversial, the elevated MECP2 can be either as a pro-inflammatory factor or a compensatory mechanism to reduce inflammation and pain. In both of the two conditions, MECP2 can be increased in pain and inflammation. However, this speculation needs more studies to further confirm. Besides, we also found that serum MECP2 was associated with patients' quality of life before study. However, different levels of MECP2 didn't influence the quality of life after one-month treatment.

Inflammation is closely related to the pain, including correlated with PHN. It was reported that PHN patients showed higher levels of IL-1β and lower levels of BDNF in cerebrospinal fluid [24]. Another study found the expression of IL-1α, IL-16, intercellular adhesion molecule-1, and monocyte chemoattractant protein-1 was elevated in skin of PHN patients [25]. Besides, Üçeyler *et al.* demonstrated that in some PHN patients, the ex-

pression of IL-10 and IL-6 on skin might increase than unaffected skin [26]. In our study, we also found that inflammatory factors CRP, IL-6 and TNF-α were increased in PHN patients. Besides, we demonstrated that serum MECP2 levels were positively correlated with serum inflammatory factors. All these results indicated that increased MECP2 was correlated with increased inflammation and pain of PHN patients.

The present study includes some limitations, The VAS scale and Pittsburg sleep quality are subjective scales, these factors depended of the subjective appreciation of the individual, so there was no confirmation that the levels of MECP2 correspond to the exact grade of pain because each subject can express the pain sensation in different form and may be an inexact measure of pain´s classification. In addition, the sample size of the study is small and we didn't investigate the molecular mechanism for MECP2 in PHN, and how the phosphorylated-MECP2 changes is also unclear, which need further investigations to reveal.

In conclusion, this observational study demonstrated that higher serum MECP2 levels were associated with a more severe pain condition and increased release of inflammatory factors, as well as a poorer quality of life of PHN patients before treatment. This study provided a novel potential biomarker for diagnosis of PHN.

ACKNOWLEDGEMENTS

We would like to acknowledge the everyone for their helpful contributions on this paper.

Funding

Science and Technology Project of Jiangxi Provincial Health Commission (220211509).

Declaration of conflict of interest

All authors declare no conflict of interest.

Authors' ORCID numbers

- Zhijian Wang
  0000-0001-6086-2241
- Wei Shen
  0000-0003-0342-3634
- Mengye Zhu
  0000-0002-6081-4490
- Mu Xu
  0000-0002-9755-3028
- Mizhen Qiu
  0000-0002-1066-1908
- Daying Zhang
  0000-0003-0975-9964
- Shibiao Chen
  0000-0002-5622-1860

Authors' contributions

Each author has made an important scientific contribution to the study and has assisted with the drafting or revising of the manuscript.

REFERENCES

1. **Mallick-Searle T, Snodgrass B, Brant JM**. Postherpetic neuralgia: epidemiology, pathophysiology, and pain management pharmacology. J Multidiscip Health 2016;9:447.
2. **Shrestha M, Chen A.** Modalities in managing postherpetic neuralgia. Korean J Pain 2018;31(4):235.
3. **Saguil A, Kane SF, Mercado MG, Lauters R.** Herpes zoster and postherpetic neuralgia: prevention and management. Am Fam Physician 2017;96(10):656-663.
4. **Gudin J, Fudin J, Wang E, Haylon T, Patel K, Goss TF.** Treatment patterns and medication use in patients with postherpetic neuralgia. J Manag Care Spec Ph 2019;25(12):1387-1396.
5. **Wei S, Li X, Wang H, Liu Q, Shao L**. Analysis of the risk factors for postherpetic neuralgia. Dermatology 2019;235(5):426-433.

6. **Saguil A, Kane S, Mercado M, Lauters R.** Herpes zoster and postherpetic neuralgia: prevention and management. Am Fam Physician 2017 15;96(10):656-663.
7. **Johnson RW, Rice ASC.** Postherpetic neuralgia. New Engl J Med 2014;371(16):1526-1533.
8. **Mari F, Azimonti S, Bertani I, Bolognese F, Colombo E, Caselli R, Scala E, Longo I, Grosso S, Pescucci C**. CDKL5 belongs to the same molecular pathway of MeCP2 and it is responsible for the early-onset seizure variant of Rett syndrome. Hum Mol Genet 2005;14(14):1935-1346.
9. **Downs J, Géranton SM, Bebbington A, Jacoby P, Bahi-Buisson N, Ravine D, Leonard H.** Linking MECP2 and pain sensitivity: the example of Rett syndrome. Am J Med Genet A. 2010;152(5):1197-1205.
10. **Zhang W, Peterson M, Beyer B, Frankel WN, Zhang Z-W.** Loss of MeCP2 from forebrain excitatory neurons leads to cortical hyperexcitation and seizures. J Neurosci 2014;34(7):2754-2763.
11. **Bodda C, Tantra M, Mollajew R, Arunachalam JP, Laccone FA, Can K, Rosenberger A, Mironov SL, Ehrenreich H, Mannan AU**. Mild overexpression of Mecp2 in mice causes a higher susceptibility toward seizures. Am J Pathol 2013;183(1):195-210.
12. Rzeszotarska E , Sowinska A , Stypinska B, Walczuk E, Wajda A, Lutkowska A, Felis-Giemza A, Olesinska M, Puszczewicz M, Majewski D, Jagodzinski PP, Czerewaty M, Malinowski D, Pawlik A, Jaronczyk M, Paradowska-Gorycka A. The role of MECP2 and CCR5 polymorphisms on the development and course of systemic lupus erythematosus. Biomolecules 2020, *10(3):494. doi: 10.3390/biom10030494.*
13. **Xie AX, Pan X-Q, Meacham RB, Malykhina AP.** The expression of transcription factors Mecp2 and CREB Is modulated in inflammatory pelvic pain. Front Syst Neurosci 2019;12:69.
14. **Manners MT, Tian Y, Zhou Z, Ajit SK.** MicroRNAs downregulated in neuropathic pain regulate MeCP2 and BDNF related to pain sensitivity. FEBS Open Bio 2015;5:733-740.
15. **Branch HzecwgoCMDAD**. Chinese Consensus of Herpes Zoster. Chin J Dermatol 2018;51:403–408.
16. **Yu S, Wan Y, Wan Q**. Chinese expert consensus on diagnosis and treatment of postherpetic neuralgia. Chin J Pain Med 2016;22:161-167.
17. **Wang Y, Liu C, Guo Q-L, Yan J-Q, Zhu X-Y, Huang C-S, Zou W-Y.** Intrathecal 5-azacytidine inhibits global DNA methylation and methyl-CpG-binding protein 2 expression and alleviates neuropathic pain in rats following chronic constriction injury. Brain Res 2011;1418:64-69.
18. **Van Der Vaart M, Svoboda O, Weijts BG, Espín-Palazón R, Sapp V, Pietri T, Bagnat M, Muotri AR, Traver D.** Mecp2 regulates tnfa during zebrafish embryonic development and acute inflammation. Dis Model Mech 2017;10(12):1439-1451.
19. **Li C, Jiang S, Liu S-Q, Lykken E, Zhao L-t, Sevilla J, Zhu B, Li Q-J.** MeCP2 enforces Foxp3 expression to promote regulatory T cells' resilience to inflammation. Proc Natl Acad Sci 2014;111(27):E2807-E2816.
20. **Ma T-t, Li X-f, Li W-x, Yang Y, Huang C, Meng X-m, Zhang L, Li J.** Geniposide alleviates inflammation by suppressing MeCP2 in mice with carbon tetrachloride-induced acute liver injury and LPS-treated THP-1 cells. Int Immunopharmacol 2015;29(2):739-747.
21. **Wittrahm R, Takalo M, Marttinen M, Kuulasmaa T, Mäkinen P, Kemppainen S, Martiskainen H, Rauramaa T, Pike I, Leinonen V**. MECP2 Increases the pro-inflammatory response of microglial cells and phosphorylation at serine 423 regulates neuronal gene expression upon neuroinflammation. Cells 2021;10(4):860.
22. **Zhang R, Huang M, Cao Z, Qi J, Qiu Z, Chiang L-Y.** MeCP2 plays an analgesic role in pain transmission through regulating CREB/miR-132 pathway. Mol Pain 2015;11:s12990-015.
23. **Zalosnik MI, Fabio MC, Bertoldi ML, Castañares CN, Degano AL**. MeCP2 deficiency exacerbates the neuroinflammatory setting and autoreactive response during an autoimmune challenge. Sci Rep 2021;11(1):1-15.

24. Zhao W, Wang Y, Fang Q, Wu J, Gao X, Liu H, Cao L, An J. Changes in neurotrophic and inflammatory factors in the cerebrospinal fluid of patients with postherpetic neuralgia. Neurosci Lett 2017;637:108-113.

25. Cao S, Zhang D, Yuan J, Deng W, Wen S, Qin B, Li Y. Inflammatory cytokine expression in the skin of patients with postherpetic neuralgia. J Int Med Res 2020;48(8):0300060520929582.

26. Üçeyler N, Valet M, Kafke W, Tölle TR, Sommer C. Local and systemic cytokine expression in patients with postherpetic neuralgia. PLoS One 2014;9(8):e105269.

Invest Clin 63(1): 92 - 99, 2022 https://doi.org/10.54817/IC.v63n1a08

Detection of the Omicron variant of SARS-CoV-2 by restriction analysis targeting the mutations K417N and N440K of the spike protein.

Rossana C Jaspe[1], José Luis Zambrano[2], Mariana Hidalgo[3], Yoneira Sulbarán[1], Carmen L Loureiro[1], Zoila C Moros[2], Domingo J Garzaro[1], Ferdinando Liprandi[2], Héctor R Rangel[1] and Flor H Pujol[1]

[1]Laboratorio de Virología Molecular, Centro de Microbiología y Biología Celular, Instituto Venezolano de Investigaciones Científicas, Caracas, Venezuela.
[2]Laboratorio de Biología de Virus, Centro de Microbiología y Biología Celular, Instituto Venezolano de Investigaciones Científicas, Caracas, Venezuela.
[3]Laboratorio de Inmunoparasitología, Centro de Microbiología y Biología Celular, Instituto Venezolano de Investigaciones Científicas, Caracas, Venezuela.

Key words: COVID-19; SARS-CoV-2; Omicron Variant of Concern; RFLP; rapid screening.

Abstract. By the end of 2021, the Omicron variant of concern (VOC) emerges in South Africa. This variant caused immediate concern, due to the explosive increase in cases associated with it and the large number of mutations it exhibits. In this study, the restriction sites that allow detecting the mutations K417N and N440K in the Spike gene are described. This analysis allows us to propose a rapid method for the identification of cases infected with the Omicron variant. We show that the proposed methodology can contribute to provide more information on the prevalence and rapid detection of cases of this new VOC.

Corresponding author: Flor H Pujol, Laboratorio de Virología Molecular, IVIC, CMBC, Caracas, Venezuela. E-mail: fhpujol@gmail.com

Detección de la Variante Ómicron del SARS-CoV-2 por análisis de restricción de dos mutaciones de la proteína de la espiga

Invest Clin 2022; 63 (1): 92 – 99

Palabras clave: COVID-19; SARS-CoV-2; Variante Omicron; RFLP; detección rápida.

Resumen. Para finales de 2021 surge la variante de preocupación (VOC por sus siglas en inglés) Ómicron en Sudáfrica. Esta variante causó de forma inmediata preocupación, debido al aumento explosivo de casos asociados a ella y al gran número de mutaciones que exhibe. En este estudio, se describen los sitios de restricción que permiten detectar dos de estas mutaciones en el gen de la espiga, las mutaciones K417N y N440K. Este análisis permite proponer un método rápido para la identificación de casos infectados con la variante Ómicron. Mostramos que la metodología propuesta puede contribuir a proporcionar más información sobre la prevalencia y a detectar rápidamente los casos de esta nueva VOC.

Received: 29-01-2022 Accepted: 05-02-2022

INTRODUCTION

The COVID-19 pandemic is caused by an emerging coronavirus, SARS-CoV-2, and has caused more than 360 million cases and more than 5 million deaths worldwide. This virus belongs to the family Coronaviridae. The tremendous number of replication events that this virus has experienced, in addition to an elevated frequency of recombination, and the probable action of host deaminases on the viral genome [1], has allowed the emergence of many mutations in the viral genome [2].

Different variants (lineages of viruses sharing particular types of mutations) have emerged since the end of 2020. Some of these variants have been defined as of interest (VOI) or concern (VOC) by WHO, associated with more transmissibility, or partial resistance to protective immunity, among other characteristics. The variants for which at least one of these characteristics has been confirmed, are named VOC [3-7]. There are at present five VOCs: Alpha, which emerged in the UK, Beta in South Africa, Gamma in Brazil, Delta in India, and Omicron in South Africa. Genomic surveillance is recommended for monitoring the introduction of SARS-CoV-2 variants of concern (VOCs) in each country [6, 7].

Since the middle of 2021, the Delta VOC (lineage B.1.617.2) was predominating in many countries and replacing the other circulating variants. However, at the end of November 2021, Omicron VOC (lineage B.1.1.529) was identified in South Africa [8]. This variant was classified as VOC in a record time because of the explosive increase of cases in South Africa, and the great number of mutations exhibited by this new lineage. Since then, up to January 15, 2022, the VOC Omicron has been detected in at least 119 countries (Complete genome sequences submitted in GISAID: https://www.gisaid.org/hcov19-variants/) and is presently replacing Delta worldwide [9].

Omicron VOC exhibits more than 50 mutations in its complete genome, com-

pared to the ancestral Wuhan strain. More than 30 of these mutations are located in the spike protein [8, 10]. Rapid detection of this variant is particularly important, due to the explosive nature of its transmission. The aim of this study was to evaluate a method for rapid detection of this mutation by restriction enzyme analysis, taking advantage of two mutations present in this VOC: K417N and N440K.

MATERIALS AND METHODS

Sequences available at GISAID on January 15, 2022, were analyzed for the presence of two mutations of the Omicron VOC: K417N and N440K. at https://www.gisaid.org. The number of sequences belonging to the Delta VOC among the ones harboring this mutation was also estimated.

This study was approved by the Bioethical Committee of IVIC. A restriction enzyme analysis was developed to detect the presence of two mutations: K417N and N440K. RNA from clinical samples positive by qRT-PCR (classified upon sequencing as Delta or Omicron) were amplified with primers 75L (AGAGTCCAACCAACAGAATCTATTGT) and 76.8R (GTTGCTGGTGCATGTAGAAGTTC) to generate an amplicon of 614 nt, with the PCR conditions previously described [11], with denaturation times of 94°C/30 sec. Six μL of the amplicon were digested with one unit of HindIII or SspI for one hour at 37°C and then loaded in a 3% agarose gel electrophoresis for band visualization with Ethidium bromide. Restriction results were compared with the sequence obtained by sending PCR purified fragments to the Macrogen Sequencing Service (Macrogen, Korea).

RESULTS

Sequences available at GISAID, belonging to the Delta or Omicron variant lineages, were analyzed for the presence of K417N and N440K. A total of 7,136,478 were available at GISAID on January 15, 2022. Only sequences of the complete genome and with high coverage were analyzed. As can be seen in Table 1, while 73% of the sequences available for the Delta variant meet both criteria, only 2% of the Omicron VOC meet them. The presence of K417N or N440K was near 90% in the Omicron VOC lineages, compared to less than 1% in the Delta VOC ones. According to this prevalence data, the detection of one of these two mutations could result in an assay with 94.4% sensitivity and 99.8% specificity.

The analysis of the restriction sites presents in the 614 nt amplicon of the spike gene

Table 1
Number of sequences available at GISAID of Delta or Omicron VOC harboring the mutations K417N and N440K.

Number of sequences (%)*	Delta (B.1.617.2)	Omicron (B.1.1529)
Total sequences	4,061,464	364,148
Sequences of complete genome with high coverage (SCH)	2,954,586 (73%)	5,995 (2%)
SCH with K417N	4,831 (0.2%)	5,415 (90%)
SCH with N440K	99 (0.002%)	5,263 (88%)
SCH with both mutations	0**	5,016 (84%)
SCH with any of the mutations	5,830 (0.2%)	5,662 (94.4%)

*Sequences available at GISAID in January 15, 2022. **12 sequences were available with both mutations among the 4,061,464 total sequences of the Delta variant.

of SARS-CoV-2 showed the presence of a restriction site in the nucleotides corresponding to the K417N and N440K mutations. Fig. 1 shows the expected restriction pattern of samples and isolates harboring mutations K417N and N440K, by using two restriction enzymes: SspI for K417N and HindIII for N440K: the SspI enzyme has an additional restriction site in the respective mutated sample and HindIII an unique restriction site in the mutation N440K. Fig. 1C shows the digestion of the PCR-amplified product with the two enzymes of two samples with the two mutations (Omicron variant) and two samples without the mutations (Gamma or Delta variant). A total of 28 samples were analyzed for their restriction pattern with these two enzymes, and compared for the presence or not of the mutations K417N and N440K in their sequence. A 100% concordance was observed in the detection of the two mutations between the two methods (Table 2). In addition, the sequence of the complete genome was available for three of the samples analyzed, and again a perfect concordance was found with the variant assigned by restriction analysis of the sequencing of the small genomic fragment: two Omicron VCs (GISAID accession numbers EPI_ISL_8063574 and EPI_ISL_8063663) and one Delta VOC (EPI_ISL_8804532). All the Omicron VOCs analyzed in this study harbored both mutations K417N and N440K.

DISCUSSION

For evaluating the projected sensitivity of restriction analysis using these two mutations as an indicator of Omicron presence, sequences available at GISAID were evaluated for the presence of the mutations K417N and N440K. The prevalence between Omicron and Delta VOCs was compared, since the Delta VOC was circulating and predominating in almost every part of the world just before the Omicron VOC rise in cases.

In addition to the huge number of mutations and rise in cases in each country, where this variant began to circulate, another peculiarity of the Omicron VOC is the variability in the number of mutations displayed by each isolate, that is, not all the isolates harbor all the mutations described for this variant. Indeed, the authors found a prevalence of less than 50% for the two mutations analyzed in this study, although they also recognized that the prevalence reported in their study might be higher for some of these mutations [8]. The rush in submitting sequences for the Omicron variant, shown by the huge predominance of complete genome sequences with low coverage (98%, compared to only 27% for Delta VOC, see Table 1), is an important factor that may hamper the real prevalence of each mutation in the Omicron VOC genomes.

According to the analysis performed on the sequences submitted to GISAID, the predicted sensitivity of the proposed restriction analysis, based on the detection of at least one of the K417N or N440K mutations, should result in a test with at least 94% sensitivity. Indeed, the sensitivity could be even higher, considering the possibility that some of the Omicron VOC sequences deposited in GISAID may harbor non-resolved nucleotides in the sites of these two mutations. In addition to few Delta VOCs, the Beta VOC harbors the mutation K417N. Thus, the detection of this mutation might not guarantee the presence of the Omicron VOC. However, the frequency of Beta VOC has been very low in the last months. A search in GiSAID resulted in only six sequences of Beta VOC from December 2021 up to January 2022.

A perfect correlation was found in this study between the restriction and sequence analysis. All the sequences analyzed harbored the two mutations, in agreement with the high prevalence of both mutations found in the sequence analyzed in this study, and providing a predictive value of almost 100% of Omicron identification. This method indeed allowed us to detect the first Omicron cases in Venezuela (Jaspe, RC, and

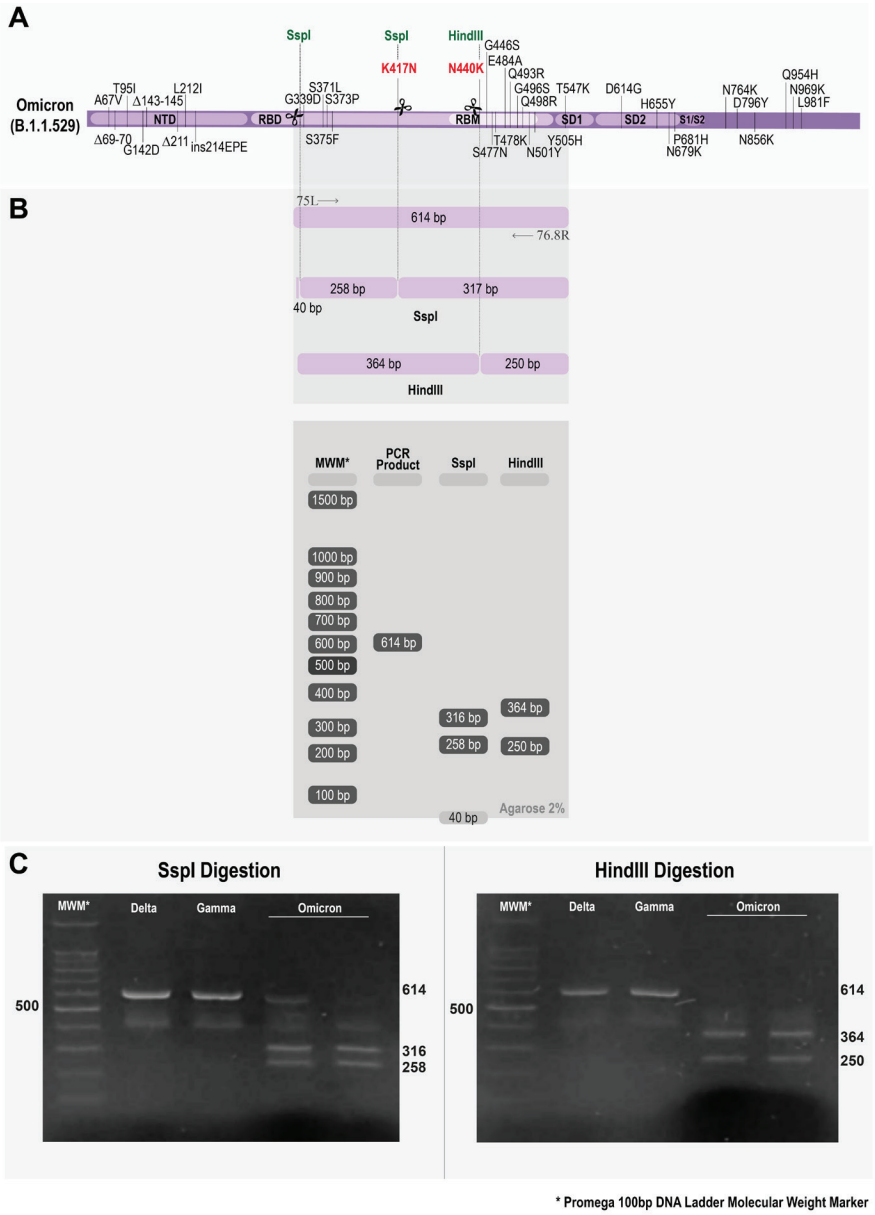

Fig. 1. Restriction analysis of amplicons with K417N and N440K mutations. A. Sequence of the amplified product showing the restriction sites which discriminate Wild-type (WT) or mutant (K417N and N440K) viruses. The use of these two enzymes generates a restriction pattern characteristic for each situation (WT, K417N, and N440K). The restriction sites are underlined. The numbers in the alignment indicate the bp position in the PCR-amplified product. Nucleotides 79-81 code for the amino acid K417 (CTG) or N417 (CGG). Nucleotides 79-81 code for the amino acid N440 (CTG) or K440 (CGG). B. Expected digestion pattern with HindIII or SspI enzymes. With HindIII digestion, the WT amplicon generates an undigested product of 614 bp, while N440K mutated amplicon generates 2 bands: one of 384 pb and one of 250 bp. With SspI digestion, WT amplicon generates two bands: one of 575 pb and one of 40 bp that is not seen in the gel, while K417N mutated amplicon generates three bands of 317, 258, and 40 bp that is not seen in the gel. C. Agarose gel electrophoresis of PCR-amplified products digested with HindIII or SspI. The PCR-amplified products digested with the enzymes were run with molecular weight markers (100bp DNA Ladder Molecular Weight Marker, Promega): smaller bands are signaled (100, 200, and 300 bp).

Table 2
Concordance between restriction enzyme analysis and sequencing results.

Sequence analysis Restriction analysis	K417 and N440 (Delta)	N417 and K440 (Omicron)	Concordance
K417 and N440	15	0	100%
N417 and K440	0	13	

A total of 28 samples were analyzed: 15 Delta VOC (lineage B.1.617.2), without any of the two mutations, and 13 Omicron VOC (lineage B.1.1.529).

Pujol, FH, personal communication). Our group has already developed several restriction analyses for the detection of key mutations present in some VOCs, like E484K and L452R [12, 13]. The method proposed in this study, together with the previously developed for other mutations, has been very useful in our hand for rapid detection of the variant in particular cases. It is important to note that complete genome sequencing is necessary for confirmation of the variant assignment, but once Omicron VOC is expanding in a particular region, the detection of these mutations is highly predictive of its presence.

Due to its explosive reproductive rate, rapid methods for detection of the Omicron VOC are warranted. In our hands, the detection of two of its mutations by restriction analysis was very useful for the rapid detection of the Omicron VOC.

Funding

This study was supported by Ministerio del Poder Popular de Ciencia, Tecnología e Innovación of Venezuela.

Declaration of conflict of interest

The authors declare no conflict of interest.

Authors' ORCID numbers

- Rossana C Jaspe (RCJ)
  0000-0002-4816-1378
- José Luis Zambrano (JLZ)
  0000-0001-9884- 2940
- Mariana Hidalgo (MH)
  0000-0002-8307-8254
- Yoneira Sulbaran (YS)
  0000-0002-3170-353X
- Carmen L Loureiro (CLL)
  0000-0003-3665-1107
- Zoila C Moros (ZCM)
  0000-0001-6322-9230
- Domingo J Garzaro (DJG)
  0000-0002-9956-5786
- Ferdinando Liprandi (FL)
  0000 0001 8084 8252
- Héctor R Rangel (HRR)
  0000-0001-5937-9690
- Flor H Pujol (FHP)
  0000-0001-6086-6883

Authorship contribution

- RCJ and JLZ contributed equally to this study.
- Design of the study and writing of the manuscript: RCJ, JLZ, FL, FHP. Experimental: RCJ, MH, YS, CLL, ZCM, DJG, HRR.
- All the authors read and approved the final version of the manuscript.

REFERENCES

1. **Pujol FH, Zambrano JL, Jaspe R, Loureiro CL, Vizzi E, Liprandi F, Rangel HR**. Biología y evolución del coronavirus causante de la COVID-19. Rev Soc Venezol Microbiol 2020; 40:63-70.
2. **Phan T**. Genetic diversity and evolution of SARS-CoV-2. Infect Genet Evol 2020; 81:104260. *https://doi.org/10.1016/j.meegid.2020.104260.*
3. **Rotondo JC, Martini F, Maritati M, Mazziotta C, Di Mauro G, Lanzillotti C, Barp N, Gallerani A, Togˊnon M, Contini C**. SARS-CoV-2 infection: new molecular, phylogenetic, and pathogenetic insights. Efficacy of current vaccines and the potential risk of Variants. Viruses 2021; 13:1687. *https://doi.org/10.3390/v13091687*
4. **World Health Organization**. Tracking SARS-CoV-2 variants. Available from: URL: https://www.who.int/en/activities/tracking-SARS-CoV-2-variants/. [revised on January 26, 2022].
5. **Mistry P, Barmania F, Mellet J, Peta K, Strydom A, Viljoen IM, James W, Gordon S, Pepper MS.** SARS-CoV-2 variants, vaccines, and host immunity. Front Immunol 2022; 12:809244. *https://doi.org/10.3389/fimmu.2021.809244.*
6. **Alefishat E, Jelinek HF, Mousa M, Tay GK, Alsafar HS.** Immune response to SARS-CoV-2 variants: A focus on severity, susceptibility, and preexisting immunity. J Infect Public Health 2022;15(2):277-288. *https://doi.org/10.1016/j.jiph.2022.01.007.*
7. **Thye AY, Law JW, Pusparajah P, Letchumanan V, Chan KG, Lee LH.** Emerging SARS-CoV-2 Variants of Concern (VOCs): an impending global crisis. Biomedicines 2021;9(10):1303. *https://doi.org/10.3390/biomedicines9101303.*
8. **Viana R, Moyo S, Amoako DG, Tegally H, Scheepers C, Althaus ChL, Anyaneji UJ, Bester PhA, Boni MF, Chand M, Choga WT, Colquhoun R, Davids M, Deforche K, Doolabh D, du Plessis L, Engelbrecht S, Everatt J, Giandhari J, Giovanetti M, Hardie D, Hill V, Hsiao NY, Iranzadeh A, Ismail A, Joseph Ch, Joseph R, Koopile L, Kosakovsky Pond SL, Kraemer MUG, Kuate-Lere L, Laguda-Akingba O, Lesetedi-Mafoko O, Lessells RJ, Lockman Sh, Lucaci AG, Maharaj A, Mahlangu B, Maponga T, Mahlakwane K, Makatini Z, Marais G, Maruapula D, Masupu K, Matshaba M, Mayaphi S, Mbhele N, Mbulawa MB, Mendes A, Mlisana K, Mnguni A, Mohale Th, Moir M, Moruisi K, Mosepele M, Motsatsi G, Motswaledi MS, Mphoyakgosi Th, Msomi N, Mwangi PN, Naidoo Y, Ntuli N, Nyaga M, Olubayo L, Pillay S, Radibe B, Ramphal Y, Ramphal U, San JE, Scott L, Shapiro R, Singh L, Smith-Lawrence P, Stevens W, Strydom A, Subramoney K, Tebeila N, Tshiabuila D, Tsui J, van Wyk S, Weaver S, Wibmer CK, Wilkinson E, Wolter N, Zarebski AE, Zuze B, Goedhals D, Preiser W, Treurnicht F, Venter M, Williamson C, Pybus OG, Bhiman J, Glass A, Martin DP, Rambaut A, Gaseitsiwe S, von Gottberg A, de Oliveira T.** Rapid epidemic expansion of the SARSCoV-2 Omicron variant in Southern Africa. Nature 2022 Jan 7. *https://doi.org/10.1038/s41586-022-04 411-y.*
9. **Health professionals and researchers from across Europe.** Europe must come together to confront omicron. BMJ. 2022;376:o90. *https://doi.org/10.1136/bmj.o90.*
10. **Ren SY, Wang WB, Gao RD, Zhou AM.** Omicron variant (B.1.1.529) of SARS-CoV-2: Mutation, infectivity, transmission, and vaccine resistance. World J Clin Cases 2022;10(1):1-11. *https://doi.org/10.12998/wjcc.v10.i1.1.*
11. **Jaspe RC, Loureiro CL, Sulbaran Y, Moros ZC, D´Angelo P, Rodríguez L, Zambrano JL, Hidalgo M, Vizzi E, Alarcon V, Aguilar M, Garzaro DJ, CoViMol Group, Rangel HR, Pujol FH.** Introduction and rapid dissemination of SARS-CoV-2 Gamma Variant of Concern in Venezuela. Infect Genet Evol 2021;96:105147. *https://doi.org/10.1016/j.meegid.2021.105147.*
12. **Jaspe RC, Sulbaran Y, Loureiro CL, D Angelo P, Rodriguez L, Garzaro D, Rangel HR, Pujol FH.** Importance of mutations in amino acid 484 of the Spike protein of SARS-CoV-2: rapid detection by restriction enzyme analysis. Invest. Clin.

2021; 62(Suppl. 2): 16–24. *https://doi.org/10.22209/IC.v62s2a02.*

13. **Jaspe RC, Sulbaran Y, Hidalgo M, Loureiro CL, Moros ZC, Garzaro D, Rangel HR, Pujol FH.** A simple method for detection of mutations in amino acid 452 of the Spike protein of SARS-CoV-2 using restriction enzyme analysis. Invest. Clin 2021; 62(4): 371-377. *https://doi.org/10.22209/IC.v62n4a07.*

Instrucciones a los Autores

Investigación Clínica publica Trabajos Originales, Revisiones y Reporte de Casos Clínicos en español e inglés, que contribuyan al avance del conocimiento en biología humana o animal. También incluye una sección de "Cartas al Editor".

Envío del manuscrito

El manuscrito (Word para Windows®), con su correspondiente lista de verificación y acompañado de una carta de presentación al editor, debe ser enviado por correo electrónico a las direcciones riclinicas@gmail.com/elenaryder@gmail.com. Las Tablas y las Figuras, sí las hubiese, deben estar al final del trabajo. Además del manuscrito, se pueden incluir los nombres de tres posibles árbitros y sus respectivas direcciones institucional y electrónica. El Comité Editorial se reserva el derecho de decidir si utiliza alguno de los revisores sugeridos. Todo lo referente a la correspondencia, incluidos la opinión de los árbitros, los requerimientos producto de la revisión del trabajo y la notificación de la decisión del Comité Editorial, será comunicado por correo electrónico. La correspondencia de seguimiento del trabajo debe incluir el código asignado por la revista en la carta de recepción.

Carta de presentación

El manuscrito debe estar acompañado de una carta firmada por todos los autores, donde manifiestan que han participado activamente en la ejecución del trabajo, que este no ha sido publicado con anterioridad y que conocen que se está enviando para su publicación a Investigación Clínica y que no ha sido enviado a otra Revista para su consideración. La autoría debe estar basada en: 1) Contribución sustancial a la concepción y diseño del estudio, obtención de datos o su análisis e interpretación, 2) Revisión crítica del artículo y 3) Aprobación de la versión final a ser publicada. La obtención de fondos, la recolección de datos o la supervisión del grupo de investigación, por sí solos, no justifican la autoría. Aquellos miembros del grupo que no cumplan con los criterios para ser autores, deben ser mencionados en la sección de Agradecimientos. El orden de aparición de los autores no se podrá modificar una vez que el trabajo haya sido aceptado. En la carta de presentación, es imprescindible colocar: financiamiento, contribución de cada uno de los autores y su número ORCID, y si hubiere algún conflicto de competencia.

Sistema de Arbitraje

Para el proceso de arbitraje se utilizará la vía electrónica. Todos los trabajos serán sometidos a la consideración del Comité Editorial de la Revista, el cual decidirá si deben ser enviados a arbitraje, o si se rechazan por no cumplir las normas editoriales o no tener la calidad suficiente. El autor de correspondencia recibirá una carta de recepción con un código numérico.

El arbitraje de Trabajos Originales y Reporte de Casos, será realizado por dos expertos en el área objeto de la comunicación y en el caso de las Revisiones, solo por uno. Los árbitros tendrán un plazo máximo de dos meses para enviar su respuesta. Si las opiniones de los dos árbitros coinciden, el Comité Editorial podrá tomar una decisión; en caso de discrepancia, esperará la opinión de un tercer árbitro. Si la situación lo amerita,

se podrán solicitar otras opiniones. El nombre de los árbitros y el de los autores del trabajo, serán estrictamente confidenciales; la Revista sigue la evaluación doble ciego. Los autores recibirán, tanto en el caso de modificaciones, como en el de rechazo, las opiniones completas respecto al trabajo. El plazo para responder a las recomendaciones de los árbitros, tendrá un máximo de dos meses, pasados los cuales el trabajo será rechazado o readmitido como nuevo.

Costo de la publicación. Todo trabajo aceptado tendrá un costo por concepto de Manejo Editorial.

Normas Editoriales

Los trabajos deben estar escritos a doble espacio, con amplios márgenes y numeración de las páginas. En Word for Windows y preferiblemente en Times New Roman 12.

Los **Trabajos Originales**, las **Revisiones** y los **Reportes de Casos,** deben ser contribuciones inéditas de importancia para el avance del conocimiento en el tema objeto de estudio. Deben incluir en la primera página:

El **Título del trabajo** con letra mayúscula al inicio o cuando se trate de nombres propios; luego el primer nombre, la inicial del segundo y el apellido completo de los autores; si usaran dos apellidos deberán separarlos con un guión. El nombre de cada autor llevará superíndices de números consecutivos que correspondan a cada una de las instituciones a las que están afiliados. No repetir si pertenecen a la misma institución, solo colocar el superíndice respectivo. No colocar títulos profesionales.

Un **Título corto** de no más de 75 caracteres, en el idioma en que fue realizado el manuscrito.

Palabras clave. En renglón aparte, se escribirán de tres a seis palabras clave en español y en inglés, evitando repetir palabras que se encuentren en el título.

Autor de correspondencia. Colocar Nombre completo, sin títulos académicos, dirección institucional, ciudad, país, teléfono y correo electrónico.

A continuación, se presentarán un **Resumen** en español y el título y el resumen (**Abstract**), ambos en inglés. Si el autor no está capacitado en el idioma inglés, es importante que consulte a un especialista en lengua inglesa, antes de enviar los trabajos o resúmenes en ese idioma. Se requiere el uso del inglés americano. Un trabajo puede ser rechazado, si requiere de muchas correcciones lingüísticas.

Los **Trabajos Originales**, estarán constituidos por: Resumen en español e inglés, Introducción, Material y Métodos o Pacientes y Métodos (si el trabajo se refiere a seres humanos), Resultados, Discusión, Tablas, Figuras, Agradecimientos y Referencias. Las Tablas y Figuras deberán presentarse aparte del manuscrito. La Revista no tiene una sección de Conclusiones, sino que estas estarán incluidas al final de la Discusión.

El **Resumen**, debe constar de un máximo de 250 palabras y establecer los objetivos, la metodología, los hallazgos originales y las conclusiones basadas en los resultados presentados. No debe contener referencias ni ser estructurado**.** Al final se debe incluir una pequeña conclusión. Se deben evitar las abreviaturas y si son necesarias, se deben definir en la primera mención.

El **Abstract** debe estar redactado en inglés americano y cumplir las mismas indicaciones del Resumen.

Introducción. Debe incluir en primer lugar, antecedentes y generalidades sobre el tema objeto del estudio, hallazgos controversiales, e interrogantes y aportaciones propias, y finalmente el objetivo principal de la investigación.

Material y Métodos. En esta sección se debe informar sobre las características y tamaño de la muestra. En los estudios con humanos deben incluir el consentimiento informado y señalar los criterios de inclusión y exclusión. En estos estudios se debe incluir en la descripción del Material utilizado, la aprobación por parte del Comité de Ética de la institución donde se realizó la investigación y seguir los lineamientos de la Declara-

ción de Helsinki de 1975, revisada en 2013. Se debe evitar el uso de iniciales o números de Historia de los Hospitales y no se aceptarán fotografías del rostro del paciente sin su consentimiento escrito. Aquellos estudios que involucren animales, también deben seguir el Código de Ética correspondiente, que cumpla con los estándares internacionales establecidos para el uso, cuidado y tratamiento de los animales de laboratorio. Los procedimientos deben ser descritos con suficiente detalle para permitir que el trabajo pueda ser duplicado. Los métodos no originales deberán tener su referencia y los equipos y reactivos utilizados deben ir acompañados del nombre y país de la compañía proveedora.

Análisis estadístico. Se debe informar cual fue la plataforma usada, mencionando la versión y las pruebas estadísticas empleadas.

Los **Resultados**, deben ser presentados en tiempo pretérito, en una secuencia lógica en el texto, Tablas y Figuras. Solo se deben resaltar las observaciones importantes. Los valores de laboratorio y las unidades deben ser expresados en el Sistema Internacional (SI). No repetir en el texto lo mostrado en las Figuras o Tablas, solo expresarlo. Las Tablas y Figuras se presentarán en hojas aparte y no en fotografías. La numeración de las Tablas y Figuras será en caracteres arábigos. No colocar en los títulos siglas que no hayan sido previamente identificadas.

Discusión. Mencionar los hallazgos principales del estudio, luego comparar los resultados con otros de la literatura, sus aportaciones y fortalezas, mencionar las limitaciones del trabajo, sugerir delineamientos de futuras investigaciones y terminar con una conclusión acorde con los resultados.

Las **Revisiones Narrativas** deben estar escritas por especialistas en el campo objeto de las mismas y contener las contribuciones del autor, ya sea en las referencias o con una discusión del tema revisado. El número máximo de autores es de cuatro. No se aceptarán revisiones que consistan meramente de una descripción bibliográfica, sin incluir un análisis. El cuerpo de las revisiones es libre, aunque es conveniente subdividirlo en secciones. Las **Revisiones Sistemáticas y Metaanalisis** deben seguir las indicaciones internacionales establecidas por PRISMA (Preferred Reporting Items for Systematic reviews and Meta-Analyses) o por cualquier otro método similar.

Los **Reportes de Casos** se refieren a la presentación de casos clínicos poco frecuentes en la práctica médica. Deben incluir una breve introducción sobre la patología a ser presentada, la descripción del caso y una discusión con el apoyo bibliográfico correspondiente. Limitar la discusión a lo más notable del caso.

Las **Cartas al Editor**, deben ser comentarios sobre publicaciones recientes en la revista y en lo posible, no deben exceder de dos páginas, incluidas las referencias.

Tablas. Las Tablas deben ocupar una página cada una y estar numeradas en caracteres arábigos Deben contener un título descriptivo escrito centrado. Las columnas no deben separarse con líneas. Las notas referentes a lo expresado en el cuerpo de la Tabla, deben ser escritas al pie de la misma, precedidas de los símbolos correspondientes. La revista no acepta la expresión "Fuente de información", cuando se refiere a resultados presentados en el mismo artículo, solo si provienen de otro material. Si el artículo está escrito en español, los números decimales se deben separar con una coma y si está escrito en inglés, con un punto.

Figuras. Para las Figuras se deben seguir los siguientes puntos generales: cada figura debe ser enviada en un archivo separado, en el programa donde fue generada (por ejemplo GraphPad Prism®). El número de la Figura debe ser arábigo y estar de acuerdo con la secuencia en el texto. Debe asegurarse que el tipo de letra y el tamaño, sean uniformes. Todas deben tener como mínimo 300dpi. Las figuras en color deben de ser enviadas en formato RGB (sigla en inglés de *red, green, blue*).Las leyendas de las figuras se deben enviar por separado, con suficiente información para no tener que recurrir al texto. Las imágenes radiográficas no deben contener

leyendas que identifiquen al paciente. Las Fotografias pueden ser en blanco y negro o en color, deben tener un contraste adecuado para su reproducción y estar en formato JPG o TIF, con las siguientes condiciones: las fotografías en color o en gradaciones de gris, deben tener un mínimo de 300 dpi. En el caso de las microfotografías electrónicas, debe extremarse el cuidado de la nitidez de los hallazgos reportados y señalarlos por medio de símbolos. También se debe indicar el aumento utilizado, de preferencia una barra indicando el valor que representa (micras, milimicras, nanómetros etc.). Las leyendas no deben estar incorporadas a la fotografía y estas deben presentarse en página aparte, en forma lo suficientemente explicativa, sin tener que acudir al texto, y cuidar la descripción si se trata de la figura a color o en tonos de grises. La Revista no aceptará fotografías o figuras tomadas de otras revistas sin la respectiva autorización.

Referencias. Todas las referencias deben estar en el texto con un número en superíndice y citadas por orden de aparición, según las normas internacionales "*Recommendations for the Conduct, Reporting, Editing, and Publication of Scholarly Work in Medical Journals*", actualizadas en Diciembre de 2021 (http:/www.icmje.org); es decir, primero el apellido con la letra inicial en mayúscula, e iniciales del nombre, también en mayúscula (sin puntos), de todos los autores. Los nombres de los autores deben ir en negritas y separados entre sí por comas. No se aceptarán los términos "y col." o "*et al.*" en la sección de las referencias.

El título completo del trabajo tendrá mayúsculas solo al inicio y en los nombres propios. El título de la revista debe ser abreviado de acuerdo al Index Medicus (http:/www.nlm.nih.gov), seguido del año de publicación; volumen: y primera y última páginas, separadas por un guión. A seguidas colocar el doi de dicho trabajo. No se aceptarán como referencias, observaciones no publicadas, comunicaciones personales o trabajos enviados a publicación; sin embargo, estos podrán aparecer citados entre paréntesis en el texto. Si el autor es una organización, se coloca el nombre de la misma como referencia.

Ejemplos:

Referencias de publicaciones periódicas: Jaspe RC, Sulbaran Y, Hidalgo M, Loureiro CL, Moros ZC, Garzaro D, Rangel HR, Pujol FH. A simple method for detection of mutations in amino acid 452 of the Spike protein of SARS-CoV-2 using restriction enzyme analysis. Invest Clin 2021; 62(4): 371-377. https://doi.org/10.22209/IC.v62n4a07.

Referencias de libros: Kandel ER, Schwartz JH, Jessell TM. Principles of neural science. New York: McGraw Hill; 2001, p 1227-1246.

Artículos en libros: Molina-Vílchez R, Diez-Ewald M, Fernández G. Anemia y Embarazo. En: Zighelboim I, Guariglia D, Eds. Clínica Obstétrica. Caracas: Disinlimed; 2000. P 570-577.

Memorias de Congresos: Metabolic benefits of lifestyle intervention in the clinical setting: a pilot study in Latinos with prediabetes form Venezuela, South América. Victoria Stepenka, Yoleida Rivas, Juan Casal, Roberto Gutiérrez, Elena Ryder, Hermes Florez. 70th. Scientific Sessions. American Diabetes Association. 25-29 junio, 2010, Orlando, USA.

Tesis: Leon-N I. Caracterización de aislamientos del complejo *Sporothrix* spp. Provenientes de diferentes regiones de Venezuela [Tesis de Maestria] Caracas: IVIC; 2013.

Revista en formato electrónico: Calvo B, Melo A, Perozo A, Hernández M, Francisco E, Hagen F, Meis J, Colombo J. First report of *Candida auris* in America: clinical and microbiological aspects of 18 episodes of candidaemia. J Infect 2016 [citado, 2017 febrero 10] Disponible en: http://dx.doi.org/10.1016/j.inf.2016.07.008.

Limitar a un máximo de 50 referencias para los artículos originales y 100 para las Revisiones Narrativas y Sistemáticas o Metanaálisis.

Se recomienda revisar cuidadosamente el último número de la Revista, como guía para la preparación del manuscrito (http://sites.google.com/site/revistainvestigacionesclinicas).

Lista de Verificación

- ☐ Carta firmada por todos los autores, donde se indique el autor de correspondencia, la participación de cada autor en la elaboración del trabajo, y se manifieste que este no ha sido publicado con anterioridad, ni está siendo enviado a otra revista para publicación.
- ☐ Páginas numeradas en forma secuencial.
- ☐ Título en español.
- ☐ Título en inglés.
- ☐ Título corto en el lenguaje principal utilizado en el manuscrito.
- ☐ Lista de Autores con nombres completos, sin títulos profesionales.
- ☐ Resumen no estructurado en inglés y español de no más de 250 palabras, que incluya introducción, procedimientos básicos, resultados y conclusión.
- ☐ Introducción sucinta y referida al objeto de estudio.
- ☐ Material y Métodos o Material y Pacientes, descritos con precisión y con referencias adecuadas.
- ☐ Especificación del análisis estadístico (cuando se requiere).
- ☐ Resultados presentados en forma clara y en orden lógico sin discusión de los mismos.
- ☐ Discusión basada en los hallazgos obtenidos.
- ☐ Referencias presentadas en orden de aparición, citadas en el texto y de acuerdo a las especificaciones de la revista.
- ☐ No se aceptan comunicaciones personales, ni presentaciones en congresos que no hayan tenido resumen.
- ☐ Tablas con las notas en la parte inferior.
- ☐ Las ilustraciones y fotografías de acuerdo a las especificaciones de la revista.
- ☐ Leyendas de las ilustraciones, figuras y fotografías en páginas separadas.
- ☐ Número ORCID de todos los autores.
- ☐ Fuente de financiamiento.
- ☐ Participación de los autores en el trabajo.
- ☐ Conflicto de competencia.

Instructions to Authors

Investigación Clínica publishes Original Research Articles, Reviews and Clinical Case Reports in Spanish and English that represent a significant contribution to the advance of knowledge in human or animal biology. It also includes a section of Letters to the Editor.

Send the manuscript (in Word for Windows ®), with its corresponding Check List and accompanied by a Cover Letter to the Editor, by e-mail to the following addresses: riclinicas@gmail.com / elenaryder@ gmail.com. The Tables and Figures, if any, should be placed at the end of the manuscript text and must be sent as individual files (one per each table and figure). The name of three possible referees, with their postal and e-mail addresses should be submitted together with the manuscript. The Editorial Board reserves the right to decide if any of them will be chosen as reviewers. Everything concerning the correspondence, including the opinion of the referees, the requirements resulting from the manuscript review and notification of the decision of the Editorial Committee, will be conducted by e-mail. The Paper follow-up correspondence must include the code assigned by the Journal in the receipt letter.

Cover Letter

The manuscript must be accompanied by a letter, addressed to the Editor, in which all authors accept, with their signature, that have actively participated in the development and execution of this work, and that the manuscript is being sent for consideration to this journal. In this letter, the authors must state that the work submitted is original, has not been published previously, and that it is not under consideration for publication. Authorship must be based in: 1) A substantial contribution to the concept and design of the study, acquisition of data or analysis and interpretation of the data; 2) Drafting or critically reviewing the manuscript; and 3) Final approval of the version of the article to be published. Raising funds, collecting data or general supervision of the research group, by themselves, do not justify authorship. Those members of the group that do not meet the authorship criteria should be recognized, with their authorization, in the **Acknowledgments** section. The author must sign a form specifying the extent of their participation in the work. The order of authorship credited should be a joint decision of the co-authors. The order of appearance of the authors, and the inclusion or exclusion of any of them, cannot be modified once the work has been accepted. In the cover letter, it is essential to include source of financing, participation of each of the authors using initials and the ORCID number (ORCID iD) of each one, and if there is any conflict of competence.

Peer-review Process

This process will be realized through electronic means. All manuscripts submitted for publication are considered by the Editorial Board of the Journal, which decides if they should be sent to review, or should be rejected because the manuscript does not meet the minimal editorial requirements or if it is not of sufficient quality to be published in the journal. The corresponding author will receive a receipt letter with a numerical code. The Original Research Articles and Clinical Case Reports will be reviewed by two

experts in the area object of the communication, and only one, in the case of Review Articles. The name of the authors and reviewers áre strictly confidential; the Journal follows the double blind review process. The reviewers will be given a maximum of a two-month period to send their evaluations. If the opinions of two of them coincide, the Editorial Board could accept these evaluations. In case of discrepancy, it will wait for a third opinion or it may even require the evaluation of additionally appointed referees. The authors will receive the complete reviewer's evaluations, both in cases of manuscript modifications, or in cases of rejections. The Editorial Committee will give the authors a two-month period to respond to the reviewer's opinions or to make the suggested modifications. If the authors take more time to answer than the stipulated, the manuscript will be rejected or considered as a new submission.

Publication Fees. A nominal publication fee will be charged upon acceptance of a paper, to contribute to the cost of Editorial Handling.

Editorial Norms

Manuscripts should be submitted in Microsoft Word® (.doc/.docx) format, preferably in Times New Roman 12 font, must be double-spaced throughout, all pages should be numbered and with ample margins in both sides.

Original Research Articles, Clinical Case Reports and Review Articles must consist of original contributions of importance to the advance of knowledge in the subject matter of the study. They must include in the first page the manuscript's:

The Title of the work, which must be with a capital letter at the beginning or in the case of proper names; then place the authors with their first name, the middle initial and the complete last name; if they use two surnames they must separate them with a hyphen. The name of each author will have superscripts of consecutive numbers that correspond to each of the institutions of affiliation. Do not repeat if they belong to the same institution, just place the respective superscript. Do not use professional titles. The author of the correspondence, his full name, without academic titles, institutional address, city, country, telephone and email must be indicated.

A short Title of no more than 75 characters, in the language in which the manuscript was written.

Keywords. In a separate line, three to six keywords will be written in Spanish and English, avoiding repeating words found in the title.

This should be followed by a summary in Spanish and the Title and Abstract, both in English. If the full text of the paper is written in English or as with the English abstract, it is important to consult with an expert if the author is not proficient in the language. A manuscript could be rejected if it requires considerable language modifications.

Original Research Articles, should be structured as follows: Abstracts in Spanish and English, Introduction, Material and Methods or Patients and Methods (if the research is related to humans), Results, Discussion, Tables, Figures, Acknowledgments and References. Tables and Figures must be presented separately from the manuscript. The Journal does not utilize a Conclusions section and these should be part of the end of the Discussion.

Abstract, must be written in American English and should establish the objectives of the study, the methodology used, the original observations and the conclusions based on the results presented. It must not contain references, nor be structured and should not exceed the limit of 250 words. A brief conclusion must be presented at the end of the abstract. Avoid the use of abbreviations and if necessary, they should be defined at the first mention in the text. The summary in Spanish must comply with the same indications as the Abstract in English.

Introduction: it should include adequate background and general information

about the subject under study, controversial findings, and own questions and contributions, and finally the main objective of the investigation.

Material and methods: this section should report on the characteristics and size of the sample. In studies with humans, they must include informed consent and indicate the inclusion and exclusion criteria. Human studies should include in the description of the Material used, the approval of the Ethics Committee of the institution where the study was realized, following the principles outlined in the Declaration of Helsinki of 1975 and revised in 2013. The use of names, initials or the clinical history number should be avoided. Photographs showing the face of patients will not be accepted without a signed statement of informed consent. Those studies involving animals must follow the corresponding ethics code, according to the established international standard guidelines for the use, care and treatment of laboratory animals. Procedures should be described with sufficient detail as to allow the work to be replicated. Non-original methods must have their reference and the equipment and reagents used must be accompanied by the name and country of the supplying companies.

Statistical analysis. The software used must be reported, mentioning the version and the statistical tests used.

Results, should be presented in past tense following a logical sequence in the Text, Tables and Figures. Laboratory values and units must be expressed in the International System of Units (SI). The information presented in Tables and Figures should not be repeated in the text. Only the important observations must be detailed.

Discussion, must emphasize on the new and important findings of the study and compare the results obtained with those previously reported on other investigations. It should present the new finding's implications, their limitations, as well as suggest the outlines of future investigations and end with a conclusion according to the results obtained.

Review Articles. Should be written, preferentially, by a specialist in the field object of the review and should contain the author's own contributions, either in the bibliography or with a discussion of the subject matter reviewed. No more than four authors are allowed. Reviews that consist only in a bibliographical description of the subject, without including an analysis, will not be accepted. The text body of the Reviews is free, although it is convenient to subdivide it in sections.

Systematic Reviews and Meta-Analyses, must follow the indications established internationally by PRISMA (Preferred Reporting Items for Systematic reviews and Meta-Analyses) or any other similar method.

Clinical Case Reports. Should consist in the presentation of uncommon clinical cases in the daily medical practice. They must include a brief introduction about the pathology to be studied, a detailed description of the case, followed by a discussion and the corresponding bibliographical support. Limit the discussion to the most notable of the case.

Letters to the Editor, should be commentaries to recent publications in our Journal and if possible, should not exceed two pages in length, including references, if any.

Tables. The Tables will be presented on separate sheets. The numbering of the Tables will be in Arabic characters. They must have their titles centered and without acronyms or abbreviations. Lines should not separate columns. The clarification notes referring to the expressed in the body of the Table should be incorporated as footnotes, with the corresponding symbol, at the bottom. The journal does not accept the expression "Source of Information" in the Tables that refer to the results presented in the manuscript, but only in those that come from other material. Care should be taken to place commas be-

fore decimals if the article is written in Spanish or periods if it is in English.

Figures, should be submitted considering the following general points: each figure should be submitted as a separate file in the same software in which it was generated (GraphPad Prism® for example). Figures should be numbered consecutively, in Arabic numerals, according to the order of citation in the text. Make sure to use uniform font size and style in all figures. Figure legends must be sent separately and not appended to the figure, indicating their number, and with sufficient information to allow their interpretation, without having to recur to the text. Color Figures must be in TIFF or RGB (red,gree,blue) and have at least 600 dpi. **Photographs,** may be in black and white or in color, they must have adequate contrast for their reproduction and be in JPG or TIF format, and comply with the following conditions: photographs in color or in shades of gray must have a minimum of 300 dpi. In the case of electronic microphotographs, extreme care must be taken with the sharpness of the reported findings and detailing them by means of symbols. The magnification used in the microphotographs should also be indicated. The legends must not be incorporated into the photograph and these must be presented on a separate page, in a sufficiently explanatory way, without having to turn to the text, and taking care of the description if the figure is in color or in shades of gray. Radiographic images should not contain legends that identify the patient. The Journal will not accept photographs or figures taken from other magazines without the respective authorization.

All **References** must be cited in the text as superscript Arabic numerals. They must be cited consecutively in the order of appearance in the text, written accurately, as they appear in the original work, and following the international norms described in "Recommendations for the Conduct, Reporting, Editing, and Publication of Scholarly Work in Medical Journals", updated in December 2021, http:// www.icmje.org; i.e., first, last name (using capitals only at the beginning) and first name initials, without periods, for all authors. The names of all authors must be typed in bold face and each one separated by commas. The terms "y col." or "et al." are not acceptable. This must be followed by the full title of the article using capital letters only at the beginning and in proper names. Next, the abbreviated journal title, according to the indications of the Index Medicus (http://nlm.nih.gov), followed by the year of publishing; volume: and first and last page numbers separated by a hyphen. This must be followed by the digital object identifier of the work (DOI). Unpublished observations, personal communications or papers sent for publication will not be accepted as references; however, these may appear in the text, in parenthesis. If the author is an Organization, its name should be cited as a reference.

Examples:

– References of periodic publications: Jaspe RC, Sulbaran Y, Hidalgo M, Loureiro CL, Moros ZC, Garzaro D, Rangel HR, Pujol FH. A simple method for detection of mutations in amino acid 452 of the Spike protein of SARS-CoV-2 using restriction enzyme analysis. Invest Clin 2021; 62(4): 371-377. *https://doi.org/10.22209/IC.v62n4a07.*

– Book References: Kandel ER, Schwartz JH, Jessell TM. Principles of neural science. New York: McGraw Hill; 2001, p 1227-1246.

– Articles in Books: Molina-Vilchez R, Diez-Ewald M, Fernández G. Anemia y Embarazo. En: Zighelboim I, Guariglia D, Eds. Clínica Obstétrica. Caracas: Disinlimed; 2000. P 570-577.

– Congress Abstracts: Metabolic benefits of lifestyle intervention in the clinical setting: a pilot study in Latinos with prediabetes form Venezuela, South América.

Victoria Stepenka, Yoleida Rivas, Juan Casal, Roberto Gutiérrez, Elena Ryder, Hermes Florez. 70th. Scientific Sessions. American Diabetes Association. 25-29 junio, 2010, Orlando, USA.

– Thesis: Leon-N I. Caracterización de aislamientos del complejo *Sporothrix* spp. Provenientes de diferentes regiones de Venezuela [Tesis de Maestria] Caracas: IVIC; 2013.

– Online Journals: Calvo B, Melo A, Perozo A, Hernández M, Francisco E, Hagen F, Meis J, Colombo J. First report of *Candida auris* in America: clinical and microbiological aspects of 18 episodes of candidaemia. J Infect 2016 [citado, 2017 febrero 10] Disponible en: *http://dx.doi.org/10.1016/j.inf.2016.07.008.*

Limit to a maximum of 50 references for original articles and 100 for Narrative and Systematic Reviews or Meta-analyses.

It is recommended to check the last number of our journal as a guide in the preparation of the manuscript consulting the web page: http://sites.google.com/site/revistainvestigacionesclinicas/home.

Check List

- ☐ Cover letter signed by all authors accepting a significant participation in the work, that are in agreement with the content of the manuscript and that the content has not been published or submitted for publication elsewhere. Corresponding author must be identified.
- ☐ Pages sequentially numerated.
- ☐ Title in English.
- ☐ Title in Spanish.
- ☐ Short Title in the main language used in the manuscript.
- ☐ Full names of the authors without professional titles.
- ☐ Postal and e-mail addresses of the institution or institutions where the work was performed.
- ☐ Non structured abstracts in English and Spanish that state the purpose, basic procedures, main findings and principal conclusions of the study. No more than 250 words.
- ☐ Concise Introduction regarding to the study.
- ☐ Precise description of Material and Methods, or Patients and Methods, with references.
- ☐ Specification of statistical analysis (when required).
- ☐ Results described clearly and in logical order without extended discussion of their significance.
- ☐ Discussion based in findings of the study.
- ☐ All references mentioned in the Reference list are cited in the text according to specifications of the journal.
- ☐ Unpublished results, personal communications or congress presentations without abstracts are not recommended in the reference list.
- ☐ Tables with footnotes below the table body.
- ☐ Illustrations and photographs according to journal specifications.
- ☐ Figures, illustrations and photographs with legends in separate pages.
- ☐ Conflict of competence.
- ☐ Source of founding.
- ☐ ORCID iD of the authors.
- ☐ Contribution of all authors to the paper.

Investigación Clínica
Vol. 63 Nº 1 / March 2022
Bilingual - Abstracts in Spanish and English

Contents

Investigación Clínica
Vol. 63 Nº 1 / Marzo 2022
Bilingüe - Resúmenes en Español e Inglés

Contenido